# Chapter 4. Results and Discussion

## 4.1. Analysis with SSPG-Methane blends

The thermodynamic-based SI engine performance prediction simulation model was initially validated with the experimental results, carried out over *Wiscon TN27* SI engine while utilizing the fuel blends of SSPG with methane. Further, specifications for the engine model have been presented in Table 4.1. The simulation model was utilized for an innovative engine performance investigation through variable compression ratio (CR), SSPG-blending proportion (SSPG), and Start-of-ignition (SOI) input settings. The considered PG blend fractions for the study have been presented in Table 4.2 along with their respective thermo-physical properties. The generated simulation results were imported into Minitab software for performing the RSM-based regression and statistical multi-objective optimization. In this analysis, the considered response parameters included six engine performance-indicating parameters (ITE, IMEP, BTE, BP, BMEP, and BSEC) and two emission-indicating parameters (for CO and NO). Finally, through the optimization operation, the best input settings were assessed orienting for enhanced performance efficiency, power, and adequately low CO-NO emissions. For executing the analysis the research procedure integrated the RSM-based approach for optimization with the novel applied modelling strategy, and the unique-cum-diverse combinations of the independent input-output parameters. With this novelty in the investigation execution, the present research work is extended toward achieving the following basic objectives:

- To present the modelling compatibility of SSPG-Methane blend fuelled engine performance prediction using a QD thermodynamic simulation approach.
- To analyze the impact of CR, SSPG-Methane blend, and SOI simultaneous variations on the engine performance (Power, fuel consumption, and emission).

- To detail the sensitivity in the selected engine performance response parameters regarding the considered independent input factor parameters.
- To carry out a detailed assessment of the input variables in the cumulative performance of SI engine.
- To develop prediction models for the particular engine model and fuelling agents through both, the thermodynamic-based QDTM and the statistically-based regression modelling.
- Present the optimal input conditions for maximizing efficiency and power, while minimizing the fuel consumption and emissions, using RSM.

Table 4.1: Engine specifications respective to simulation

| Particular | Engine Specification |
|---|---|
| Engine make | Wiscon TM27, freely aspirated [65] |
| Engine type | 4 Stroke-Spark Ignition Engine |
| Compression ratio (r) | 10-13:1 *(variable)* |
| Bore Diameter (mm) | 91.0 |
| Stroke (mm) | 103.2 |
| Connecting rod length (mm) | 136.5 |
| Start of ignition (crank angle) | 30-45 bTDC *(variable)* |
| Equivalence ratio | 1.0 |
| PG fraction by volume% to methane | 10-90% *(variable)* |
| RPM | 1500 |

Table 4.2: Thermophysical properties of considered PG~$CH_4$ blends

| **Fuel** | **Fuel composition by V%** | **Calorific Value (MJ/kg)** | **Reference** |
|---|---|---|---|
| Sewage sludge Producer gas (SSPG) | $H_2$: 13%<br>CO: 16%<br>$CH_4$: 3%<br>$CO_2$: 15%<br>$N_2$: 53%<br>Density: 1.1 kg/$m^3$ | 4.05 | [26], [49] |
| Methane | CH4:100% | 50.33 | [49] |
| SSPG10 | 10% SSPG+90% methane | 42.82 | Calculated |
| SSPG25 | 25% SSPG+75% methane | 35.59 | |

| | | |
|---|---|---|
| SSPG50 | 50% SSPG+50% methane | 21.28 |
| SSPG75 | 75% SSPG+25% methane | 11.70 |
| SSPG90 | 90% SSPG+10% methane | 6.92 |

### 4.1.1. Engine performance Validation

Results of the developed quasi-dimensional computational model and the respective experimental outcomes for pressure vs crank angle traces have been presented in Figure 4.1.1**.** The correspondingly configured engine specifications were matched with the engine specifications of that of the experimental reference, as also consolidated in Table 4.1. The fuel composition of SSPG and the concerned CV (as Lower calorific value (LCV)) have also been set as per reference, as presented in Table 4.2. According to the figure, quasi-dimensional (QD) simulation-modelled results closely intercepted the corresponding previous experimental trace of reference[49] for the in-cylinder pressure variation. The maximum crank angle deviation is within 5%. From Figure 4.1.1, it is also noticed that the position of pressure throughout the compression is found to be deviating by less than 4 crank angle degrees, however, the peak pressure closely matches. In experimental results from the reference [49], performance results are based on neglecting the effect of misfiring and the obtained results represent an ensemble of 100 cyclic traces of pressure-crank angle. Therefore, the maximum pressure range has been considered for the validation. Thus, the QD model validates the experimental result with a marginal difference (within 5%) at fixed $35^{\circ}$ BTDC SOI and 10 CR, which shows the satisfactory capability of the simulation model. This difference may be due to the effect of assumptions considered in the simulation program. Concerning the engine output power validation, the experimental outcomes at different relative air-fuel ratios for 0, 20, 40 and 50% SSPG blend with methane, are consolidated in Figure 4.1.2. Thereafter, the validated quasi-dimensional model was implemented through FORTRAN for accessing the engine performance (Power, fuel consumption, and emission) with varying SSPG-Methane blend, CR, and SOI levels.

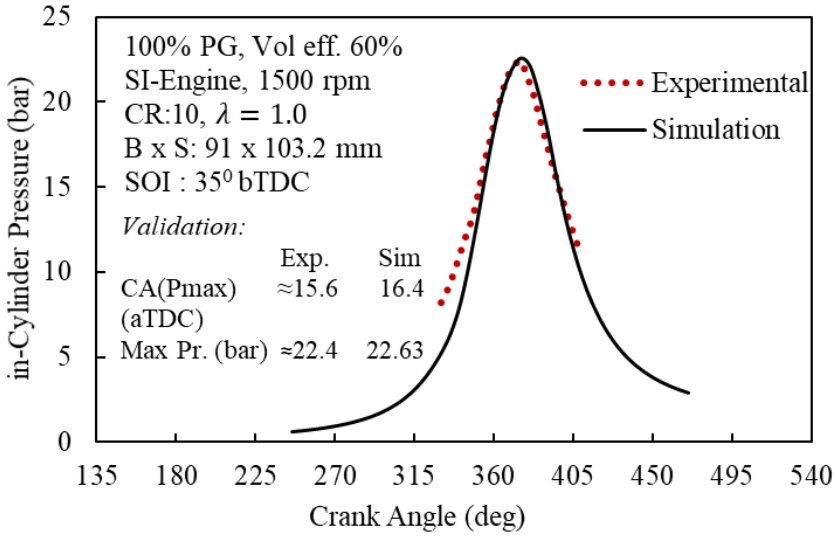


Figure 4.1.1. Model validation with experimental with pressure vs crank angle

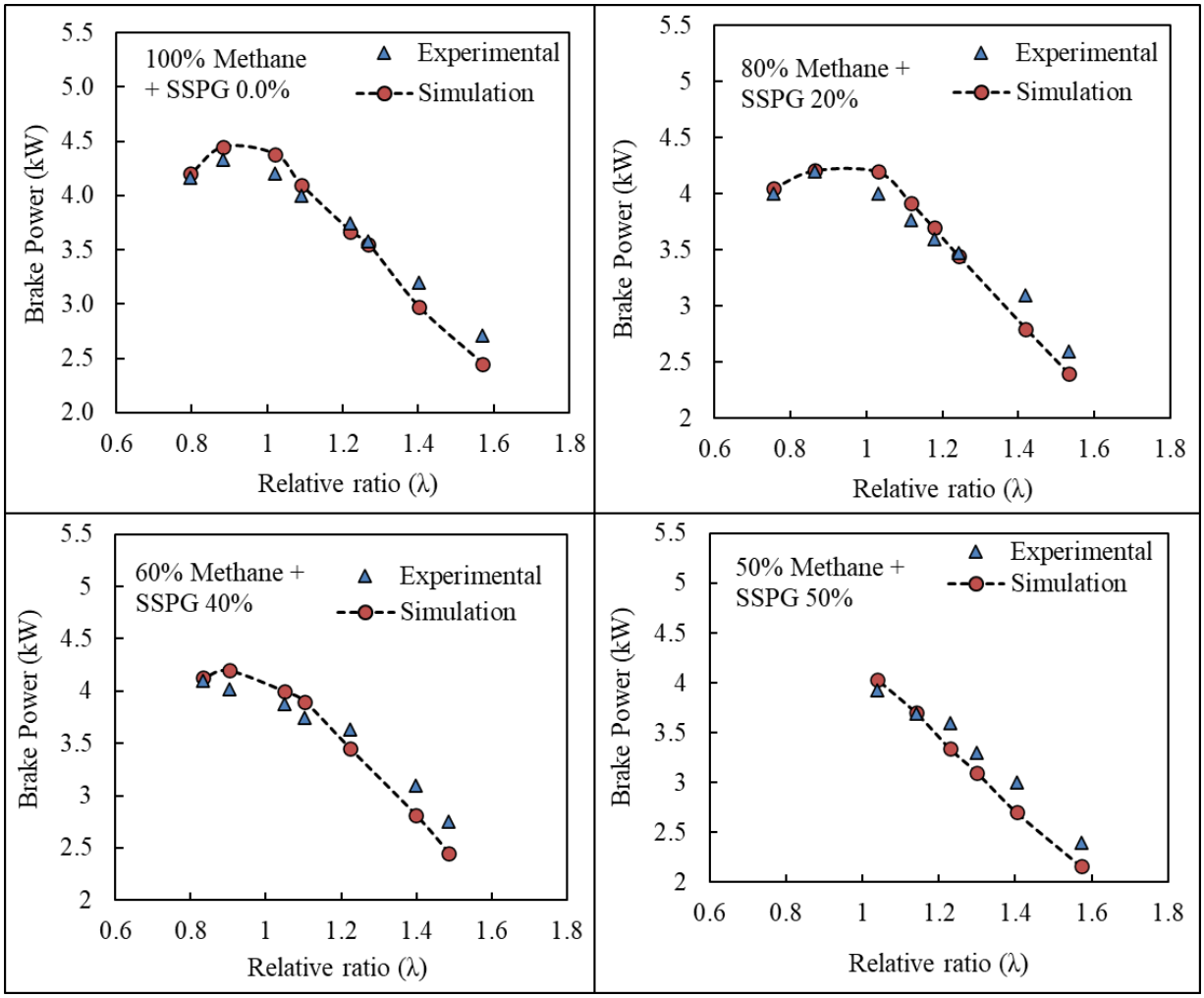


Figure 4.1.2. Model validation with brake power vs relative ratio

### 4.1.2. Significant Decision parameters

To assess the sensitivities of all eight selected response parameters towards the three considered independent input factors (CR, blend fraction, and spark timing inputs), the Pareto charts were formed with respect to the simulation results, and the statistical tool of ANOVA analysis was utilized.

#### *4.1.2.1.* Pareto chart

The predominant influence of the considered vital input parameters over the performance and emission responses is confirmed using the Pareto charts [168, 200], developed using Minitab software. Figure 4.1.3 and Figure 4.1.4 represent the Pareto charts for performance and emissions responses, respectively. In the figure, the red line represents a 95% confidence level. In such representations, the higher the value of standardized effect for a response parameter (beyond level of significance, that is: >1.99) is, the more dominant the particular independent input parameter is. This strategy identified the identification and evaluation of the particular independent input parameters which laid a higher degree of influence on the respective output responses variable. For instance, in the Pareto chart for IMEP, the influence of variations in factor B (which denotes SS-PG blend fraction as intake fuel proportions) imparts the most significant variations on the IMEP response of the engine. This strategy of evaluation further enabled the classification of the performance parameters based on their factor of influence. For instance, it could be inferred from Figure 4.1.3 that at overall, all the performance parameters are basically significantly affected by the PG blend (SS PG%) variations. This could be attributed to the influence laid by PG blendings on the calorific value of net charge present inside the combustion chamber [195]. All the power-indicating responses, like IMEP, BP, and BMEP are also subsequently and significantly affected by the square term variations in SOI (CC-term) and SSPG (BB-term), and linear term variation of CR (A-term). The linear-term

interaction for the parameter SOI (C-term) is observed to have the least effect on the considered performance parameters.

Similarly, from Figure 4.1.4 it is observed that CO-emission is most affected by linear term variations of SSPG, whereas, NO emission is most influenced by linear term SOI variation. This effect could pertain to the significant influence of PG concentration (SS PG%) on valence oxygen availability in input charge[136] and significant influences of SOI on peak combustion temperature [116, 201].

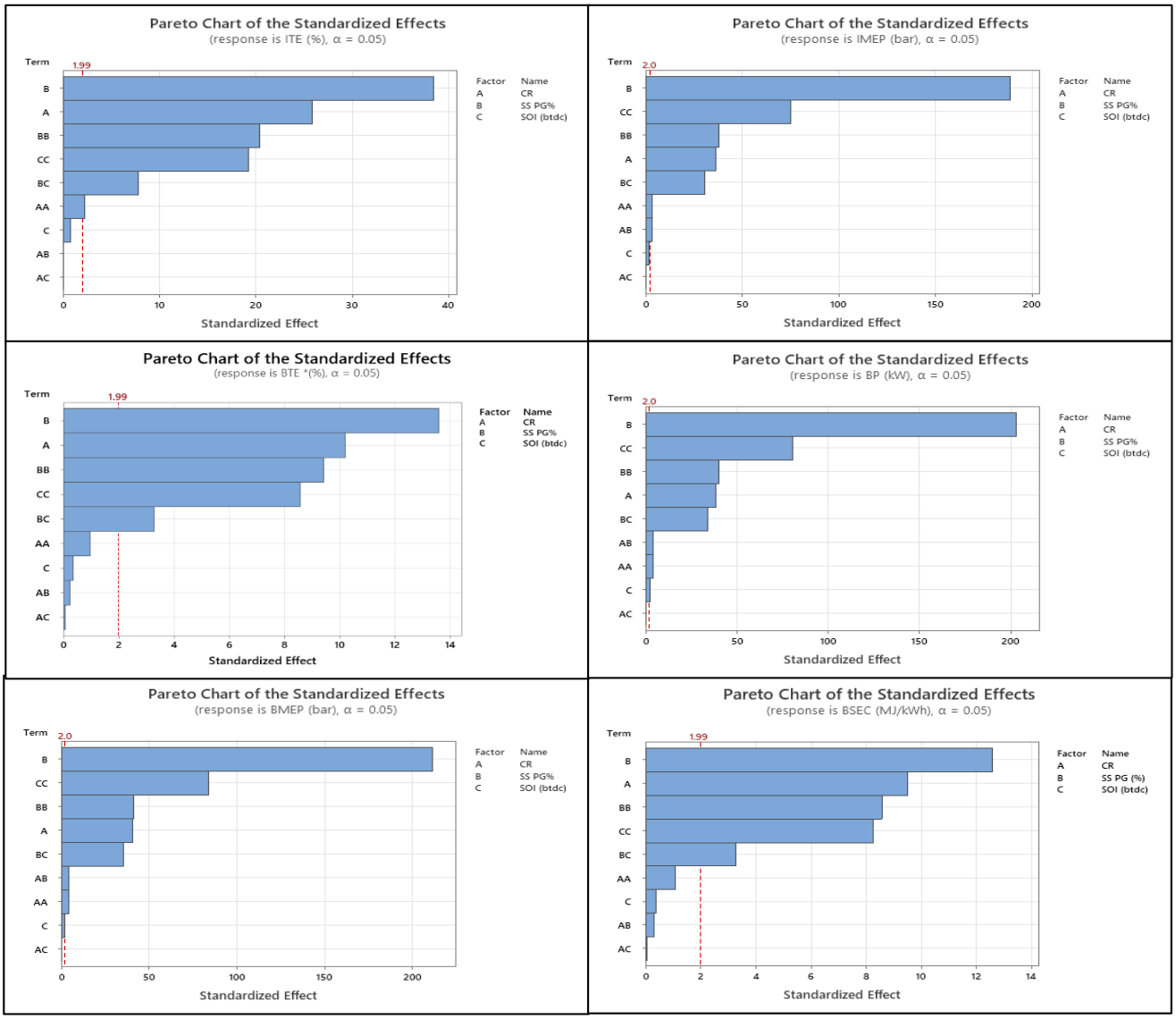


Figure 4.1.3. Pareto chart for the performance parameters of the engine

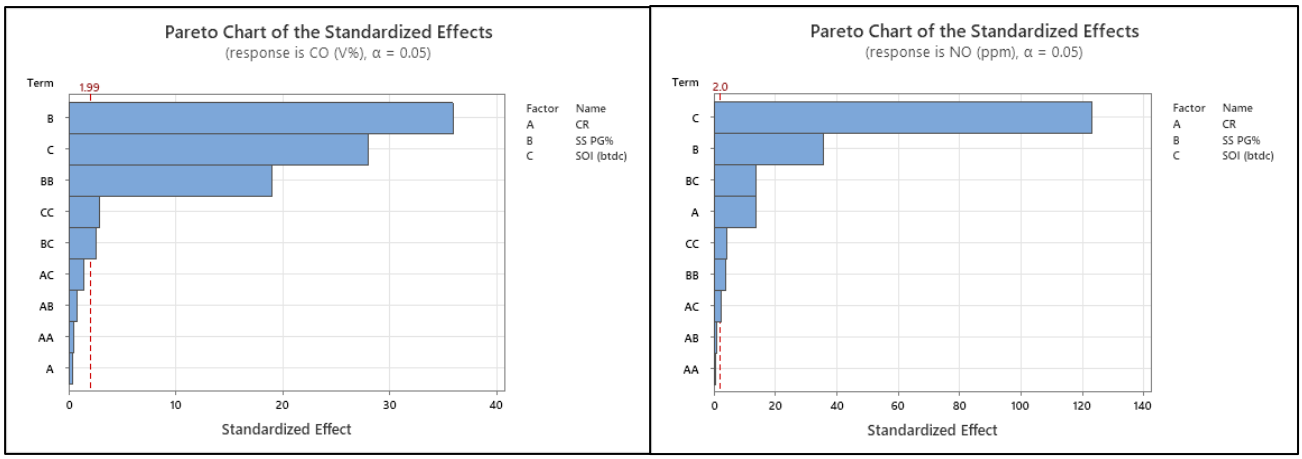


Figure 4.1.4. Pareto chart for emission parameters of the engine

***4.1.2.2.*** RSM regression analysis

Consistency of the RSM-developed statistical-based polynomial regression model for the eight response parameters is confirmed with the acquirement of higher coefficient of determination ($R^2$) values through ANOVA analysis. On the other hand, the consistency with the optimal response outcomes is confirmed by the acquirement of the higher composite desirability (D) values, thereby supporting the attainment of the most desired and optimal results. RSM-constructed second-order regression equations for the performance and emission response estimations are presented in Eqs. 56-61 and Eqs. 62-63, respectively. In these equations, the interpretations of contributions of the multi-ordered independent input terms over the responses are indicated via magnitudes of corresponding coefficient values. For instance, the 'CR*SOI' two-way interaction term is statistically modeled to have negligible impacts on the BP, as the coefficient tends to zero.

$$\begin{aligned} \text{ITE} \;=\; & -6.74 + 1.888\ \text{CR} - 0.1060\ \text{SS PG} + 1.551\ \text{SOI} \\ & - 0.0572\ \text{CR*CR} + 0.000826\ \text{SS PG*SS PG} - 0.02176\ \text{SOI *SOI} \\ & + 0.000067\ \text{CR*SS PG} + 0.00016\ \text{CR*SOI} + 0.001483\ \text{SS PG*SOI} \end{aligned} \tag{56}$$

$$\begin{aligned} \text{IMEP} \;=\; & 0.325 + 0.1441\ \text{CR} - 0.009853\ \text{SS PG} + 0.29935\ \text{SOI} \\ & - 0.00440\ \text{CR*CR} - 0.000076\ \text{SS PG*SS PG} - 0.004211\ \text{SOI *SOI} \\ & - 0.000130\ \text{CR*SS PG} + 0.000115\ \text{CR*SOI} + 0.000292\ \text{SS PG*SOI} \end{aligned} \tag{57}$$

$$\begin{aligned} BTE &= -11.45 + 1.72\,CR - 0.1124\,SS\,PG + 1.505\,SOI \\ &\quad - 0.0529\,CR*CR + 0.000825\,SS\,PG*SS\,PG - 0.02095\,SOI*SOI \\ &\quad + 0.00038\,CR*SS\,PG - 0.0006\,CR*SOI + 0.001353\,SS\,PG*SOI \end{aligned} \quad (58)$$

$$\begin{aligned} BP &= -0.861 + 0.1288\,CR - 0.008429\,SS\,PG + 0.25092\,SOI \\ &\quad - 0.003900\,CR*CR - 0.000063\,SS\,PG*SS\,PG - 0.003522\,SOI * SOI \\ &\quad - 0.000122\,CR*SS\,PG + 0.000014\,CR*SOI + 0.000251\,SS\,PG*SOI \end{aligned} \quad (59)$$

$$\begin{aligned} BMEP &= -1.027 + 0.1536\,CR - 0.010086\,SS\,PG + 0.29896\,SOI \\ &\quad - 0.00470\,CR*CR - 0.000074\,SS\,PG*SS\,PG - 0.004202\,SOI*SOI \\ &\quad - 0.000153\,CR*SS\,PG + 0.000068\,CR*SOI + 0.000299\,SS\,PG*SOI \end{aligned} \quad (60)$$

$$\begin{aligned} BSEC &= 32.79 - 0.930\,CR + 0.0497\,SS\,PG - 0.738\,SOI \\ &\quad + 0.0301\,CR*CR - 0.000386\,SS\,PG*SS\,PG + 0.01039\,SOI*SOI \\ &\quad + 0.000268\,CR*SS\,PG - 0.00037\,CR*SOI - 0.000698\,SS\,PG*SOI \end{aligned} \quad (61)$$

$$\begin{aligned} CO &= 1.158 - 0.0532\,CR - 0.00671\,SS\,PG - 0.01800\,SOI \\ &\quad + 0.00110\,CR*CR + 0.000072\,SS\,PG*SS\,PG + 0.000306\,SOI*SOI \\ &\quad + 0.000053\,CR*SS\,PG + 0.000650\,CR*SOI + 0.000047\,SS\,PG*SOI \end{aligned} \quad (62)$$

$$\begin{aligned} NO &= -1182 - 261\,CR - 35.52\,SS\,PG + 180.5\,SOI \\ &\quad + 3.32\,CR*CR + 0.03652\,SS\,PG*SS\,PG - 1.109\,SOI *SOI \\ &\quad + 0.189\,CR*SS\,PG + 2.78\,CR*SOI + 0.6026\,SS\,PG*SOI \end{aligned} \quad (63)$$

***4.1.2.3.*** ANOVA analysis

The ANOVA results for performance and emission parameters are presented in Table 4.3 and Table 4.4, respectively. The statistical-based significance of the model, with its variables and their interactions, is presented in ANOVA-result tables via the F-value magnitudes. A greater F-value shows a higher influence of the corresponding factor on the concerned response parameter. The p-value, then again, is the most crucial model indicator as it confirms model validity. If the p-value is greater than 0.05, the model is considered inconsistent [202]. Considering linear term relations, it can be inferred from Table 4.3 that the impact of SOI upon

the response of ITE and BTE could be neglected as the p-value is major (or, more than 0.05). Whereas, most performance response parameters are affected majorly by variations in SSPG, followed by CR variations that are reflected from the higher F-values. On the other hand, square terms also verify the greater influence of SSPG on the performance response parameters. Considering the 2-way interactions, it could be observed that the simultaneous variations in SSPG and SOI impart a greater effect over ITE, IMEP, BP, and BMEP pertaining to zero P-value and comparatively greater F-values.

It can be inferred from Table 4.4 that CO and NO emissions are highly sensitive to SSPG variation and SOI variations, respectively. This sensitivity aligns with the results portrayed in the Pareto charts as well. Besides this, concerning the statistical model efficiency, the results also feature $R^2$ values (adj. and pred.) lie higher values equal to the range of 95% - 99%, which is in a very acceptable range.

Table 4.3: ANOVA for engine performance parameters.

| | **ITE** | | **IMEP** | | **BTE** | | **BP** | | **BMEP** | |
|---|---|---|---|---|---|---|---|---|---|---|
| **Source** | **F-Value** | **P-Value** | **F-Value** | **P-Value** | **F-Value** | **P-Value** | **F-Value** | **P-Value** | **F-Value** | **P-Value** |
| Model | 371.75 | 0.000 | 4596.81 | 0.000 | 57.34 | 0.000 | 5324.48 | 0.000 | 5760.74 | 0.000 |
| **Linear** | 721.25 | 0.000 | 12498.87 | 0.000 | 96.55 | 0.000 | 14486.62 | 0.000 | 15692.74 | 0.000 |
| **Interaction** | | | | | | | | | | |
| CR | *671.26 | 0.000 | *1329.77 | 0.000 | *104.03 | 0.000 | *1494.31 | 0.000 | *1649.90 | 0.000 |
| SS PG | **1482.32 | 0.000 | **35704.77 | 0.000 | **184.55 | 0.000 | **41412.24 | 0.000 | **44866.44 | 0.000 |
| SOI | 0.60 | 0.441 | 4.02 | 0.048 | 0.13 | 0.719 | 6.40 | 0.013 | 3.45 | 0.067 |
| **Square** | 281.67 | 0.000 | 2265.67 | 0.000 | 57.75 | 0.000 | 2605.87 | 0.000 | 2809.31 | 0.000 |
| **Interaction** | | | | | | | | | | |
| CR*CR | 5.19 | 0.025 | 12.44 | 0.001 | 0.94 | 0.334 | 16.16 | 0.000 | 17.85 | 0.000 |
| SS PG*SS PG | **417.72 | 0.000 | *1447.00 | 0.000 | **88.75 | 0.000 | *1622.58 | 0.000 | *1714.61 | 0.000 |
| SOI*SOI | *372.38 | 0.000 | **5652.83 | 0.000 | *73.39 | 0.000 | **6537.64 | 0.000 | **7079.00 | 0.000 |
| **2-Way** | 20.12 | 0.000 | 320.21 | 0.000 | 3.58 | 0.017 | 390.55 | 0.000 | 424.46 | 0.000 |
| **Interaction** | | | | | | | | | | |
| CR*SS PG | 0.01 | 0.930 | *12.09 | 0.001 | 0.05 | 0.817 | *17.65 | 0.000 | *20.91 | 0.000 |
| CR*SOI | 0.00 | 0.973 | 0.24 | 0.628 | 0.00 | 0.957 | 0.01 | 0.939 | 0.10 | 0.748 |
| SS PG*SOI | **60.35 | 0.000 | **948.44 | 0.000 | **10.68 | 0.002 | **1153.97 | 0.000 | **1252.45 | 0.000 |

| | | | | | |
|---|---|---|---|---|---|
| $R^2$ | 97.38 | 99.78 | 85.15 | 99.81 | 99.83 |
| $R^2$-(Adj.) | 97.12 | 99.76 | 83.67 | 99.79 | 99.81 |
| $R^2$-(Pred.) | 96.81 | 99.74 | 81.75 | 99.77 | 99.78 |

***Note:*** *The greater the F-value (** > *) shows the higher influencing factor*

Table 4.4: ANOVA for engine emission parameters

| | | BSEC | | CO | | NO | |
|---|---|---|---|---|---|---|---|
| **Source** | **DF** | **F-Value** | **P-Value** | **F-Value** | **P-Value** | **F-Value** | **P-Value** |
| Model | 9 | 50.13 | 0.000 | 301.43 | 0.000 | 1899.71 | 0.000 |
| **Linear** | 3 | 83.36 | 0.000 | 767.44 | 0.000 | 5312.10 | 0.000 |
| CR | 1 | *90.66 | 0.000 | 0.16 | 0.688 | 184.47 | 0.000 |
| SS PG | 1 | **158.57 | 0.000 | **1289.04 | 0.000 | *1286.81 | 0.000 |
| SOI | 1 | 0.13 | 0.715 | *782.87 | 0.000 | **15206.66 | 0.000 |
| **Square** | 3 | 50.76 | 0.000 | 121.80 | 0.000 | 11.95 | 0.000 |
| CR*CR | 1 | 1.16 | 0.285 | 0.22 | 0.643 | 0.33 | 0.568 |
| SS PG*SS PG | 1 | **73.64 | 0.000 | **362.11 | 0.000 | *15.30 | 0.000 |
| SOI*SOI | 1 | *68.54 | 0.000 | *8.30 | 0.005 | **18.13 | 0.000 |
| **2-Way Interaction** | 3 | 3.63 | 0.016 | 3.18 | 0.028 | 64.82 | 0.000 |
| CR*SS PG | 1 | 0.10 | 0.750 | 0.56 | 0.456 | 1.18 | 0.281 |
| CR*SOI | 1 | 0.00 | 0.945 | *2.09 | 0.152 | *6.35 | 0.013 |
| SS PG*SOI | 1 | **10.80 | 0.001 | **6.76 | 0.011 | **186.60 | 0.000 |
| $R^2$ | | 83.37 | | 96.79 | | 99.48 | |
| $R^2$-(Adj.) | | 81.71 | | 96.47 | | 99.42 | |
| $R^2$-(Pred.) | | 79.41 | | 95.96 | | 99.33 | |

## 4.1.3. 3D-Surface and Contour plots

The significant influences of CR, SSPG, and SOI control parameters over engine efficiency and emissions when dealing with naturally aspirating engines operating on blended PG have already been evident in studies of Ref.s-[110, 116]. However, the novel approach to interpreting the simultaneous impacts of the considered input variables on eight selected response output parameters is discussed in this section, in the following sub-sections with the presentation of three-dimensional (3D) surface and contour plots. This enhances the interception of influences imparted by the three-factor parameters on the selected response parameters.

***4.1.3.1.*** Indicated thermal efficiency

Indicated thermal efficiency(ITE) is the ratio of IP to the calorific value in the consumed rate of fuel [110, 133]. Figure 4.1.5 presents the simultaneous impact of CR, SSPG, and SOI on ITE. It can be observed from the surface plots that a steady increase in ITE results with CR increase simultaneous to any SSPG or SOI settings. This could pertain to increased combustion efficiency at higher CRs[201]. Considering the effects of PG-blending, it is observed that after an initial decrease, the ITE gradually increases with increasing SSPG for any CR or SOI. The initial decrease might be attributed to the lower calorific value of PG[195], and the following increase (by a minimum 7.48%) could pertain to the increased fuel-to-power conversion efficiency with increased PG blend-fraction [191]. Moreover, the highest ITE values for any specific CR and SSPG combinations are observed when the SOI is limited within 35º to 40º BTDC. Simulation results verify that ITE increased with increasing SOI, peaking at 38.36% for 40º SOI, followed by a gradual decrease. This effect could be attributed to the development of suitable power-conversion conditions that results from the advancements in spark timing and start of ignition (or, SOI). This contributes to increase of in-cylinder average temperature, initially[191]. However, excessive increase in SOI leads to unstable combustion[45, 195, 203], and consequently, it could be observed from the surface plots that the development of the highest ITE is at increased SSPG and CR values, with mid-ranged SOI. A simultaneous depiction drawn using the contour plots confirms this by showing that increased CR (higher than 11), increased SSPG (beyond 80%), and medium spark advancing (SOI at 35º to 40º) results in higher ITE (above 35%).

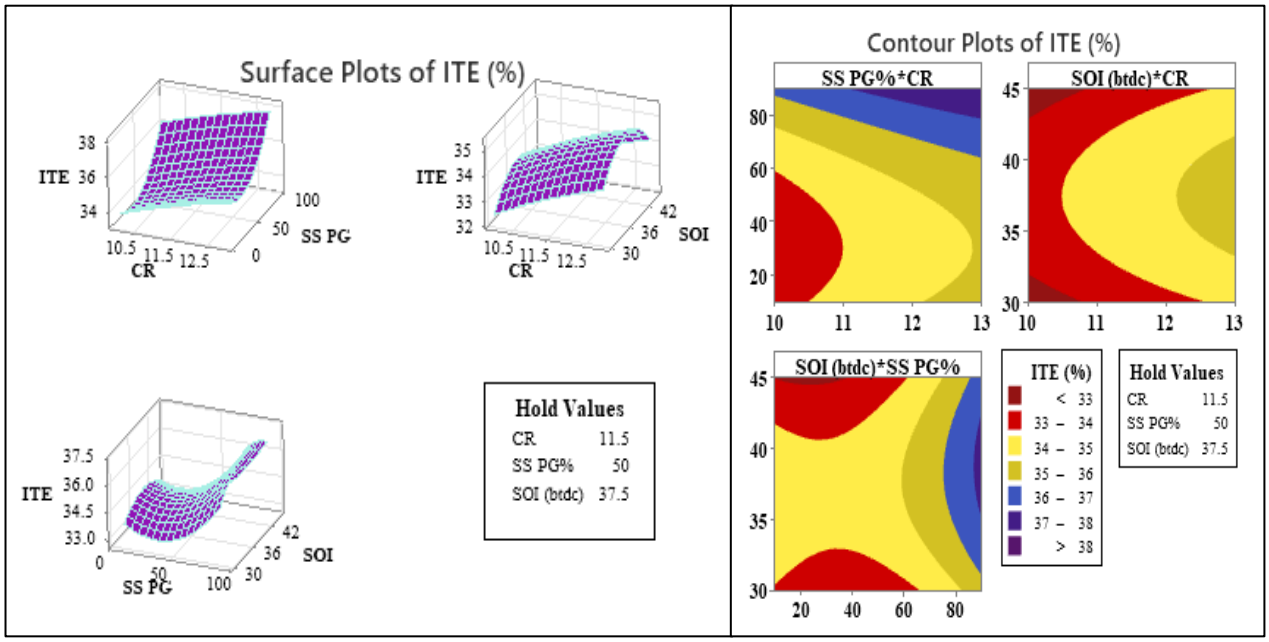


Figure 4.1.5. Simultaneous effects of decision variables on ITE

***4.1.3.2.*** Indicated mean-effective pressure

Indicated mean effective pressure (IMEP) is a significant factor in comparing the performances of engines as it characterizes an engine's power irrespective of its size (displacement volume) [110]. Corresponding 3D surface and contour plots have been depicted in Figure 4.1.6.

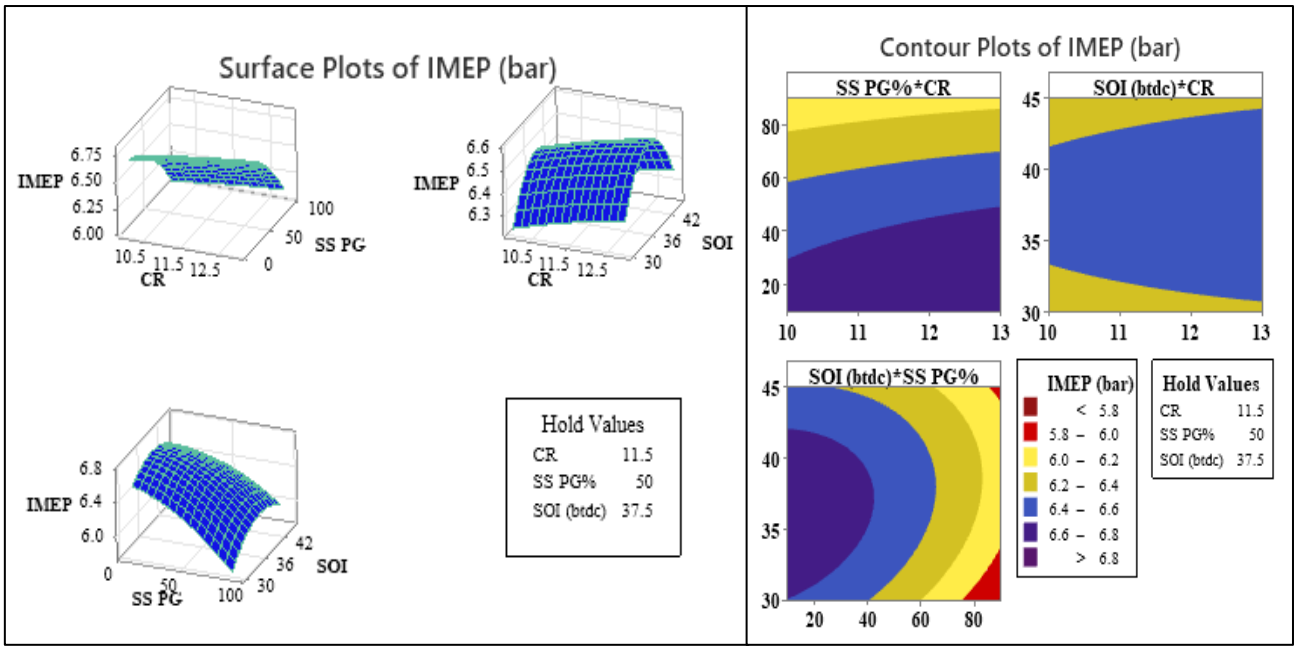


Figure 4.1.6. Simultaneous effects of decision variables on IMEP

The surface plots indicate a gradual rise of IMEP (about 1.9% increase) with the full-ranged increase in CR (10 to 13), majorly unaffected by simultaneous SSPG or SOI variations. This could result from the higher combustion efficiency at higher CR-based operations[153]. IMEP is also observed to decrease, by a minimum of 7.43% with an increase in PG content. This could again be attributed to the low calorific value of SSPG, which leads to lower heat release and eventually lower power output [204]. The contour plots confirm the above trends and quantify lower SSPG (up to 40%) and greater CRs, to result in higher IMEP(greater than 6.4 bar) outcomes. Moreover, a moderate spark advancing and inception of combustion (SOI at the range of 35º to 40º BTDC), aids in keeping the IMEP above this 6.4 bars mark. This possibly again attributes to suitable power-conversion conditions as also pointed out in some references, like [45, 195, 203]. A maximum IMEP of 6.82 bar was obtained at CR of 13, 10% SSPG-blending in net SSPG-$CH_4$ intake fuel, and 35º-37º SOI (bTDC).

***4.1.3.3.*** Brake Thermal Efficiency

Brake thermal efficiency (BTE) is an important performance metric for assessing and comparing fuel energy to power conversion [110]. Figure 4.1.7 presents the simultaneous impacts of input variations upon BTE. It is observed that BTE increases gradually with increasing CR by a maximum of 6.77%. This probably results from increased power output from better combustion occurring when the engine operates at greater CR [153, 201]. It is also noticed that following an initial decrease (by at least 4.3%), the BTE increases sharply with an increase of SSPG-blend (minimum increase of 10.2%). The initial decrease is certainly attributed to the lowering of the net C.V. of the total computed fuel-air charge with the increase in SSPG blend [195] and the following increase is probably attributed to better fuel-to-power conversion efficiency when $H_2$-content increases increase in the PG-fraction at the fuel-intake composition [191]. An optimal SOI-input closer to 35º to 37º (BTDC) range is observed to feature better BTE outputs. Contour plots show the that region of better BTE shifts towards

advanced SOI when the SSPG content increases. This certainly pertains to slower flame propagation and delayed combustion completion for increased PG content at the intake. Slower flame propagation leads to delayed heat release and thereby requires more crank-angle time for attaining peak output power [153]. Contour plots confirm that better BTE (> 26%) results from greater CR (more than 11) and any SSPG % provided that SOI ranges close to 35º (BTDC).

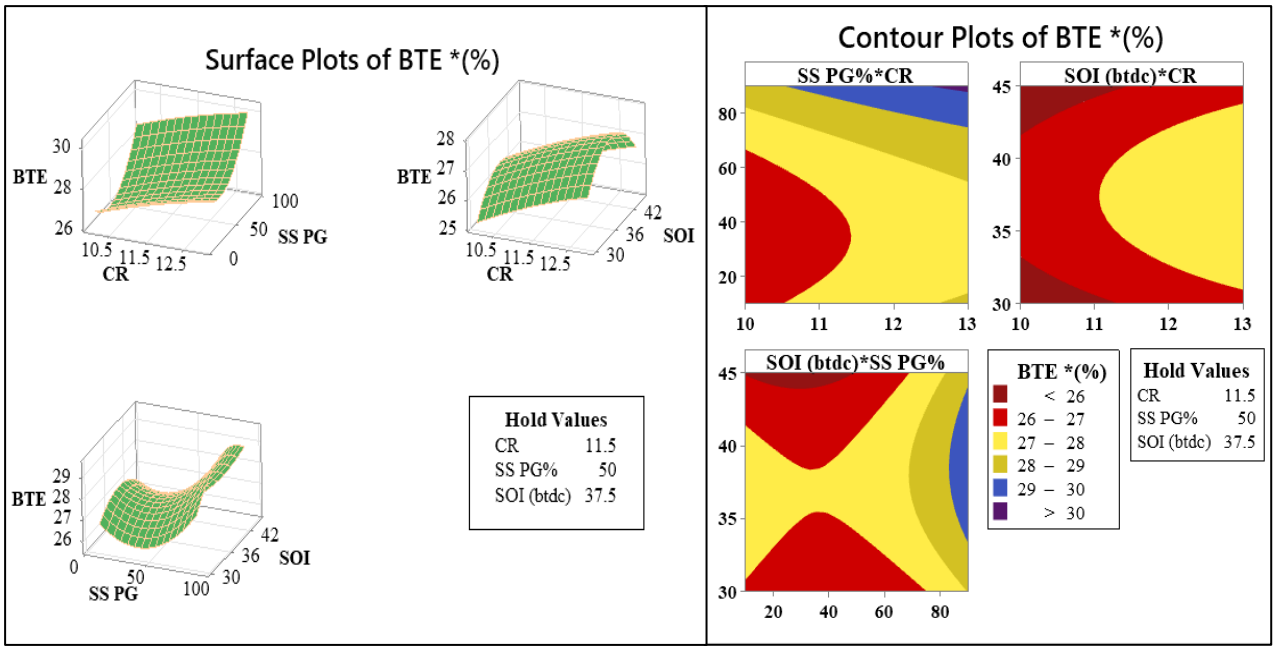


Figure 4.1.7. Simultaneous effects of decision variables on BTE

### *4.1.3.4.* Brake Power

Brake power(BP) is the net power available at the crankshaft after countering the internal frictional and other thermal losses [131]. The simultaneous effects on BP are shown in Figure 4.1.8. The figure depicts a consistent decrease in BP with increasing SSPG. Simulation results confirm this decrease to 11.36%. This decrease could be due to the inhibition of sufficient air by excessive PG substitution [201]. The insufficiency of oxidizers could be confirmed by the rapid rise of CO emissions, as discussed later in section 3.5.6. Further, BP also increases gradually with an increase in CR attributing to increased efficiency[131]. Simulation results confirm that the lowest obtained BP was 3.84 kW at the upper blending margin (90% SSPG)

and the lowest CR margin of 10. Corresponding to any CR or SSPG, an initial rise is followed by a gradual decrement of BP concerning increasing SOI. This effect might be attributed to the suitability of high temperatures and pressure conditions for flame propagation, resulting in increased power generation[195]. The contour plots confirm these features, with higher BP (more than 4.4 kW) being observed for the mid-SOI range (from 35º to 40º bTDC) and higher CR values (from 12 to 13 CR). Literature review revealed that PG-operated engines produce a one-third power drop compared to gasoline operations[49], besides increasing emissions. Thus the producer gas possesses lower average power than gasoline or natural gas. But, the significant optimization operation potentially demonstrates better waste-to-energy conversion outcomes, besides requiring minimal engine modifications[110].

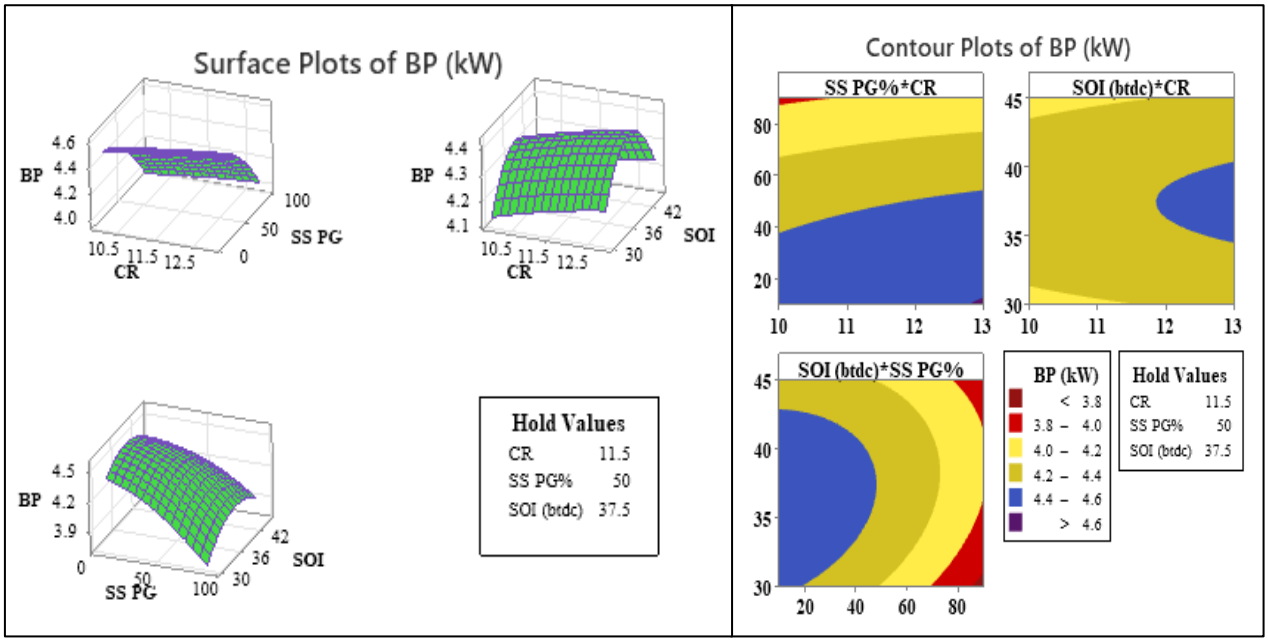


Figure 4.1.8. Simultaneous effects of decision variables on BP

***4.1.3.5.*** Brake-mean effective pressure

Brake mean effective pressure (BMEP) characterizes the size-independent power-producing capability of an engine for developing a comparative performance analysis, especially when fueled for dual-mode operations [205, 206]. BMEP dependency on the considered independent parameters is presented in Figure 4.1.9. It is inferred from surface plots that BMEP decreases

with the increase of SSPG similar to IMEP and BP, for any simultaneous CR or SOI variations. On the other hand, BMEP also tends to increase with increasing CR, attributing again to better combustion and more heat release[153]. Besides, mid-ranged SOI values, from 35º to 40º BTDC, there is better BMEP, which is mostly due to the simultaneous increased BP. Contour plots mark that higher CR (above 12) and low SSPG (below 20%) characterize BMEP greater than 5.25(bars), provided the SOI is of mid-range of 33º to 38º (BTDC).

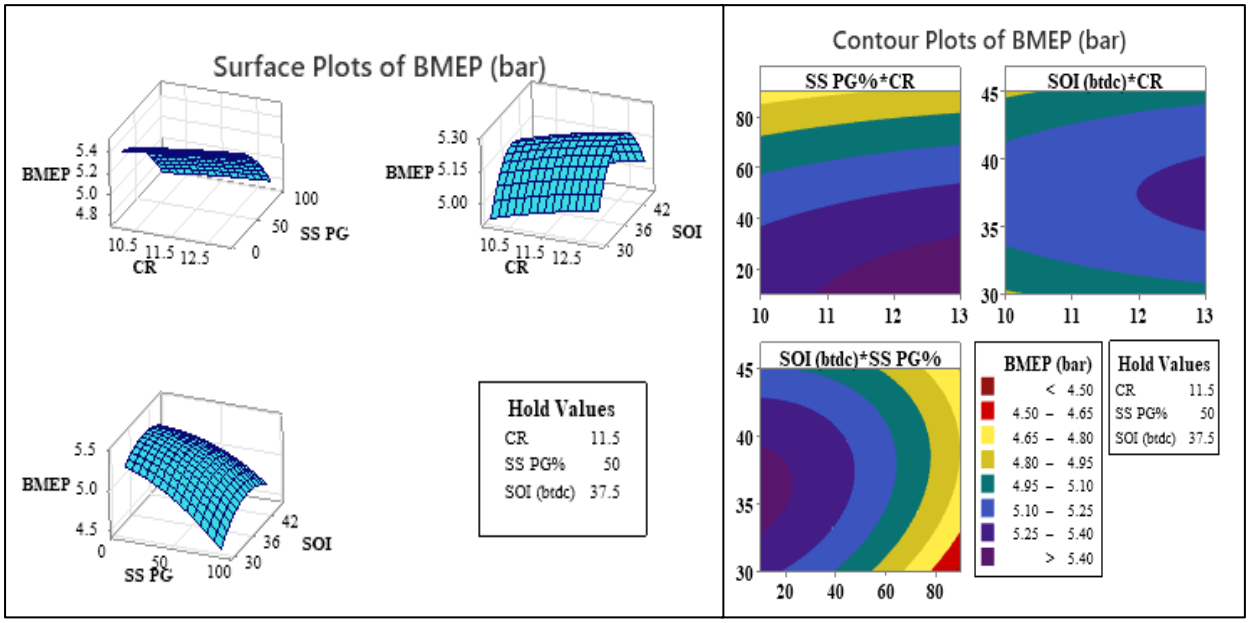


Figure 4.1.9. Simultaneous effects of decision variables on BMEP

***4.1.3.6.*** Brake-specific energy consumption

As this study utilizes two fuels (Methane and SSPG) with different energy densities, the parameter of brake-specific energy consumption (BSEC) is considered[134, 135]. BSEC could be computed as the product of BSFC and net calorific value in the consumed fuel rate [189]. Simultaneous effects of input variations over BSEC are depicted in Figure 4.1.10. It is observed from the figure that BSEC gradually decreases with increasing CR by at least 6.42%. It certainly results due to simultaneously increasing combustion efficiency and greater heat release[201]. Increasing SSPG% also features a dominating decrease in BSEC (maximum by 13.44% ) possibly due to increased conversion efficiency at greater PG-fractions [191]. Low

BSEC values consistently featured at SOI ranging between 35º to 40º (bTDC) certainly due to occurrences of maximum BP at this range. Minimum BSEC of 11.9 (MJ/kWh) featured at input factor parameters of 13 CR, maximum SSPG-blend (90%) and 40º SOI, thereby verifying the 3D-surface plots. Contour plots reflect that BSEC potentially features below 13(MJ/kWh) for simultaneous CR being greater than 11 and for all SSPG fractions provided SOI is set closeer to the range of 35º to 40º (BTDC).

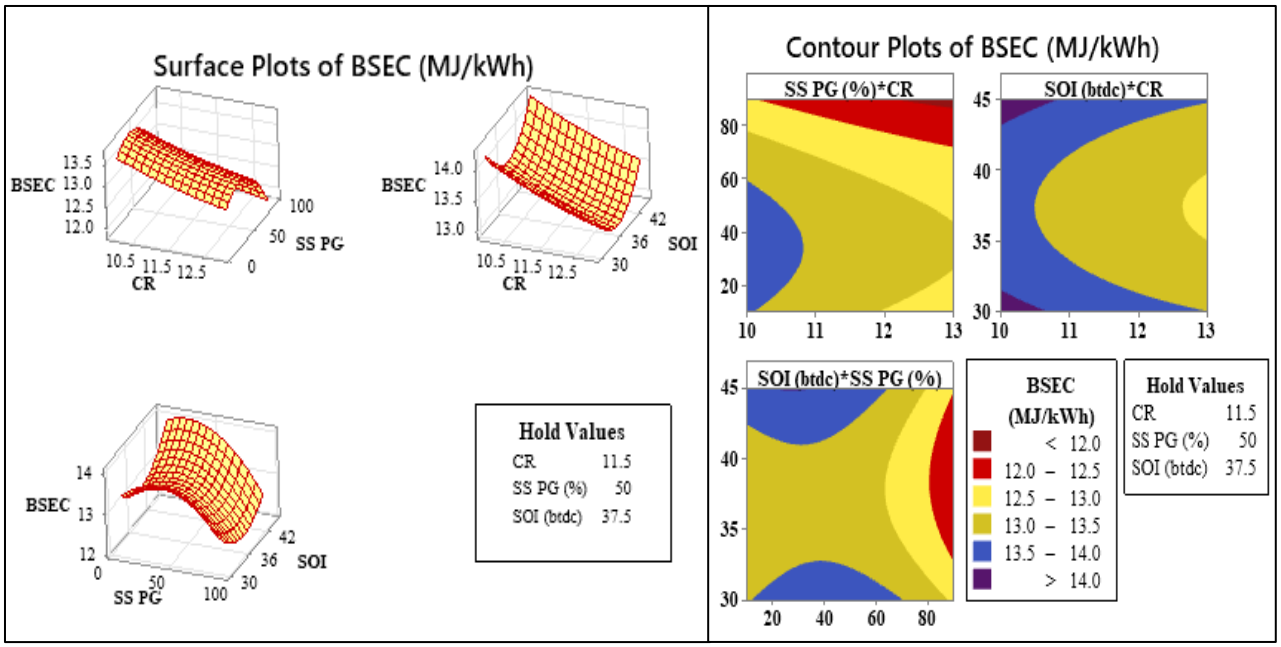


Figure 4.1.10. Simultaneous effects of decision variables on BSEC

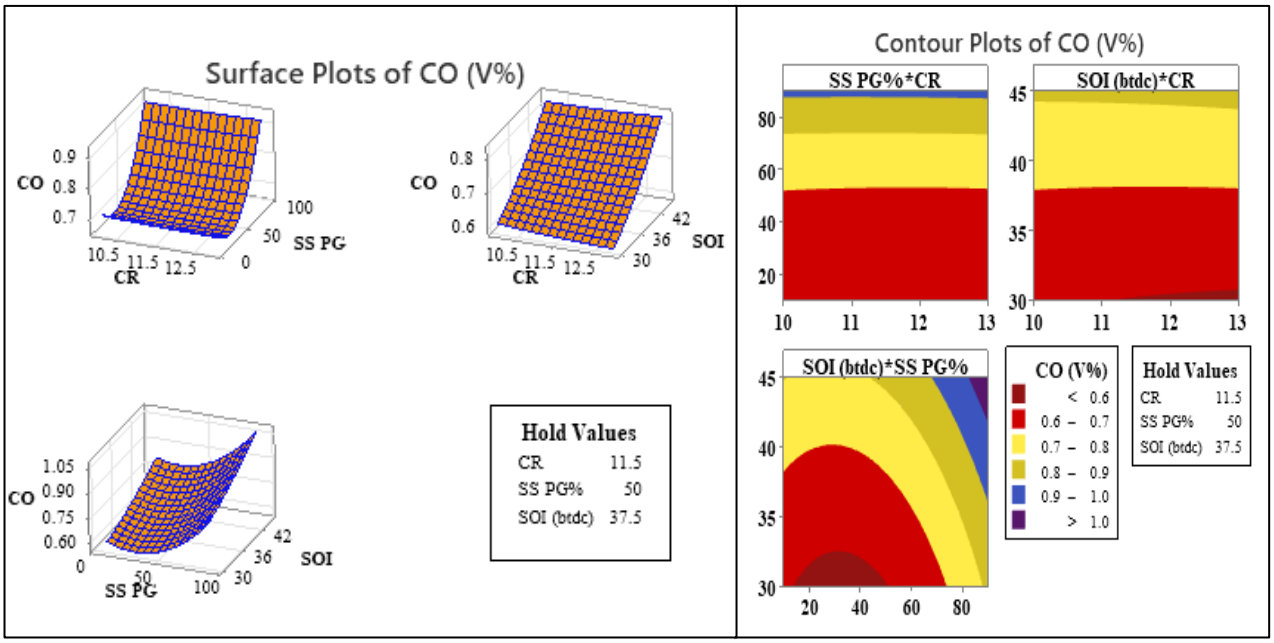


Figure 4.1.11. Simultaneous effects of decision variables on CO emission

***4.1.3.7.*** Carbon mono-oxide emission

Carbon monoxide emission (CO) from IC engines broadly indicates the occurrence of incomplete combustion [153, 207]. CO emission's dependency on the considered independent parameters is presented via 3D surface and contour plots in Figure 4.1.11. It can be noticed from contour plots and FORTRAN-based computational results that increasing SSPG results in an increase of CO emission by at least 40.6%. Possible incomplete combustion is more likely at increased SSPG blends, thereby attributing to more supply of lean mixture and increased CO-generation[49]. Besides, CO emissions also tend to increase with increasing SOI, with a minimum increment of 229.46% (from numeric results). This is because of increased chamber temperature when more simultaneous power and heat are produced with increasing SOI and result in $CO_2$ dissociation into CO [110]. The contour plots also describe that CO emissions largely remain less affected by CR variations, thereby confirming its insignificance from ANOVA analysis.

***4.1.3.8.*** Nitrogen mono-oxide emission

Nitrogen is an inert gas at room temperature. It can only react when the temperature is extremely hot, above $1100^0$C [208], and transforms into oxides of nitrogen [209]. NO emissions dependency on the input parameters is presented in Figure 4.1.12. Increasing SSPG is prompt to decrease NO emission, by at least 29.94%, attributed to the increased oxygen unavailability [136]. Increasing SOI results in an increase of NO emissions (on an average of 40.625%), which is collinear with the expected increase in chamber temperature with increasing SOI[191]. These trends are also observed in experimental works-[49, 116]. Besides, 3D surface and

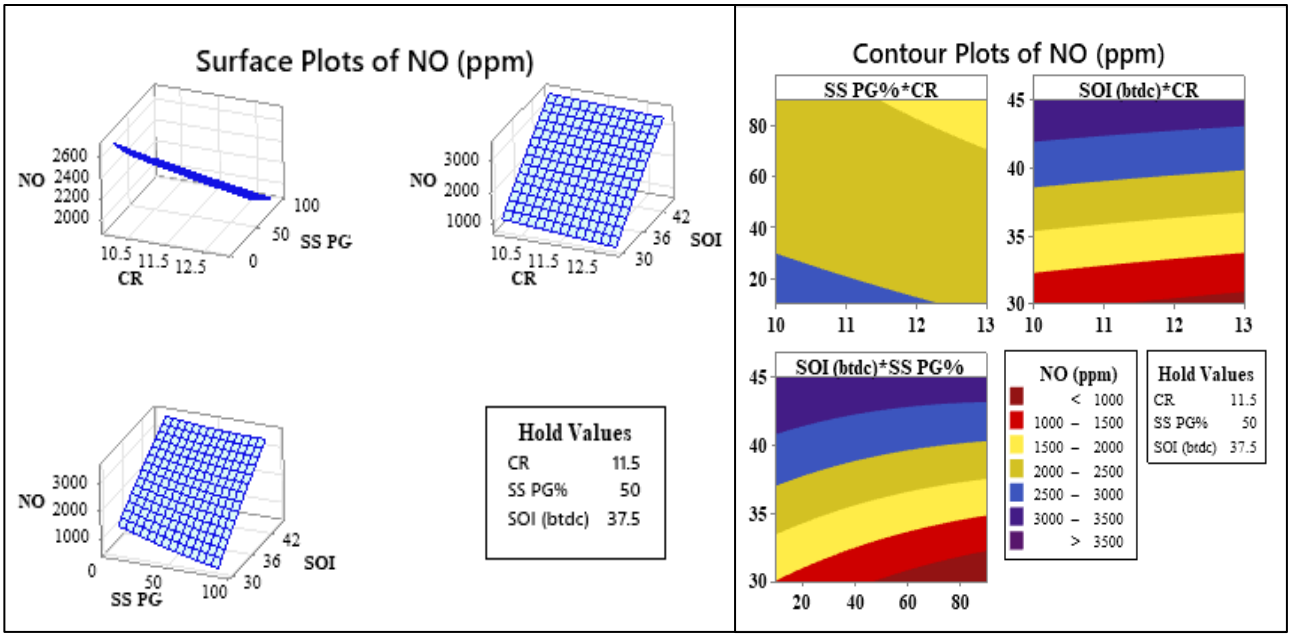


Figure 4.1.12. Simultaneous effects of decision variables on NO emissions

contour plots also indicate that NO emissions are not considerably affected by CR as compared to SOI and blend percentage of PG (Figure 4.1.12). As CR increases, although the cylinder temperature increases, the expansion ratio also increases, which might result in the freezing of the dissociation of NO-formation. Similar reasons have also been reported for the decreasing NO-emission trends while dual fuel engines run, with simultaneous CR increase in the experimental works [160, 210]. Summarily, a compromised blending magnitude for SSPG and a smaller SOI value are desired from the emissions perspective.

### 4.1.4. Optimization and significant verdicts

The RSM optimizer module of Minitab software was used to execute the multi-objective optimization. Dimensionless desirability (d) values were obtained which ranged between 0 and 1, where 0 denoted definite unacceptable response and 1 denoted absolute desired optimal response outcome. The cumulative composite desirability (D) for the model was obtained as 0.7671. Figure 4.1.13 presents the RSM optimization results considering the applied constraints. The optimum values of ITE, IMEP, BTE, BP, BMEP, BSEC, CO, and NO were found to be 35.3498%, 6.7928 bar, 28.1039%, 4.601 kW, 5.4873 bar, 12.8067 MJ/kWh, 0.645 V%, and 1967.102 ppm respectively. The optimum magnitude of independent parameters- CR, SSPG, and SOI are found to be 13, 10%, and $34.0909^0$ (BTDC) respectively. A comparable improvement in the performance responses could be drawn with regards to the experimental reference considered for the validation, the Szwaja et al. [49]. This work considered the same engine configurations with methane-SSPG fuel blends. The maximum ITE reported by them was 35.35% which is in the comparable limits with the simulated and RSM-predicted optimal ITE response of 35.3498%. On the other hand, their best IMEP was found relatively lower, at 4~4.5 bar for operations at stoichiometric equivalence, whereas the optimal IMEP found in our investigation was 6.7928 bar. This IMEP improvement should attribute to the consideration of higher CR (13) in our statistically determined RSM-based optimization, whereas the referenced work considers 10/11 CR. Further, the engine size-independent parameter, the BMEP, was also found comparable to the experimental reference. The optimal BMEP was determined as 5.4873 bar, whereas the reference work BMEP ranged within 5.39 to 6.11 bars. Further, comparisions also reveal that although the ITE is insignificantly affected, significant IMEP and BMEP improvement by up to around 32 % and 10.94% could be gained via SSPG-blending to the fuel considering the unmodified $CH_4$-run SI engine. The effects could certainly attribute to the positive impacts on engine power pertaining to participation of the $H_2$-rich producer-gas in

improving the in-cylinder combustion [191], although with SSPG-blending the net heating value of the fuel reduced ([26], Table 3.1). Table 4.5 shows the deviation of the parametric statistical-based response of the RSM-optimizer model from the mathematical model response results after a confirmation run. The fine capability of the statistical-based prediction model to mimic the simulation outcomes is indicated by the minuscule tracking error of less than 2.4%.

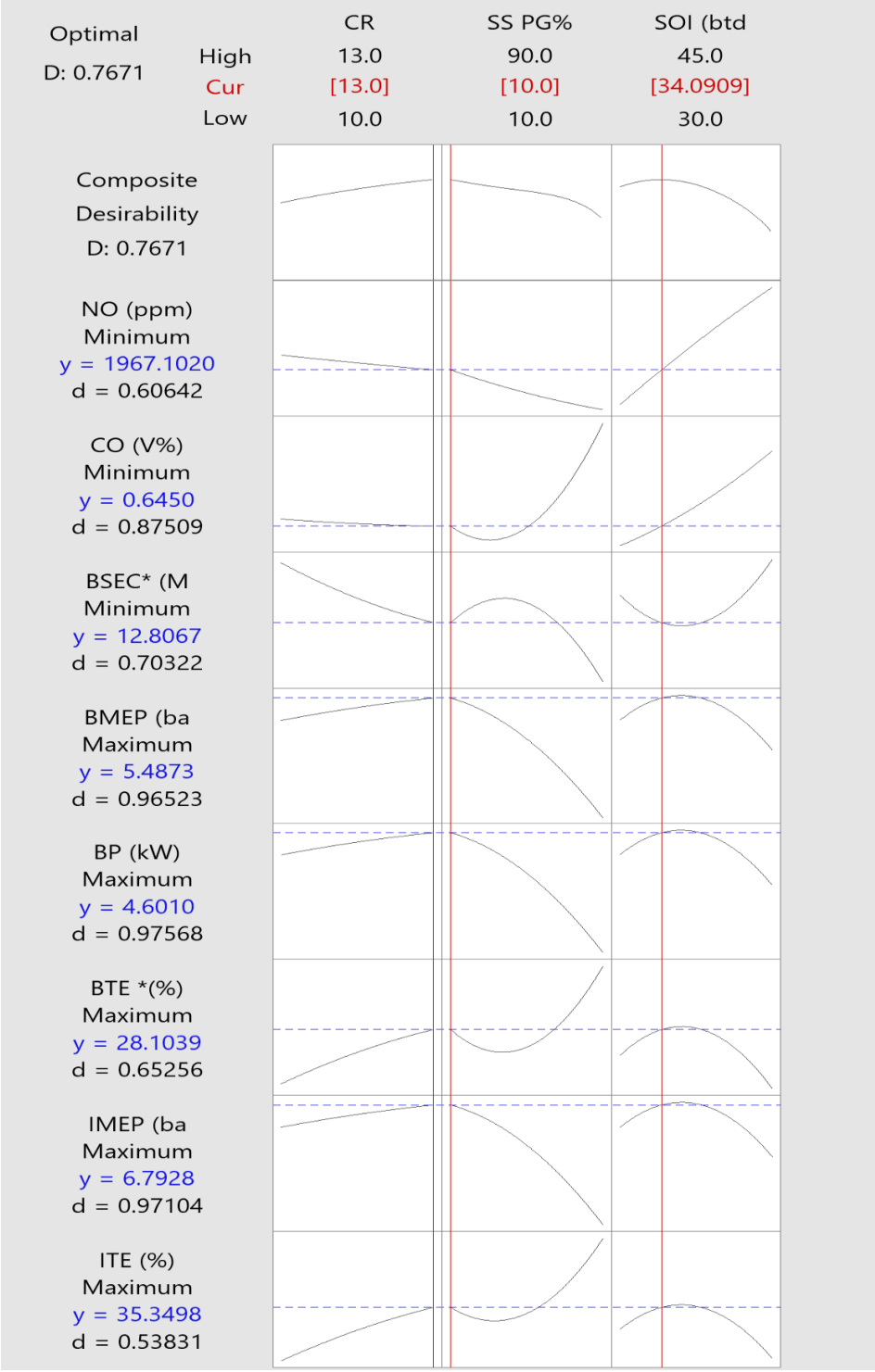


Figure 4.1.13. RSM optimizer plot

Table 4.5: Results from confirmation run at optimized input-levels

| Parameters | NO (ppm) | CO (V%) | BSEC (MJ/kWh) | BMEP (bar) | BP (kW) | BTE (%) | IMEP (bar) | ITE (%) |
|---|---|---|---|---|---|---|---|---|

| | | | | | | | | |
|---|---|---|---|---|---|---|---|---|
| Predicted statistical response | 1967.1 | 0.645 | 12.807 | 5.4873 | 4.601 | 28.10 | 6.793 | 35.349 |
| Numerical model values: | 1928.1 | 0.63 | 12.63 | 5.497 | 4.61 | 28.48 | 6.804 | 35.24 |
| Percentage deviation in %: | -2.02 | -2.38 | -1.4 | +0.176 | +0.19 | +1.33 | +0.161 | -0.31 |

The following major aspects were drawn from this analysis:

- The quasi-dimensional thermodynamic model has been successfully employed to simulate the performance and emission of the spark ignition engine. The findings of computational simulations are in good accord with data from the literature.
- According to the simulation results, sewage-sludge producer gas (SSPG) percentage and compression ratio (CR) have a substantial impact on the engine's performance.
- It is also found that the variable start of ignition (SOI) has a greater impact on emissions.
- The cumulative composite desirability was found to be 0.7671.
- The optimum magnitude of operating input parameters SSPG, CR, and SOI was found to be 10%, 13 and $34.09^0$ BTDC, respectively.
- The optimum values of ITE, IMEP, BTE, BP, BMEP, BSEC, CO, and NO were found to be 35.35%, 6.793 bar, 28.104%, 4.601 kW, 5.487 bar, 12.81 MJ/kWh, 0.645 V%, and 1967.102 ppm respectively
- ITE, IMEP, BTE, BP, BMEP, and BSEC are predominately affected by the SSPG and CR variation, whereas, CO and NO emissions are majorly affected by spark timing (SOI).

In summary, the thermodynamic model-based numerical method and subsequent data analysis through RSM optimization and ANOVA analysis revealed that the SI engine fueled with methane and PG blends enhances the performance and minimizes the exhaust emissions if the engine runs with the engine-optimized operating conditions.

## 4.2. Analysis with Miller Cycle strategy

For enhancing the effective sewage sludge-waste to end-use electricity generation by engine integration, this work aimed to simulate and investigate thermal efficiency enhancement for a specified SI engine model by employing variations in the Late inlet valve close (LIVC) strategy in the 12.0:1 geometrical compression ratio. This leads to the investigation of the Miller cycle-based engine performance investigation through the simulated approach. In order to effectively optimize the engine operating parameters in reference to the desired performance responses, variations in SSPG and $CH_4$ fuel blend proportions and suitable SOI timing were implemented and considered for optimization. A similar quasi-dimensional thermodynamic model is simulated to explore the SI engine performance outcomes, after validation from an experimental reference. Effects of blending SSPG to methane, varying LIVC, and spark timing were analyzed respective to ITE, IP, BTE, BP, and BSEC engine performance parameters, and the unstable emission constituents of CO and NO emissions. RSM technique was feasibly utilized towards identifying and analyzing the parametric trade-off nature respective to engine efficiency and power. The ANOVA-based regression model showed a composite desirability of 0.8 with 95% confidence level. In summary, the optimization method and optimal operation parameters prove significant for improving the engine performance when operating with the high CR input constraint and the miller cycle-based LIVC approach integrated engine performance model.

With the applied novelties, this analysis included the following mentioned objectives:

- To validate the QDTM modelling for accessing the LIVC-Miller Cycle strategy investigation.
- To access the benefits in efficiency through the Miller cycle strategy

- Analyze the impacts of the miller cycle on engine efficiency, energy efficiency, and unstable emission components of CO and NO.
- To inspect the sensitivities of influence of the three-factor parameters on the evaluated engine performance and emission responses
- Interception of the variations of each response parameter corresponding to the changes in each independent input parameter.
- To determine the ideal operating conditions through multi-objective optimization while utilizing the LIVC-based Miller cycle strategy.

### 4.2.1. Validation for BTE and CO, NO emission models

This generated QDTM-based simulation model was validated using the results from experimental data of ref.[49] and similarly tracing the pressure vs. crank angle (P-θ) data and BP outcomes with respect to differing PG-blend proportions in SSPG-$CH_4$ charge (particularly the 0V%, 20V%, 40V%, and 50V% SSPG mix with methane by volume). The P-θ results traced the experimental outcomes by less than 5% pressure outcome of the total range. The neat traces are observable in Figure 4.2.1**(A)**. The comparative depiction of the stated fuel blends in terms of BP versus the air-fuel relative ratios is again presented in Figure 4.2.1 (B,C,D) with respect to the modified and specific engine specifications. The figure ensured close tracing as the deviation was within 5%. 35º BTDC SOI, 10 CR, and ER 1 were considered fixed for this simulation program. Additional validations for NO and CO emission outcomes have also been presented via Table 4.6 and Figure 4.2.2, respectively. In these depictions as well, the maximum deviation in the simulation prediction extends within 5.5% and 9.2% of the maximum range. Thus, the QD model is considered to be verified despite of the appearance of minuscule deviations in prediction and is further applied to access the engine performance and emission outcomes when operating on SSPG-methane fuel blends while enabled with the LIVC-strategy of high geometric CR settings.

Table 4.6: Validation for NO

| PG-types | PG-composition | | | | | Experimental NO (g/kWh) | Simulated NO (g/kWh) | Deviation (g/kWh) |
|---|---|---|---|---|---|---|---|---|
| | $H_2$ | CO | $CH_4$ | $CO_2$ | $N_2$ | | | |
| A | 16 | 18 | 1 | 12 | 53 | 1.15 | 1.12 | 0.03 |
| B | 16 | 18 | 2.5 | 12 | 51.5 | 0.81 | 0.85 | -0.04 |
| C | 16 | 18 | 4 | 12 | 50 | 0.87 | 0.79 | 0.08 |

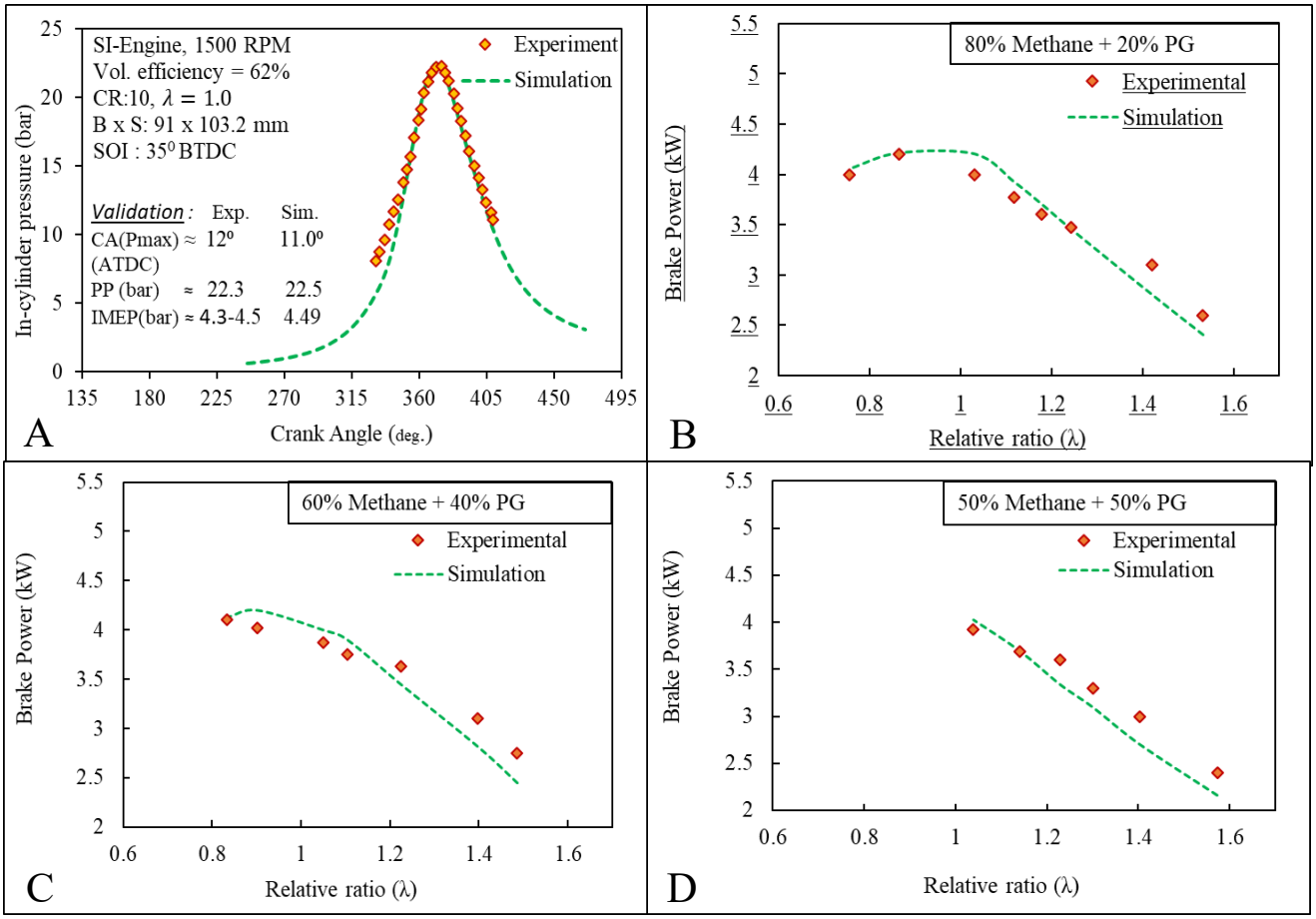


Figure 4.2.1. Simulated peak pressure and Brake power Validation

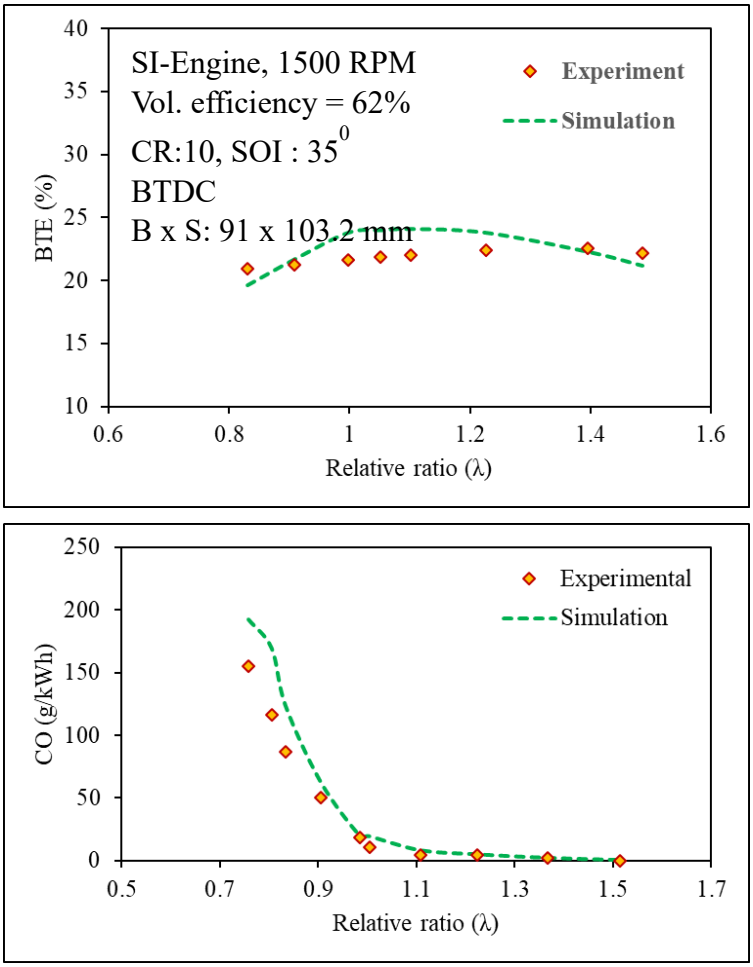


Figure 4.2.2. Efficiency and CO-emission validation

## 4.2.2. Quadratic and quartic Regression

The QDTM model and the statistical prediction model include four performances (ITE, IP, BTE, and BP), an energy efficiency term (BSEC), and two emissions (CO and NO) output parameters. The statistically developed regression models for each response are depicted in expressions: 64-70. The models were considered valid as the simulated outputs were intercepted very closely with the RSM predictions. This is observed in the prediction vs, actual plots in Figure 4.2.3. It was observed that though the quadratic regression models traced the actual outcomes very closely for performance parameters, the energy efficiency parameter of BSEC, and emission responses required the cubic regression model. By applying this, the

intersecting data points were observed precisely close to the diagonal line. Hence the RSM-developed regression models are considered valid for mimicking the QD model outcomes effectively [211] and suitable for RSM-based optimization.

$$ITE = -1.71860 - 0.079996 \times SSPG + 0.084290 \times LIVC + 1.81424 \times SOI + 0.000190 \times SSPG \times LIVC + 0.001467 \times SSPG \times SOI - 0.002170 \times LIVC \times SOI + 0.000349 \times SSPG^2 + 0.000293 \times LIVC^2 - 0.023415 \times SOI^2 \quad (64)$$

$$IP = + 1.93471 - 0.014181 \times SSPG + 0.010147 \times LIVC + 0.256651 \times SOI + 0.000055 \times SSPG \times LIVC + 0.000247 \times SSPG \times SOI - 0.000126 \times LIVC \times SOI - 0.000049 \times SSPG^2 - 0.000308 \times LIVC^2 - 0.003501 \times SOI^2 \quad (65)$$

$$BTE = - 9.10518 - 0.072607 \times SSPG + 0.157578 \times LIVC + 1.81414 \times SOI + 0.000090 \times SSPG \times LIVC + 0.001475 \times SSPG \times SOI - 0.002165 \times LIVC \times SOI + 0.000203 \times SSPG^2 - 0.000659 \times LIVC^2 - 0.023429 \times SOI^2 \quad (66)$$

$$BP = + 0.873576 - 0.014533 \times SSPG + 0.009634 \times LIVC + 0.256259 \times SOI + 0.000054 \times SSPG \times LIVC + 0.000251 \times SSPG \times SOI - 0.000123 \times LIVC \times SOI - 0.000046 \times SSPG^2 - 0.000305 \times LIVC^2 - 0.003503 \times SOI^2 \quad (67)$$

$$BSEC = + 13.01659 + 0.107162 \times SSPG + 0.149627 \times LIVC + 0.164915 \times SOI + 0.000288 \times SSPG \times LIVC + 0.001314 \times SSPG \times SOI - 0.004581 \times LIVC \times SOI - 0.003615 \times SSPG^2 - 0.001543 \times LIVC^2 - 0.012636 \times SOI^2 - 4.22230E\text{-}06 \times SSPG \times LIVC \times SOI - 2.58849E\text{-}07 \times SSPG^2 \times LIVC - 2.05003E\text{-}06 \times SSPG^2 \times SOI - 1.24869E\text{-}06 \times SSPG \times LIVC^2 - 0.000022 \times SSPG \times SOI^2 + 0.000017 \times LIVC^2 \times SOI + 0.000047 \times LIVC \times SOI^2 + 0.000028 \times SSPG^3 + 6.14583E\text{-}06 \times LIVC^3 + 0.000192 \times SOI^3 \quad (68)$$

$$CO = + 0.576675 + 0.003975 \times SSPG + 0.001207 \times LIVC - 0.018613 \times SOI - 0.000040 \times SSPG \times LIVC - 0.000090 \times SSPG \times SOI + 0.000066 \times LIVC \times SOI - 0.000037 \times SSPG^2 - 0.000031 \times LIVC^2 + 0.000682 \times SOI^2 + 4.51467E\text{-}07 \times SSPG \times LIVC \times SOI + 6.70077E\text{-}08 \times SSPG^2 \times LIVC + 3.56275E\text{-}07 \times SSPG^2 \times SOI + 1.32215E\text{-}07 \times SSPG \times LIVC^2 + 6.47533E\text{-}07 \times SSPG \times SOI^2 + 7.14286E\text{-}08 \times LIVC^2 \times SOI - 1.14286E\text{-}06 \times LIVC \times SOI^2 + 3.92889E\text{-}07 \times SSPG^3 + 1.25000E\text{-}07 \times LIVC^3 - 4.00000E\text{-}06 \times SOI^3 \quad (69)$$

$$NO = + 10339.61933 + 51.61569 \times SSPG + 20.66911 \times LIVC - 1032.20659 \times SOI + 0.026930 \times SSPG \times LIVC - 3.49191 \times SSPG \times SOI - 0.761664 \times LIVC \times SOI - 0.027127 \times SSPG^2 - 0.233922 \times LIVC^2 + 34.52541 \times SOI^2 - 0.000073 \times SSPG \times LIVC \times SOI + 0.000010 \times SSPG^2 \times LIVC + 0.000625 \times SSPG^2 \times SOI \quad (70)$$

$$- 0.000401 \times SSPG \times LIVC^2 + 0.050306 \times SSPG \times SOI^2 + 0.007024 \times LIVC^2 \times SOI + 0.004799 \times LIVC \times SOI^2 + 0.000036 \times SSPG^3 - 0.000173 \times LIVC^3 - 0.332843 \times SOI^3$$

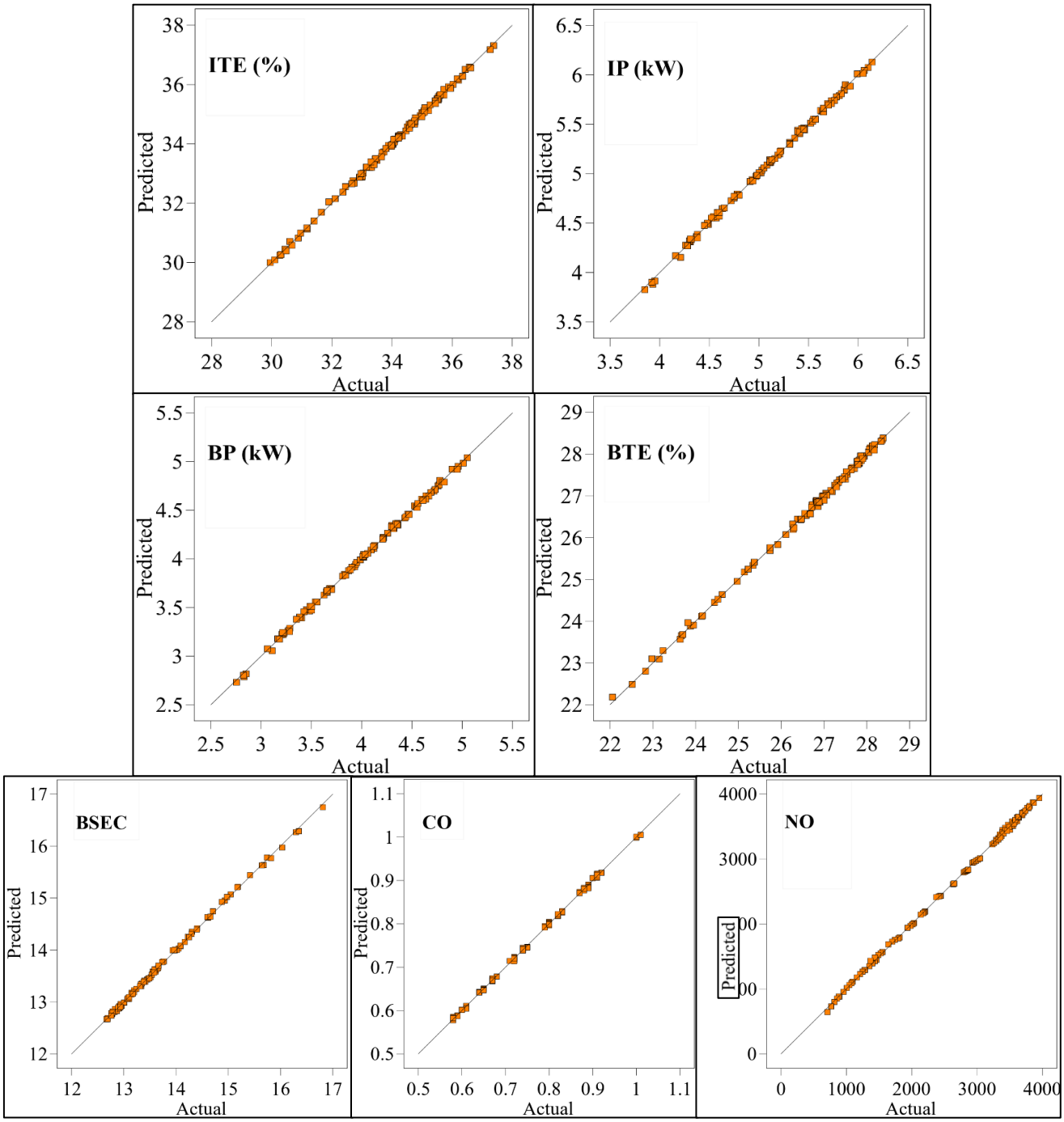


Figure 4.2.3. Modelled outputs vs. predicted response plots

### 4.2.3. ANOVA of the regression for trade-off sensitivity

ANOVA analysis assesses the goodness of fit for the RSM regression models[190]. Table 4.7 presents the ANOVA results for engine performance responses. As the p-value of the model and performance responses were less than 0.05 corresponding to the factors, the developed predictive model and the factors needed to be statistically significant. The significant impacts of considered inputs on engine performance and emissions, particularly for naturally aspirated IC Engines, have also been demonstrated in many previous literature [116, 212]. Considering linear-term interactions, the efficiency parameters (ITE and BTE) were influenced most by SOI, followed by LIVC variations pertaining to greater F-values. From the square-term interaction aspect, all the performance responses are evidently influenced the most by SOI variations.

Table 4.8 presents the ANOVA results for energy efficiency and emission responses. It is found that CO and NO responses are most influenced by SOI, followed by PG-blend variations, whereas the BSEC is influenced most by SSPG, followed by SOI variations contrarily. These contrary attributes might pertain to the dependency of these parameters on elementary molar fractions during chemical conversion and energy transformations [177, 180]. Along with F and p-values, the fit statistics were also added to these tables. For a consistent fit and effective response estimation, the predicted and adjusted $R^2$-values ($R_{pred}^2$ and $R_{adj}^2$) should differ by less than 0.2, with the $R_{adj}^2$ being closer to unity [191]. These constraints were observed to be abided. Further, for tracing of QD model with reliable preciseness, greater coefficient of determination ($R^2$)-values needed to be ensured [190, 191]. Greater $R^2$ values (minimum 0.998) were attained by assigning cubic regression models for BSEC, CO and NO responses, and the rest responses were assigned quadratic models.

Table 4.7: Performance parameters ANOVA analysis

| Source | df | ITE | | IP | | BTE | | BP | |
|---|---|---|---|---|---|---|---|---|---|
| | | F-value | p-value | F-value | p-value | F-value | p-value | F-value | p-value |
| **Model** | 9 | 8236.66 | < 0.0001 | 9313.31 | < 0.0001 | 9022.03 | < 0.0001 | 10470.65 | < 0.0001 |
| ***Linear*** | | | | | | | | | |
| A-SSPG | 1 | 6728.91 | < 0.0001 | 3378.39 | < 0.0001 | 1848.55 | < 0.0001 | 3877.03 | < 0.0001 |
| B-LIVC | 1 | 10465.34 | < 0.0001 | 66210.08 | < 0.0001 | 2097.76 | < 0.0001 | 74335.43 | < 0.0001 |
| C-SOI | 1 | 28482.15 | < 0.0001 | 6484.15 | < 0.0001 | 39010.09 | < 0.0001 | 7350.53 | < 0.0001 |
| ***Two-way interaction*** | | | | | | | | | |
| AB | 1 | 122.66 | < 0.0001 | 108.64 | < 0.0001 | 37.90 | < 0.0001 | 116.81 | < 0.0001 |
| AC | 1 | 1837.09 | < 0.0001 | 547.17 | < 0.0001 | 2522.97 | < 0.0001 | 634.65 | < 0.0001 |
| BC | 1 | 1160.74 | < 0.0001 | 41.12 | < 0.0001 | 1571.55 | < 0.0001 | 43.91 | < 0.0001 |
| ***Square*** | | | | | | | | | |
| $A^2$ | 1 | 851.28 | < 0.0001 | 174.54 | < 0.0001 | 391.84 | < 0.0001 | 174.25 | < 0.0001 |
| $B^2$ | 1 | 59.33 | < 0.0001 | 687.35 | < 0.0001 | 408.05 | < 0.0001 | 756.13 | < 0.0001 |
| $C^2$ | 1 | 23653.46 | < 0.0001 | 5557.12 | < 0.0001 | 32206.38 | < 0.0001 | 6241.65 | < 0.0001 |
| ***Fit Statistics*** | | | | | | | | | |
| $R^2$ | | 0.9988 | | 0.9989 | | 0.9989 | | 0.9990 | |
| Adjusted $R^2$ | | 0.9987 | | 0.9988 | | 0.9988 | | 0.9990 | |
| Predicted $R^2$ | | 0.9985 | | 0.9985 | | 0.9986 | | 0.9987 | |
| Adeq. Precision | | 363.1443 | | 370.7319 | | 359.2685 | | 393.5054 | |

Table 4.8: Energy efficiency and emission parameters ANOVA analysis

| Source | BSEC | | CO | | NO | |
|---|---|---|---|---|---|---|
| | F-value | p-value | F-value | p-value | F-value | p-value |
| **Model** | 5159.98 | < 0.0001 | 6715.55 | < 0.0001 | 7340.52 | < 0.0001 |
| ***Linear*** | | | | | | |
| A-SSPG | 7281.77 | < 0.0001 | 412.14 | < 0.0001 | 406.76 | < 0.0001 |
| B-LIVC | 62.23 | < 0.0001 | 2.35 | 0.1293 | 1.01 | 0.3172 |
| C-SOI | 2013.92 | < 0.0001 | 9225.21 | < 0.0001 | 15527.77 | < 0.0001 |
| ***Two-way interaction*** | | | | | | |
| AB | 88.57 | < 0.0001 | 4.07 | 0.0470 | 19.51 | < 0.0001 |
| AC | 3102.51 | < 0.0001 | 150.22 | < 0.0001 | 1654.40 | < 0.0001 |
| BC | 1895.76 | < 0.0001 | 0.6034 | 0.4396 | 519.69 | < 0.0001 |
| ***Square*** | | | | | | |
| $A^2$ | 4900.61 | < 0.0001 | 2272.29 | < 0.0001 | 0.3441 | 0.5591 |
| $B^2$ | 403.98 | < 0.0001 | 2.93 | 0.0906 | 0.1129 | 0.7378 |
| $C^2$ | 31705.86 | < 0.0001 | 351.52 | < 0.0001 | 2356.10 | < 0.0001 |
| ***Higher order interaction*** | | | | | | |
| ABC | 13.61 | 0.0004 | 12.98 | 0.0005 | 0.0053 | 0.9421 |
| $A^2B$ | 0.4198 | 0.5189 | 2.35 | 0.1295 | 0.0008 | 0.9773 |
| $A^2C$ | 6.58 | 0.0122 | 16.58 | 0.0001 | 0.7962 | 0.3749 |
| $AB^2$ | 3.33 | 0.0717 | 3.12 | 0.0813 | 0.4472 | 0.5056 |
| $AC^2$ | 64.37 | < 0.0001 | 4.67 | 0.0337 | 439.57 | < 0.0001 |

| | | | | | | |
|---|---|---|---|---|---|---|
| $B^2C$ | 42.58 | < 0.0001 | 0.0657 | 0.7984 | 9.91 | 0.0023 |
| $BC^2$ | 84.23 | < 0.0001 | 4.20 | 0.0436 | 1.16 | 0.2856 |
| $A^3$ | 6499.79 | < 0.0001 | 109.31 | < 0.0001 | 0.0143 | 0.9050 |
| $B^3$ | 12.00 | 0.0009 | 0.4139 | 0.5219 | 0.0123 | 0.9118 |
| $C^3$ | 183.51 | < 0.0001 | 6.62 | 0.0119 | 714.85 | < 0.0001 |
| ***Fit Statistics*** | | | | | | |
| $R^2$ | 0.9992 | | 0.9994 | | 0.9994 | |
| Adjusted $R^2$ | 0.9990 | | 0.9992 | | 0.9993 | |
| Predicted $R^2$ | 0.9986 | | 0.9990 | | 0.9990 | |
| Adeq. Precision | 302.9974 | | 290.0071 | | 279.0127 | |

## 4.2.4. Parametric response impacts study

Response of each considered output parameter to the simultaneous variations in three input parameters for the SI engine-simulation model is demonstrated and discussed in the following sections using RSM-developed 3D contour and surface plots. The average of input-variables parametric range is considered as the hold value for the corresponding 3D plots.

***4.2.4.1.*** Indicated thermal efficiency (ITE)

ITE is the ratio of indicated power to the calorific value of consumed fuel rate [133]. Figure 4.2.4 presents the effects of simultaneous input variations on the ITE output. It is observed that increasing PG-fraction or LIVC results in a gradual ITE increase, by a minimum of 3.24% and 5.15%, respectively. These respective effects could be attributed to improved combustion with an increase in PG-fraction and an increase in relative over-expansion[213]. With the increase in SSPG%, the $H_2$ and CO- composition at the intake also rises, thus resulting in improved combustion and increased power-conversion efficiency [48]. A typical ITE variation is observable respective to increasing SOI [116, 214], where ITE initially increases till 35º-40º SOI, and then decreases. Overall, the surface plots indicate that increased PG blend and LIVC settings potentially result in superior ITE outcomes at an optimized SOI. Maximum modelled ITE of 37.38% resulted at peak of considered PG-blend(75%), max LIVC(90º), and 35º SOI. This is collinear with the surface-plot depictions. At hold values of 70º LIVC, contour plots in Figure 4.2.4 imply that high ITE responses (>34%) result at preferably greater SSPG-fraction,

and the simultaneous LIVC greater than 60º ABDC, with SOI ranging between 30º to 45º BTDC.

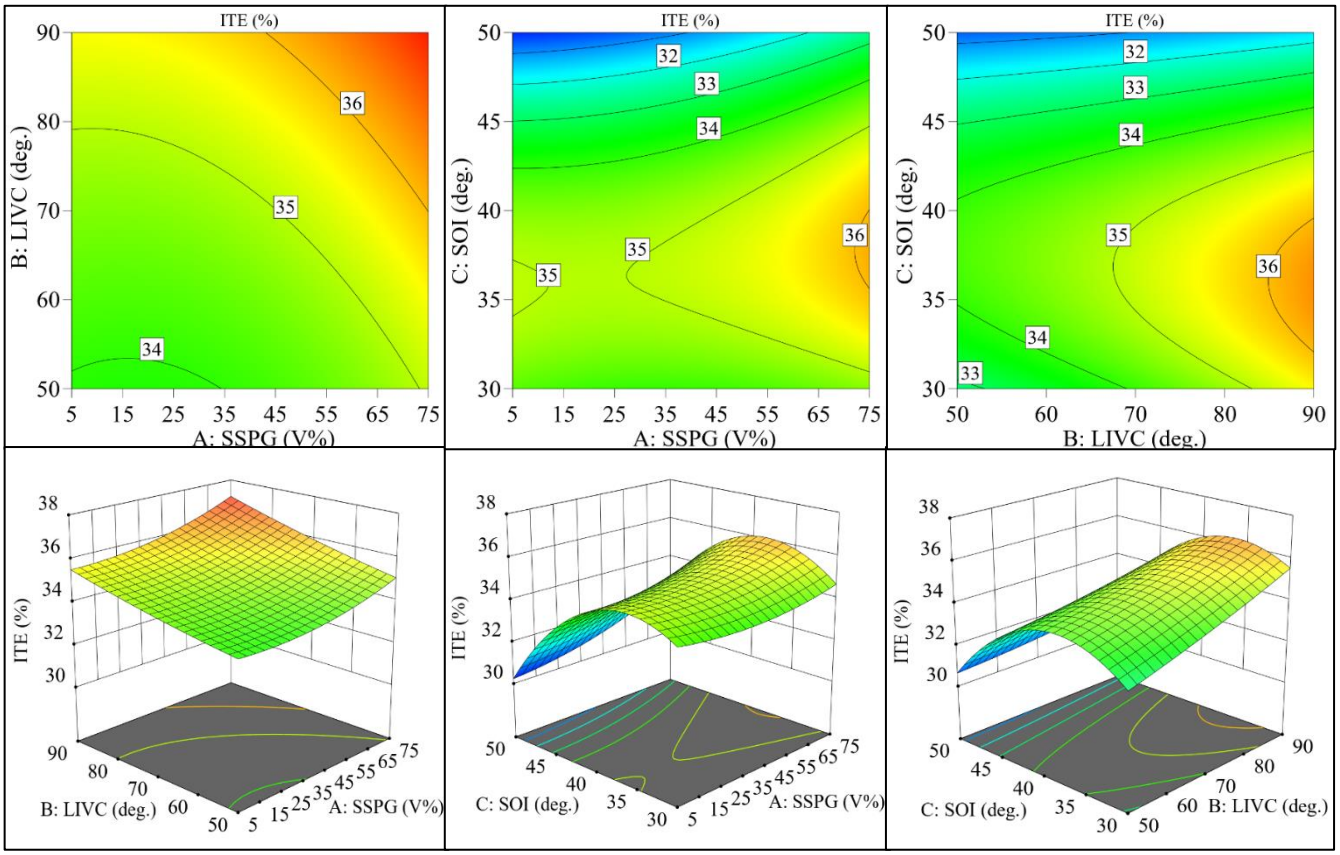


Figure 4.2.4. Effects on ITE

***4.2.4.2.*** Indicated Power

Indicated Power (IP) is defined as the power developed at the piston of the IC engine [39]. Effects of simultaneous input variations on IP are presented in Figure 4.2.5. It is observed that, unlike ITE, IP exhibits a gradual decline (by min. 5.7% at 50º LIVC) with increasing SSPG%. This could pertain to a lower CV of the PG than methane, as also mentioned in [39]. IP is also observed to decrease with increasing LIVC, by a minimum of 24.83%, which might pertain to the decreasing volumetric trapped charge inside the cylinder with the increase of LIVC. A low fuel-air charge ultimately reduces net heat release and output power [128]. The tradeoff between ITE and IP respective to SSPG% and LIVC variations demands optimization to obtain better results. Around 30º to 45º SOI range is observed to exhibit better IP, which indicates the

development of suitable high-pressure and temperature conditions for quicker flame propagation. This possibly results in better combustion and increased power as stated in [39]. Surface plots specify that lower PG-blend and LIVC, alongwith optimum SOI should exhibit better IP. Justifying this depiction, maximum simulated IP output of 6.06 kW, was obtained for 25% blend, 50º LIVC and 35º SOI. Contours convey that greater IP values (>5.2 kW) certainly result at simultaneous SSPG% less than 55%, LIVC not more than 70º (aBDC) and SOI-operating close to 35º-40º range.

***4.2.4.3.*** Brake thermal efficiency

BTE is a vital performance metric to evaluate and compare the fuel-to-power conversion in an IC engine operation [80]. Figure 4.2.6 shows the impacts of simultaneous input variations on BTE. The surface plots approve ANOVA reports of minimal BTE influence by simultaneous two-way interaction of SSPG and LIVC. With a full range increase in SSPG and a simultaneous decrease in LIVC inputs, the BTE demonstrates a maximum increment of only around 4.7%. On the other hand, with the increase in SOI, the BTE initially increases to 28.36% and then decreases by 10.7%. The peak BTE is also observable at around 35º~40º SOI range for any SSPG-blend. From contour plots, SSPG decrease and LIVC increase are observed to shift the peak BTE towards lesser SOI advance. This is probably attributed to the increased fraction of methane and the consequent increase in flame speed while the trapped fuel-air charge decreases with the LIVC increase. This results in faster combustion complete, low heat release [39, 107, 109], and decreased requirement for SOI advance. The 3D plots specify that SSPG-fractions away from 15-25%, lesser LIVC, and SOI inputs being close to 35º-40º SOI exhibit better BTE response. A maximum BTE of 28.38 % was found for 75% SSPG, 60º LIVC, and 40º SOI, which justifies the above-depicted statistical report.

***4.2.4.4.*** Brake power

The net power available at the crankshaft is Brake power(BP) [202]. Figure 4.2.7 depicts the effects of simultaneous input variations on BP. According to the 3D-surface plots, BP gradually decreases with increasing SSPG-fraction by a minimum of 6.12% at 90º LIVC. This effect is due to the low CV of PG than methane [39]. The BP trend is slightly similar to that of IP, pertaining to their representation of engine power at different engine ends. Further, LIVC increase is observed to significantly decrease BP-response, by a max. 33.7% at least SSPG% and SOI input. This effect is associated with the diminishing trapped charge with increasing LIVC [128]. A tradeoff nature for better ITE and BP also needed optimization corresponding to SSPG% and LIVC inputs. For any SSPG% or LIVC, the BP is observed to peak at the 35º~40º SOI range. Contour plots reflect that lower SSPG%, low LIVC settings, and 30º~40º SOI input settings could potentially result in better BP. At a simultaneous 25% SSPG, 50º LIVC (ABDC), and 35º SOI (BTDC), a maximum BP output of 4.96 (kW) was achieved. As per contours greater BP (>4 kW) was achievable for any SSPG%, when the LIVCs were less than 70º, and SOIs were close to 40º.

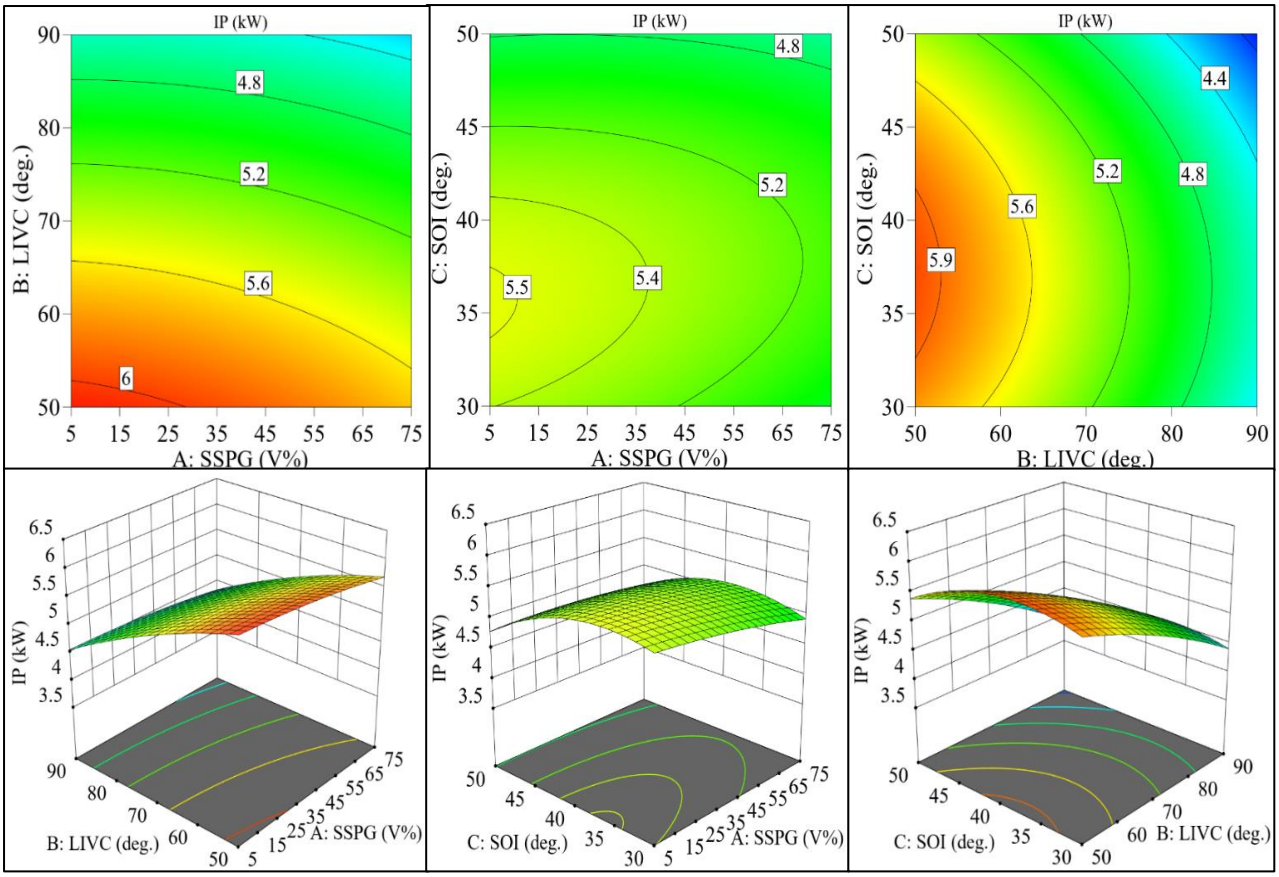


Figure 4.2.5. Effects on IP

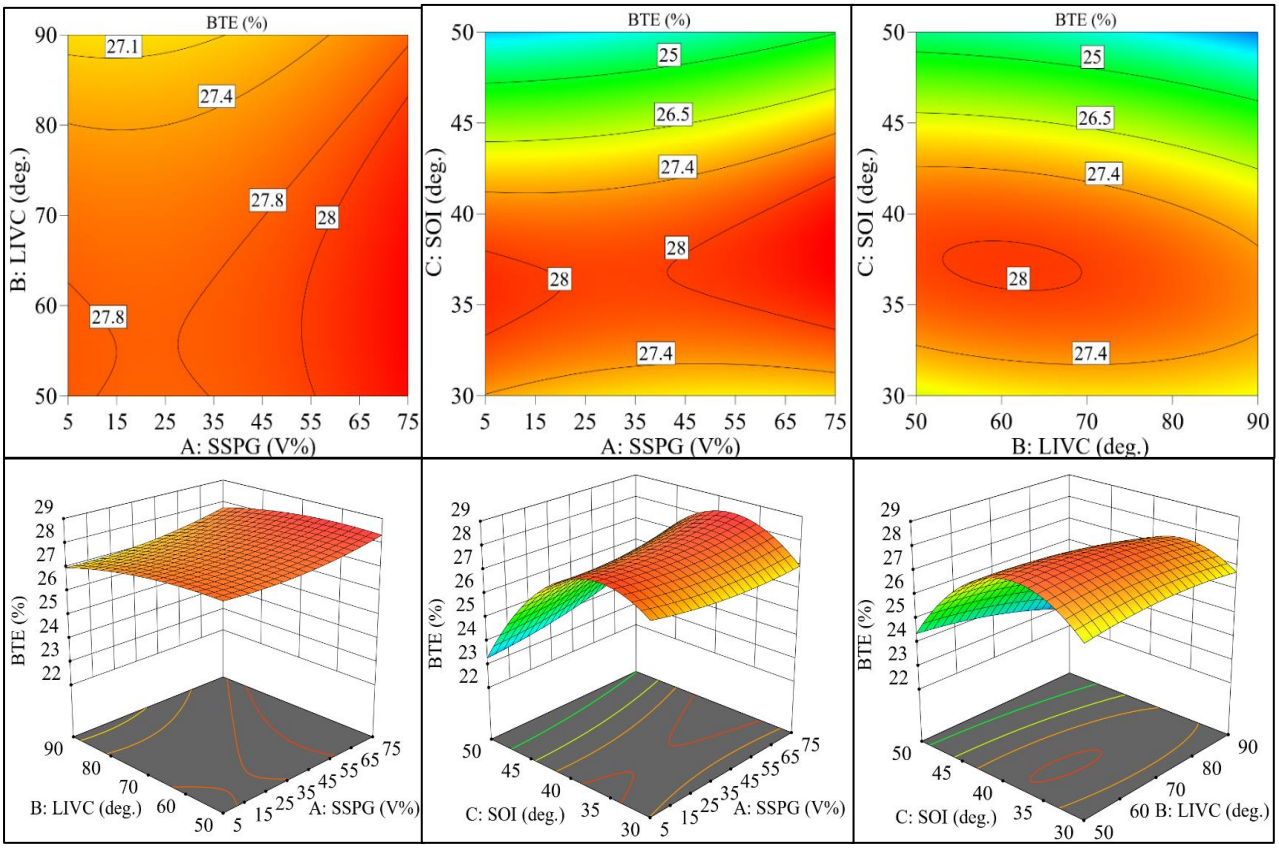


Figure 4.2.6. Effects on BTE

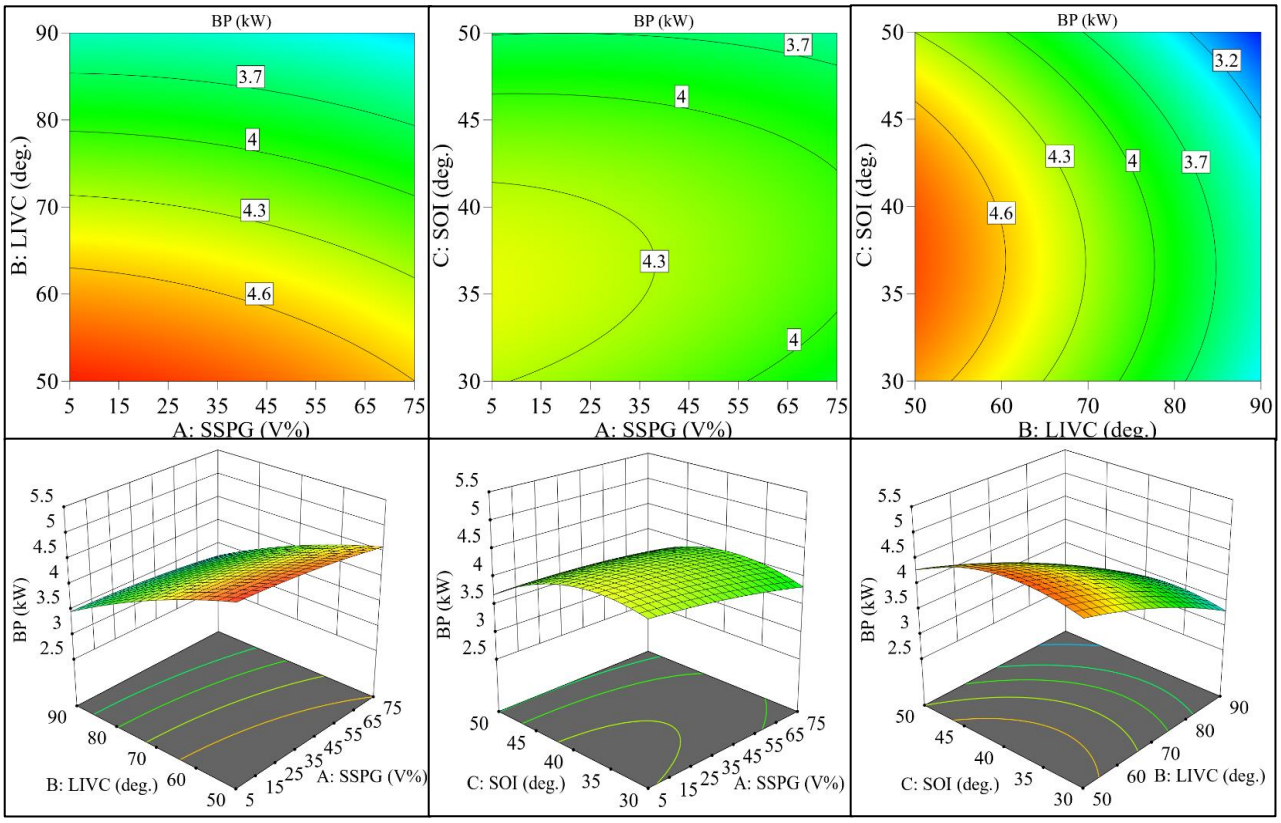


Figure 4.2.7. Effects on BP

***4.2.4.5.*** Brake-specific energy consumption

The parameter of brake-specific energy consumption (BSEC) is considered in this research as it utilizes two unlike gaseous fuel mixtures: methane and SSPG, that possess varying energy densities [134, 135]. Figure 4.2.8 presents the effects of simultaneous input variations on BSEC. The product of net calorific value for a specific fuel blend and BSFC provided the BSEC outcome response [189]. It is theoretically inversely proportionate to BTE[135]. Thus, an inverse trend of BTE could be verified for BSEC from the plots depicting simultaneous input variations. For a major portion of SSPG-increase, the BSEC is observed to decrease for any LIVC input (maximum decrease of around 8% at 70º LIVC). Improved combustion at greater SSPG-blend proportions might be attributed to BSEC decrements [48]. Further, for any LIVC or SSPG inputs, attributing to better performance at 35º-40º SOI range, the BSEC response simultaneously minimizes at this range. Better performance of methane-fueled engines at this

SOI range was also typical in some previous studies [116, 215]. 3D plots indicate that PG-blends away from the 15~35(V%) range, LIVC closer to 60º~70º (ABDC), and an optimized SOI should lessen BSEC. At 25% SSPG-blend, 60º and 70º LIVC, and 35º SOI minimum BSFC of 0.383 kg/kWh was attained from simulation.

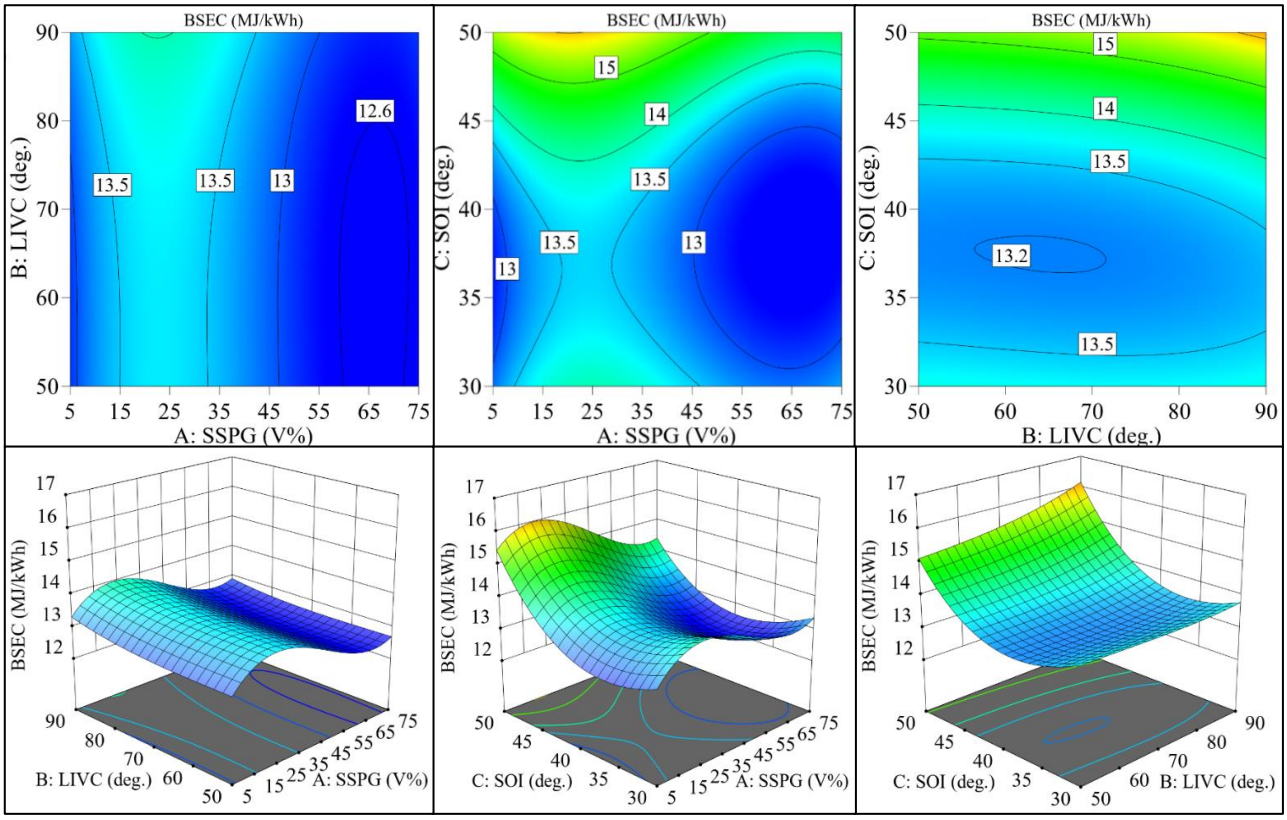


Figure 4.2.8. Effects on BSEC

***4.2.4.6.*** Carbon mono-oxide emission

Emissions of CO from I.C. Engines primarily indicate incomplete combustion and how far a mixture departs from the stoichiometric state [153, 207]. Thus, its inspection could potentially decipher the combustion quality of the intake blended fuel composition. Figure 4.2.9 shows the CO emission response respective to simultaneous input variations. Surface plots indicate that the CO emissions increase slightly, by at least 13.4%, with an SSPG% increase. SSPG possibly utilizes more available oxygen pertaining to wider flammability limit-cum-lower auto-ignition temperature and thereby deprives the methane and remaining charge from complete

combustion [201], more heat release and work output. CO emission is also observed to significantly increase with SOI increment (by a minimum of 50.8%). This conventional trend is also reported in [195], which occurs as beyond a threshold SOI level the peak in-cylinder temperature and pressure drops, leading to incomplete combustion and CO-increase [116]. Overall, as depicted in model results and 3D plots, at low SSPG-blend (<45%), SOI (<40º), and preferably greater LIVCs (70º, 80º and 90º), lesser CO emission results (less than 0.74 (V%).

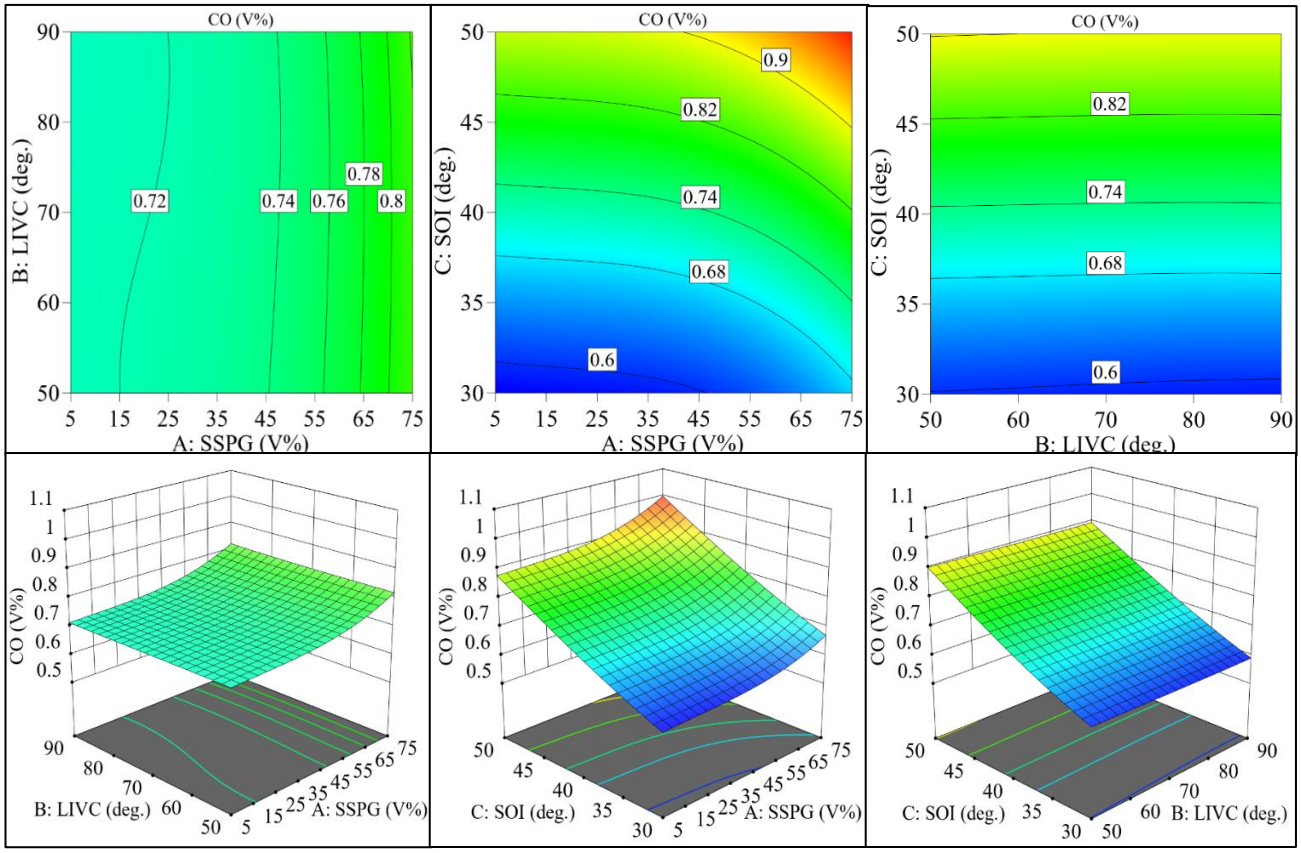


Figure 4.2.9. Effects on CO-emissions

***4.2.4.7.*** Nitrogen mono-oxide emission

Though nitrogen is an inert gas at room temperature, it can oxidize readily at temperatures over $1100^0$C[208], and form nitrogen oxides [209]. Due to oxygen scarcity, low temperature, or dissociation at greater chamber temperatures, formation of the unstable and harmful NO-emissions could upsurge[216]. Figure 4.2.10 presents the NO-variation respective to

simultaneous input variations. With the increase of SSPG%, the NO-emission is observed to linearly decrease gradually, by a minimum of 12.53% at the simultaneously applied least LIVC and SOI inputs. This effect could be attributed to greater SSPG participation in combustion and thereby liberating lesser heat (due to lesser CV of SSPG [39]), which lowers in-cylinder temperature while hindering complete combustion. Thus, NO decreases in tradeoff to the CO emission, which increased respective to SSPG-fraction, thereby signifying multi-objective optimization for optimal declaration. NO emission is also observed to significantly increase with SOI increase (maximum of 78.8%). This happens because advancing the combustion inception simultaneously increases in-cylinder temperature following the early and accumulative heat release[116]. 3D response plots indicate that greater SSPG-blending and

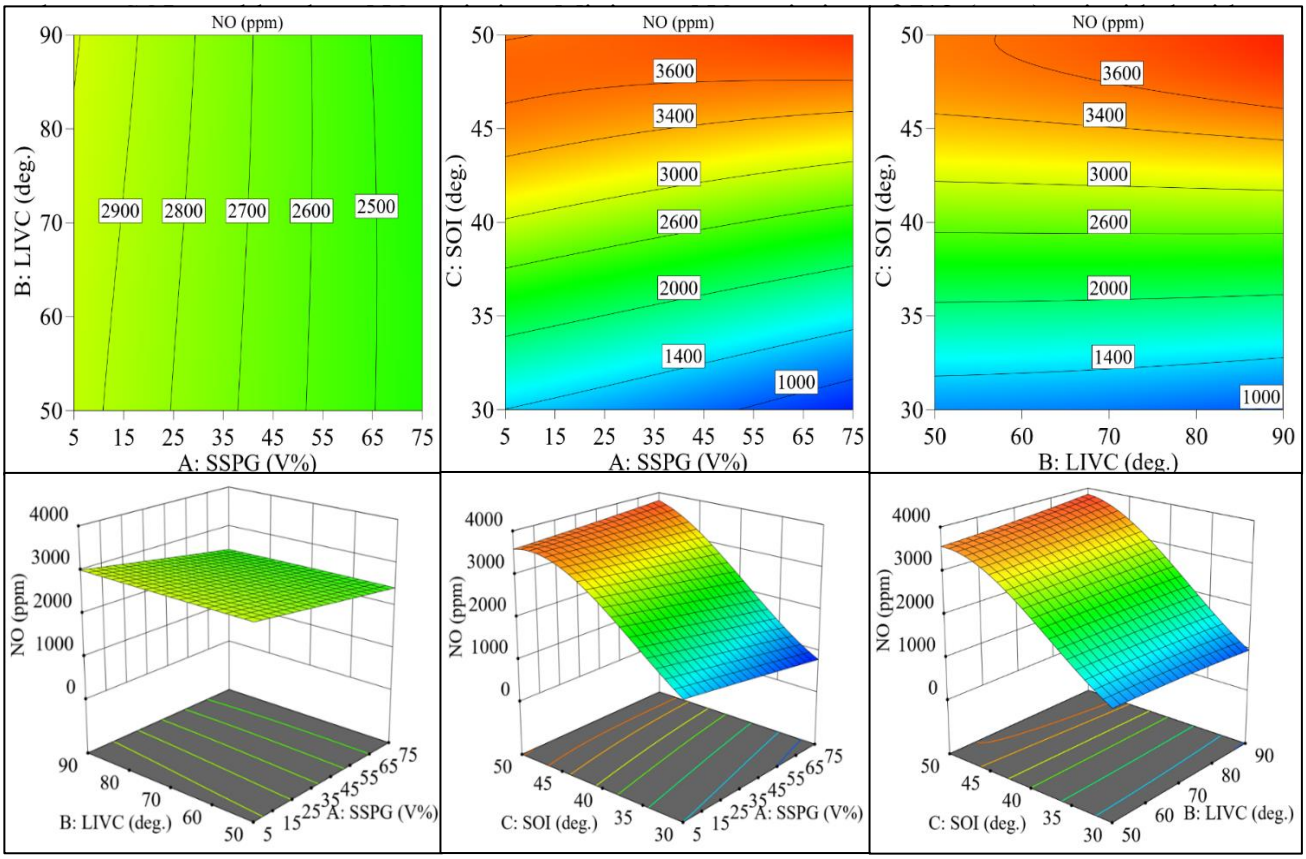


Figure 4.2.10. Effects on NO-emissions

### 4.2.5. Optimization results and findings

For the defined configurations listed in Table 4.9, multi-objective optimization was executed by the RSM approach through Design-Expert-13 software. The optimal outcome of the greatest composite desirability is presented in ramp-view mode in Figure 4.2.11 along with the individual and combined desirability values. The combined (or composite) desirability, D (shown as 'Desirability' in the figure) for the obtained optimum results was 0.800743 (≈0.801). Typically, a result with D more than 0.7 and a minimum $R^2$-value of 80% (0.8) is considered acceptable [217]. As the mentioned constraints are attained, the RSM depiction of the simulation model is adequate. In Figure 4.2.11, the left and right ramp-limit vertical lines inside each parameter box indicate the lower and upper limits (minimum and maximum values, respectively) of each parameter. The positive and negative slopes inside the parametric boxes indicate the set maximize and minimize goals of response parameters (Table 4.9), respectively. Further, the observed red and blue points on the ramps indicate the optimum value position for the input and output parameters, respectively. The observed optimum operating inputs were 64.703% SSPG, 70.329º LIVC (ABDC), and 34.03º SOI (BTDC). The correspondingly obtained optimum response parameters were 35.466% ITE, 5.176(kW) IP, 27.948% BTE, 4.08(kW) BP, 12.671(MJ/kWh) BSEC and emissions of 0.688(V%) CO, and 1456.93(ppm) NO, respectively. Additionally, Table 4.10 presents the confirmation run outcomes for verifying the RSM-predicted optimum response accuracy with the actual simulation results at optimum. The calculation showed less than a 3.5 % validation error and close confirmation of the regression-based statistical prediction model.

Table 4.9: Optimizer Constraints

| Parameters | Units | Goal | Lower limit | Upper Limit | Regression order | Importance |
|---|---|---|---|---|---|---|
| Inputs: | | | | | | |

| | | | | | | |
|---|---|---|---|---|---|---|
| SSPG | % | in range | 5 | 75 | - | 3 |
| LIVC | º ABDC | in range | 50 | 90 | - | 3 |
| SOI | º BTDC | in range | 30 | 50 | - | 3 |
| Output: | | | | | | |
| ITE | % | maximize | 29.95 | 37.38 | Quadratic | 4 |
| IP | kW | maximize | 3.85 | 6.14 | Quadratic | 1 |
| BTE | % | maximize | 22.06 | 28.38 | Quadratic | 4 |
| BP | kW | maximize | 2.756 | 5.05 | Quadratic | 1 |
| BSEC | MJ/kWh | minimize | 12.668 | 16.811 | Cubic | 3 |
| CO | % V. | minimize | 0.58 | 1.01 | Cubic | 3 |
| NO | ppm | minimize | 711.5 | 3951.2 | Cubic | 3 |

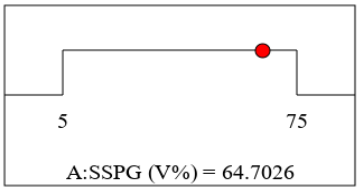


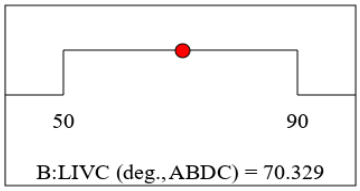


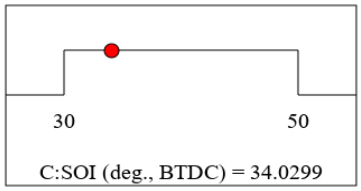


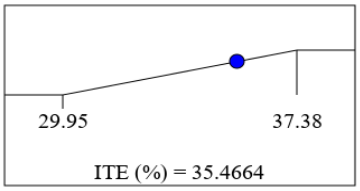


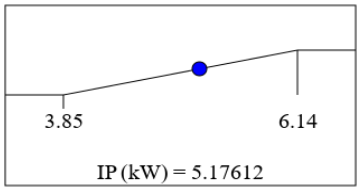


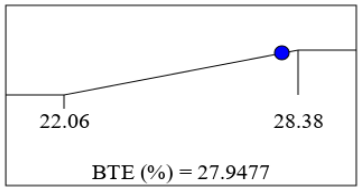


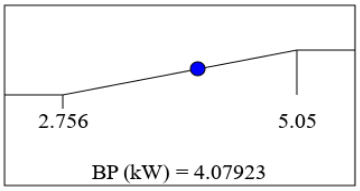


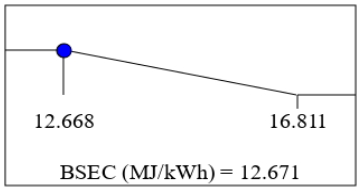


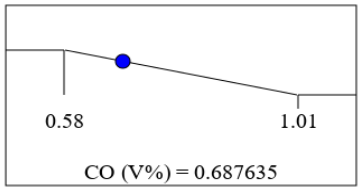


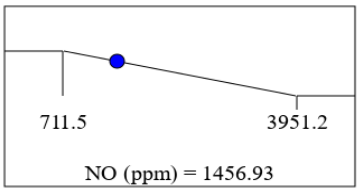


Desirability = 0.801

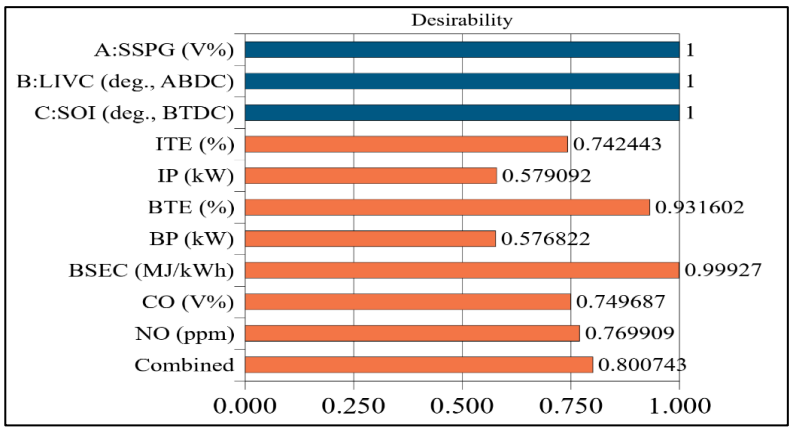

Figure 4.2.11. Optimized results and corresponding desirability values

Table 4.10: Optimum responses and confirmation run

| **Parameters** | **ITE (%)** | **IP (kW)** | **BTE (%)** | **BP (kW)** | **BSEC (MJ/kWh)** | **CO (V%)** | **NO (ppm)** |
|---|---|---|---|---|---|---|---|
| Predicted optimum responses: | 35.46 | 5.17 | 27.95 | 4.079 | 12.771 | 0.687 | 1456.93 |
| Simulation-model results: | 35.33 | 5.18 | 27.87 | 4.08 | 12.912 | 0.68 | 1440.2 |
| Maximum: | 37.38 | 6.14 | 28.38 | 5.05 | 16.811 | 1.01 | 3951.2 |
| Minimum: | 29.95 | 3.85 | 22.06 | 2.756 | 12.668 | 0.58 | 711.5 |
| Deviation in predictions (%): | +1.7% | -0.4% | 1.3% | -0.04% | -3.4% | +1.6% | 0.5% |

Although this LIVC Miller Cycle-based investigation improved the thermal efficiency, the statistically determined optimal BP (4.079 kW) verifies to be comparable with the BP trends (within 3.95 kW to 4.1 kW) that are presented in the experimental investigations of Szwaja et al. [49], which considered similar engine configurations and methane-SSPG fuel blends. Moreover, the RSM-determined optimal BTE (27.95%) improved from the experimentally verified BTE outcome (as 21.1%~21.8%). This possibly pertains to the consideration of higher optimal blend fraction for SSPG (64.7V% SSPG) in this Miller Cycle-intact investigation. Similar to the previous investigation, a comparative analysis among the SSPG-blend fueled (60V%) simulated engine performances and the neat methane-based unmodified SI Engine performance (depicted in Ref-[49]) was performed. The comparison reveals that the LIVC-implemented Miller Cycle -based operation could significantly improve the engine BTE. The improvement corresponding to the SSPG-blended methane-fuelled unmodified SI Engine could potentially be as much as 27.4%. This improvement sould certainly attribute to positive engine efficiency impacts pertaining to consideration of the Miller Cycle-based increased effective CR [153]. The significant findings of this simulated analysis are as follows:

- A trade-off pattern between thermal efficiency (ITE) and output powers (IP, BP) was observed for varying SSPG and LIVC input parameters.
- Maximum BTE of 28.38% and ITE of 37.38% are attained at separate lateness values of IVC.
- An ignition timing (SOI) close to the obtained optimum would result in better engine performance efficiency as well as greater power output.
- A trade-off pattern between carbon mono-oxide(CO) and nitrogen mono-oxide(NO) emissions was also noticeable with respect to SSPG variations.
- Through RSM-based multi-objective optimization, 64.7% SSPG%, 70.33º (CA-ABDC) LIVC, and 34.03º (CA-BTDC) SOI were found as optimum operating inputs.
- The corresponding optimum response values were: 36.46% ITE, 5,17(kW) IP, 27.94% BTE, 4.08(kW) BP, 12.671(MJ/kWh) BSFC, and emissions of 0.688(V%) CO with 1456.93(ppm) NO.
- Though LIVC was introduced to enhance performance efficiency, its variations were observed to lay greater influence on engine power (IP, BP) as evident from ANOVA analysis.
- CO and NO emissions are found to be most influenced by SOI variations.

Overall, the numerical thermodynamic-based model and the subsequent data analysis through ANOVA analysis and RSM optimization revealed that the methane and PG blends-fuelled SI engine enhances performance and minimizes exhaust emissions if the engine runs close to the optimized operating conditions.

## 4.3. Analysis with Intake-boosting

An appealing alternative solution for lowering both reliance on the power grid and pollution is by adopting decentralized power generation using gasifier-engine integrated systems. However, the utilization of gasification-derived producer gas (PG) leads to low engine power output and efficiency as compared to conventional fuels. This pertains to its low Calorific value (CV) and low flame speed. Therefore, this simulation study aimed to simulate and investigate the improvements in these parameters by inspecting various boosted-intake pressures and blends of high-CV methane with PG as inputs along with the implementation of boosted Pressure at intake valve closure (PIVC) and Late inlet valve close (LIVC)-Miller cycle strategy on a 1500 RPM Dual-fuel(DF) SI engine model. Quasi-dimensional thermodynamic modelling (QDTM) was applied to simulate this performance and emission investigation by considering Sewage sludge-based PG (SSPG) as the PG variant. Best operational input settings were found using the Response Surface Methodology (RSM)-based multi-objective optimization. With the ANOVA-based analysis and the desirability approach in the RSM-based optimization, an optimum input setting to enhance efficiency and power while quantifying emissions decrease was achieved following a 95% confidence level-set statistical optimization model.

Thus, through the novel numerical methodology, the following potential objectives were anticipated to be addressed.

- Validation for integration of thermodynamic power cycle modelling, coupled with the two zone-based turbulent flame propagation and a fundamental heat transfer sub-model principles into the QDTM simulation for inspecting intake boosting.
- Verification of the empirically calibrated polynomial coefficients and functions for assessing the internal energy variation of reactant and exhaust species.
- Nobility is also extended towards optimizing intake-boosting, Miller cycle limits, and PG-blending ranges by using the RSM through the desirability approach.

- The extent of energy efficiency enhancements, fuel-saving, and low NO emissions reduction from an unmodified SI engine of 12 geometrical compression ratio Miller cycle was also inspected.

## 4.3.1. Model validation (performance, emissions)

***4.3.1.1.*** Flame speed calibration coefficients

The calibrated constants used in assessing the flame propagation velocities have been presented in Table 4.11. Here, the flame speed for PG are independent of the considered Equivalence ratio (ER), whereas the flame speeds for methane fuel are considered a function of the ER (0.8 for this analysis). However, for both the fuel components the flame speed is considered a function of temperature in the simulation model.

Table 4.11: Laminar flame-speed computational constants

| **Constants** | **particular to PG** | **particular to Methane gas** |
|---|---|---|
| $\alpha_T$ | 2.0 | $5.75\phi^2 - 12.15\phi + 7.98$ |
| $\beta_P$ | -0.4 | $-0.925\phi^2 + 2\phi - 1.473$ |
| $S_{l0}$ | $0.56-0.827(Ø-1.186)^2$ | $-177.43\phi^3 + 340.77\phi^2 - 123.66\phi - 0.0097$ |

***4.3.1.2.*** Model Validation

The adopted QDTM-simulation model is validated using experimental findings from ref-[49]. For validation, first, the engine specifications were configured identically to the referred experimentation. The particular engine specifications are presented in Figure 4.3.1 as well. The trace of simulated in-cylinder pressures is plotted simultaneously with the experimental outcomes corresponding to the crank angles(θº CA) in Figure 4.3.1. The deviation in the simulated Peak pressure (PP) is inspected to be less than 1.03% for crank angles ranging within 0.8º CA., The PP position from TDC has significant effects on net-work output and towards achieving the maximum brake torque [218]. As the experimental results are prone to frequent

misfiring, the pressure tracings of higher magnitude were again recorded for validation. The simulated in-cylinder peak pressure accurately matches the experimental outcomes, whereas minuscule deviations were observed at the early compression stage only. The maximum deviations were within 4% and possibly attributed to the modelling assumption of homogeneous intake charge[66]. Figure 4.3.2 confirmed validation with respect to the QDTM-based BP outcomes for different relative methane blends and air-fuel ratios. With a satisfactory degree of closeness in the traced experimental outcomes, the QDTM simulation model is considered valid for predicting the engine performance respective to different levels of engine intake boosting (PIVC), SSPG-Methane blending (SSPG), and LIVC inputs. The validations for the CO and NO emission outcomes have emerged similar to the previous analysis case and have been presented at Figure 4.3.3 and Table 4.12, thus also confirming the nature of combustion.

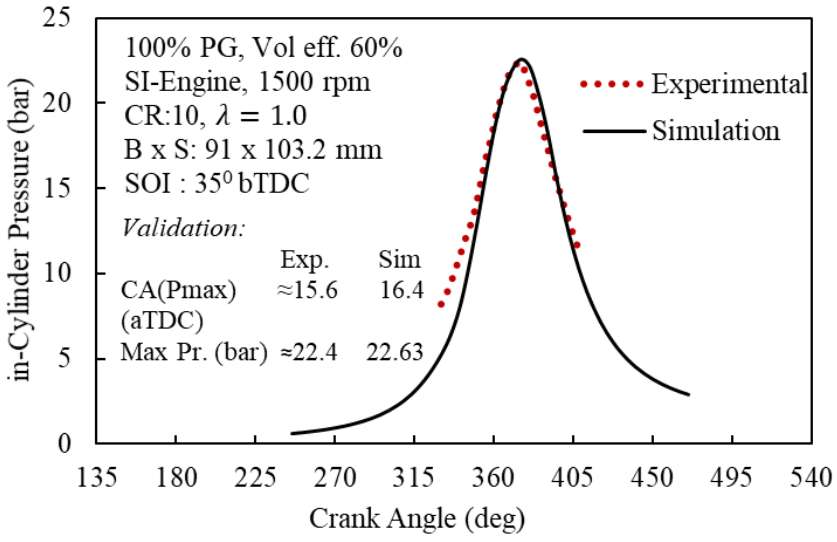


Figure 4.3.1. Pressure vs crank angle plots for model validation

Table 4.12: Validation for NO

| PG-types | PG-composition | | | | | Experimental NO (g/kWh) | Simulated NO (g/kWh) | Deviation (g/kWh) |
|---|---|---|---|---|---|---|---|---|
| | $H_2$ | CO | $CH_4$ | $CO_2$ | $N_2$ | | | |
| A | 16 | 18 | 1 | 12 | 53 | 1.15 | 1.12 | 0.03 |
| B | 16 | 18 | 2.5 | 12 | 51.5 | 0.81 | 0.85 | -0.04 |

| | | | | | | | | |
|---|---|---|---|---|---|---|---|---|
| C | 16 | 18 | 4 | 12 | 50 | 0.87 | 0.79 | 0.08 |

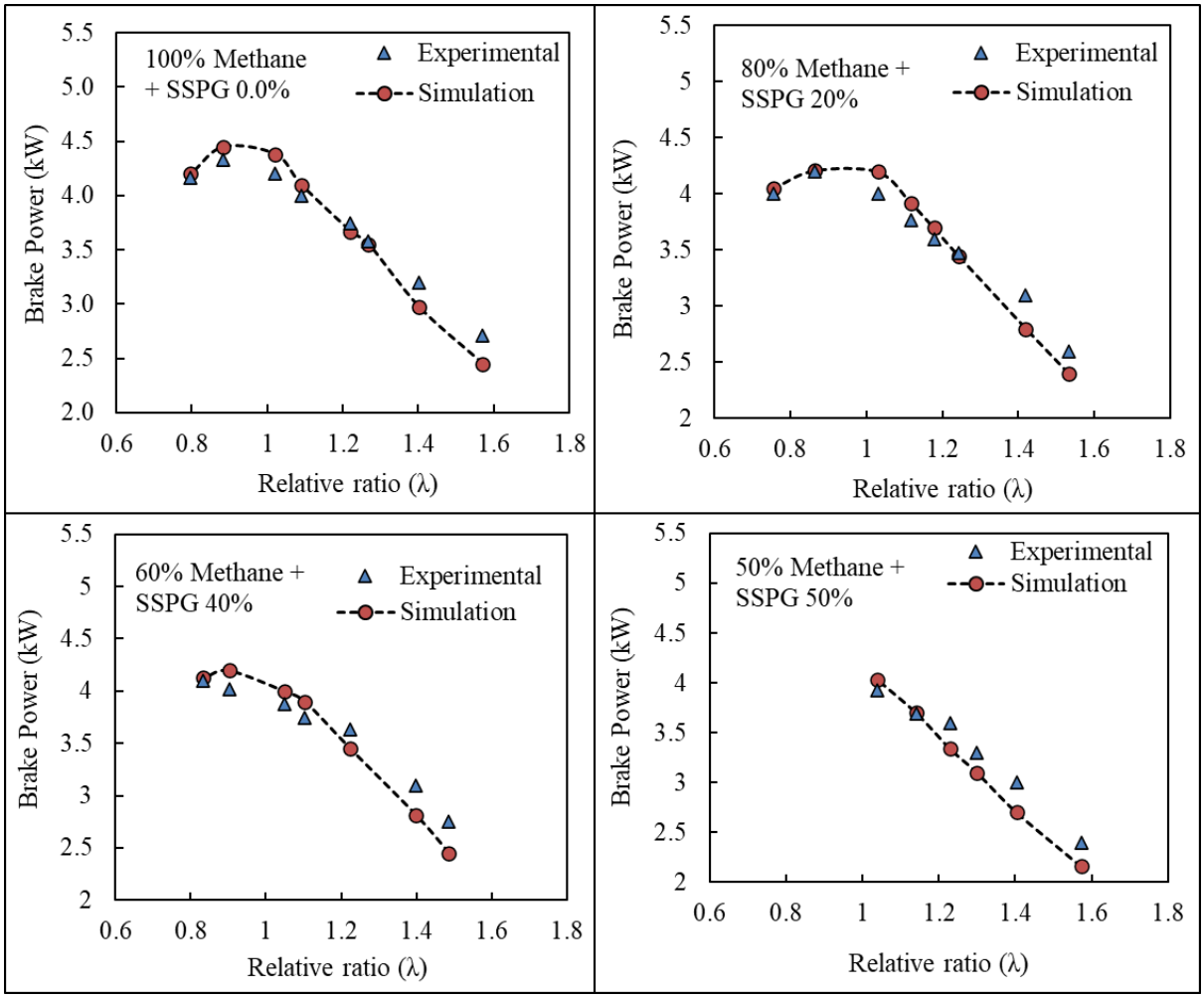


Figure 4.3.2. Power vs relative ratio for different blend validation

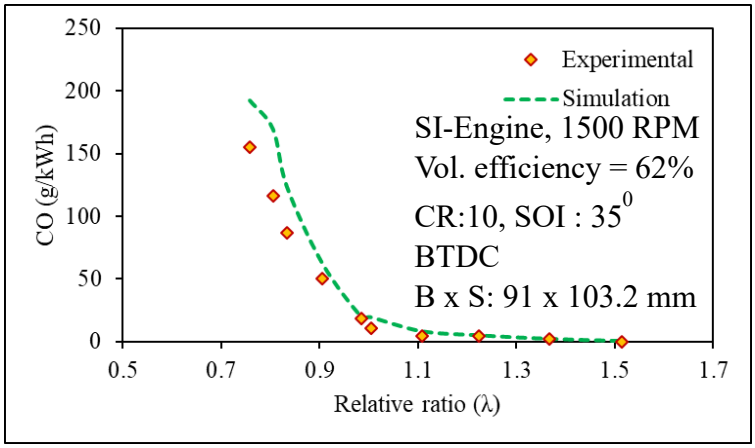


Figure 4.3.3. Efficiency and CO-emission validation

***4.3.1.3.*** Simulation Results

After the satisfactory validation, QDTM outcomes were obtained corresponding to the design-matrix inputs and were tabulated as in Table 4.13 of the supplementary. Trade-off scenarios of the desired performance and emission parametric characteristics are noticed relative to variations in the three input factors. This confirmed the vital obligations for multi-objective optimization in this study.

Table 4.13: Design matrix associated simulation results

| | **Inputs** | | | **Outputs** | | | | | | | | | |
|---|---|---|---|---|---|---|---|---|---|---|---|---|---|
| TN | **PIVC (bar)** | **SSPG (V%)** | **LIVC (ABDC)** | **CD** | **CA-PP** | **PP** | **ITE (%)** | **IMEP (bars)** | **BP (kW)** | **BMEP (bars)** | **BSEC (MJ/kWh)** | **CO (V%)** | **NO (ppm)** |
| 1 | 1 | 50 | 50 | 82.75 | 10 | 54.16 | 36.4 | 8.24 | 5.81 | 6.93 | 11.74 | 0.11 | 2468.4 |
| 2 | 1 | 50 | 60 | 82.12 | 10.3 | 51.41 | 36.95 | 7.89 | 5.52 | 6.58 | 11.67 | 0.11 | 2333.5 |
| 3 | 1 | 50 | 70 | 81.37 | 10.8 | 48.12 | 37.59 | 7.45 | 5.15 | 6.14 | 11.61 | 0.11 | 2170 |
| 4 | 1 | 50 | 80 | 80.37 | 11 | 44.35 | 38.33 | 6.92 | 4.7 | 5.614 | 11.57 | 0.11 | 1978.8 |
| 5 | 1 | 50 | 90 | 79.25 | 11.5 | 40.17 | 39.17 | 6.3 | 4.19 | 4.99 | 11.58 | 0.11 | 1765.9 |
| 6 | 1 | 60 | 50 | 82.75 | 10 | 53.32 | 36.46 | 8.14 | 5.73 | 6.84 | 11.75 | 0.11 | 2281.5 |
| 7 | 1 | 60 | 60 | 82 | 10.3 | 50.58 | 37.02 | 7.8 | 5.44 | 6.5 | 11.67 | 0.11 | 2152 |
| 8 | 1 | 60 | 70 | 81.25 | 10.5 | 47.33 | 37.69 | 7.37 | 5.08 | 6.06 | 11.6 | 0.11 | 1996.8 |
| 9 | 1 | 60 | 80 | 80.37 | 11 | 43.6 | 38.45 | 6.85 | 4.65 | 5.54 | 11.56 | 0.11 | 1819.4 |
| 10 | 1 | 60 | 90 | 79.25 | 11.5 | 39.47 | 39.32 | 6.24 | 4.14 | 4.94 | 11.56 | 0.11 | 1619.7 |
| 11 | 1 | 70 | 50 | 82.62 | 9.8 | 52.4 | 36.62 | 8.03 | 5.64 | 6.72 | 11.73 | 0.12 | 2106 |
| 12 | 1 | 70 | 60 | 82 | 10 | 49.71 | 37.22 | 7.7 | 5.36 | 6.39 | 11.64 | 0.12 | 1985.3 |
| 13 | 1 | 70 | 70 | 81.25 | 10.5 | 46.48 | 37.9 | 7.28 | 5 | 5.97 | 11.57 | 0.12 | 1838.4 |
| 14 | 1 | 70 | 80 | 80.25 | 10.8 | 42.8 | 38.7 | 6.77 | 4.58 | 5.46 | 11.52 | 0.12 | 1672.7 |
| 15 | 1 | 70 | 90 | 79.25 | 11.3 | 38.43 | 39.59 | 6.17 | 4.08 | 4.87 | 11.52 | 0.12 | 1446.8 |
| 16 | 1 | 80 | 50 | 83.12 | 9.5 | 51.4 | 37.6 | 7.9 | 5.53 | 6.59 | 11.63 | 0.14 | 1961.2 |
| 17 | 1 | 80 | 60 | 82.5 | 9.8 | 48.43 | 37.64 | 7.57 | 5.25 | 6.26 | 11.55 | 0.14 | 1822.3 |
| 18 | 1 | 80 | 70 | 81.5 | 10.3 | 45.28 | 38.38 | 7.16 | 4.91 | 5.86 | 11.46 | 0.14 | 1688.6 |
| 19 | 1 | 80 | 80 | 80.5 | 10.8 | 41.64 | 39.22 | 6.67 | 4.5 | 5.36 | 11.41 | 0.14 | 1534.2 |
| 20 | 1 | 80 | 90 | 79.37 | 11.3 | 37.63 | 40.18 | 6.09 | 4.01 | 4.78 | 11.4 | 0.14 | 1363.1 |
| 21 | 1.5 | 50 | 50 | 84.75 | 9.8 | 80.03 | 36.98 | 12.56 | 9.43 | 11.25 | 10.85 | 0.09 | 2994.1 |
| 22 | 1.5 | 50 | 60 | 84 | 10 | 75.93 | 37.55 | 12.02 | 8.98 | 10.71 | 10.75 | 0.09 | 2857.3 |
| 23 | 1.5 | 50 | 70 | 83.12 | 10.3 | 71.03 | 38.2 | 11.35 | 8.42 | 10.04 | 10.64 | 0.09 | 2684.6 |
| 24 | 1.5 | 50 | 80 | 82.12 | 10.8 | 65.43 | 38.96 | 10.55 | 7.75 | 9.24 | 10.54 | 0.09 | 2479.5 |

| | | | | | | | | | | | | | |
|---|---|---|---|---|---|---|---|---|---|---|---|---|---|
| 25 | 1.5 | 50 | 90 | 81 | 11.3 | 59.22 | 39.83 | 9.61 | 6.96 | 8.31 | 10.45 | 0.09 | 2239.1 |
| 26 | 1.5 | 60 | 50 | 84.62 | 9.5 | 78.89 | 37.04 | 12.41 | 9.31 | 11.11 | 10.85 | 0.1 | 2800 |
| 27 | 1.5 | 60 | 60 | 83.87 | 9.8 | 74.82 | 37.62 | 11.89 | 8.87 | 10.58 | 10.74 | 0.1 | 2666.9 |
| 28 | 1.5 | 60 | 70 | 83.12 | 10.3 | 69.97 | 38.3 | 11.23 | 8.32 | 9.93 | 10.63 | 0.1 | 2499.8 |
| 29 | 1.5 | 60 | 80 | 82.12 | 10.8 | 64.42 | 39.08 | 10.45 | 7.66 | 9.14 | 10.52 | 0.1 | 2303.4 |
| 30 | 1.5 | 60 | 90 | 80.87 | 11.3 | 58.27 | 39.98 | 9.53 | 6.89 | 8.22 | 10.43 | 0.1 | 2075.6 |
| 31 | 1.5 | 70 | 50 | 84.5 | 9.5 | 77.64 | 37.23 | 12.25 | 9.17 | 10.94 | 10.82 | 0.11 | 2615.6 |
| 32 | 1.5 | 70 | 60 | 83.87 | 9.8 | 73.62 | 37.83 | 11.74 | 8.74 | 10.43 | 10.7 | 0.11 | 2487.5 |
| 33 | 1.5 | 70 | 70 | 83 | 10 | 68.83 | 38.53 | 11.1 | 8.21 | 9.79 | 10.58 | 0.1 | 2330.1 |
| 34 | 1.5 | 70 | 80 | 82.12 | 10.5 | 63.32 | 39.34 | 10.32 | 7.56 | 9.01 | 10.47 | 0.1 | 2139.4 |
| 35 | 1.5 | 70 | 90 | 80.87 | 11 | 57.24 | 40.27 | 9.42 | 6.8 | 8.11 | 10.37 | 0.1 | 1924.9 |
| 36 | 1.5 | 80 | 50 | 85 | 9.3 | 76.25 | 37.68 | 12.05 | 9.01 | 10.75 | 10.71 | 0.12 | 2467.4 |
| 37 | 1.5 | 80 | 60 | 84.12 | 9.5 | 72.27 | 38.3 | 11.55 | 8.59 | 10.24 | 10.6 | 0.12 | 2361.3 |
| 38 | 1.5 | 80 | 70 | 83.12 | 10 | 67.55 | 39.05 | 10.93 | 8.07 | 9.63 | 10.46 | 0.12 | 2212.8 |
| 39 | 1.5 | 80 | 80 | 82.25 | 10.3 | 62.11 | 39.91 | 10.18 | 7.44 | 8.87 | 10.34 | 0.12 | 2032.8 |
| 40 | 1.5 | 80 | 90 | 81.12 | 11 | 56.11 | 40.88 | 9.3 | 6.7 | 7.99 | 10.24 | 0.12 | 1828.1 |
| 41 | 2 | 50 | 50 | 85.87 | 9.5 | 106.19 | 37.37 | 16.92 | 13.09 | 15.61 | 10.43 | 0.08 | 3404.3 |
| 42 | 2 | 50 | 60 | 85.12 | 9.8 | 100.74 | 37.94 | 16.2 | 12.49 | 14.89 | 10.31 | 0.08 | 3276.1 |
| 43 | 2 | 50 | 70 | 84.25 | 10.3 | 94.22 | 38.6 | 15.3 | 11.73 | 13.99 | 10.19 | 0.08 | 3109 |
| 44 | 2 | 50 | 80 | 83.25 | 10.5 | 86.78 | 39.37 | 14.21 | 10.82 | 12.91 | 10.06 | 0.08 | 2904.2 |
| 45 | 2 | 50 | 90 | 82 | 11.3 | 78.53 | 40.25 | 12.96 | 9.77 | 11.65 | 9.94 | 0.08 | 2654.8 |
| 46 | 2 | 60 | 50 | 85.75 | 9.5 | 104.77 | 37.44 | 16.73 | 12.93 | 15.42 | 10.42 | 0.09 | 3212.6 |
| 47 | 2 | 60 | 60 | 85.12 | 9.8 | 99.35 | 38.03 | 16.03 | 12.34 | 14.72 | 10.3 | 0.09 | 3083.7 |
| 48 | 2 | 60 | 70 | 84.25 | 10 | 92.89 | 38.71 | 15.14 | 11.6 | 13.83 | 10.17 | 0.09 | 2919.3 |
| 49 | 2 | 60 | 80 | 83.25 | 10.5 | 85.51 | 39.5 | 14.08 | 10.71 | 12.77 | 10.04 | 0.09 | 2718.9 |
| 50 | 2 | 60 | 90 | 82 | 11 | 77.34 | 40.41 | 12.84 | 9.67 | 11.53 | 9.91 | 0.09 | 2478.1 |
| 51 | 2 | 70 | 50 | 85.75 | 9.3 | 103.18 | 37.63 | 16.51 | 12.75 | 15.2 | 10.38 | 0.1 | 3025.3 |
| 52 | 2 | 70 | 60 | 85 | 9.5 | 97.82 | 38.24 | 15.82 | 12.17 | 14.51 | 10.25 | 0.1 | 2900.5 |
| 53 | 2 | 70 | 70 | 84.25 | 10 | 91.42 | 38.95 | 14.96 | 11.45 | 13.65 | 10.12 | 0.09 | 2738.5 |
| 54 | 2 | 70 | 80 | 83.12 | 10.3 | 84.12 | 39.77 | 13.92 | 10.57 | 12.61 | 9.98 | 0.09 | 2545.5 |
| 55 | 2 | 70 | 90 | 82 | 11 | 76.03 | 40.71 | 12.7 | 9.55 | 11.39 | 9.85 | 0.09 | 2315.4 |
| 56 | 2 | 80 | 50 | 86.25 | 9.3 | 101.41 | 38.11 | 16.26 | 12.53 | 14.95 | 10.26 | 0.11 | 2875.9 |
| 57 | 2 | 80 | 60 | 85.25 | 9.5 | 96.107 | 38.73 | 15.58 | 11.97 | 14.27 | 10.14 | 0.11 | 2770.5 |
| 58 | 2 | 80 | 70 | 84.37 | 9.8 | 89.8 | 39.49 | 14.74 | 11.27 | 13.44 | 9.99 | 0.11 | 2617.4 |
| 59 | 2 | 80 | 80 | 83.37 | 10.3 | 82.58 | 40.35 | 13.73 | 10.41 | 12.42 | 9.85 | 0.11 | 2431 |
| 60 | 2 | 80 | 90 | 82.15 | 10.8 | 74.58 | 41.34 | 12.54 | 9.42 | 11.23 | 9.71 | 0.11 | 2209.6 |
| 61 | 2.5 | 50 | 50 | 86.75 | 9.5 | 132.3 | 37.66 | 21.31 | 16.77 | 20 | 10.18 | 0.08 | 3704.6 |
| 62 | 2.5 | 50 | 60 | 86 | 9.8 | 125.5 | 38.23 | 20.4 | 16.01 | 19.09 | 10.05 | 0.08 | 3589.4 |
| 63 | 2.5 | 50 | 70 | 85.12 | 10 | 117.39 | 38.89 | 19.27 | 15.06 | 17.96 | 9.92 | 0.08 | 3434.7 |
| 64 | 2.5 | 50 | 80 | 84.12 | 10.5 | 108.1 | 39.67 | 17.9 | 13.92 | 16.6 | 9.78 | 0.08 | 3238.2 |

| | | | | | | | | | | | | | |
|---|---|---|---|---|---|---|---|---|---|---|---|---|---|
| 65 | 2.5 | 50 | 90 | 82.87 | 11 | 97.82 | 40.55 | 16.32 | 12.6 | 15.01 | 9.64 | 0.08 | 2993.6 |
| 66 | 2.5 | 60 | 50 | 86.62 | 9.3 | 130.62 | 37.73 | 21.08 | 16.57 | 19.77 | 10.16 | 0.08 | 3516.7 |
| 67 | 2.5 | 60 | 60 | 85.87 | 9.5 | 123.86 | 38.32 | 20.18 | 15.83 | 18.88 | 10.04 | 0.08 | 3400.4 |
| 68 | 2.5 | 60 | 70 | 85 | 10 | 115.8 | 39.01 | 19.07 | 14.9 | 17.76 | 9.9 | 0.08 | 3245.5 |
| 69 | 2.5 | 60 | 80 | 84 | 10.5 | 106.6 | 39.81 | 17.73 | 13.77 | 16.43 | 9.75 | 0.08 | 3051.6 |
| 70 | 2.5 | 60 | 90 | 82.75 | 11 | 96.39 | 40.72 | 16.17 | 12.47 | 14.87 | 9.61 | 0.08 | 2810.4 |
| 71 | 2.5 | 70 | 50 | 86.62 | 9.3 | 128.73 | 37.93 | 20.8 | 16.35 | 19.49 | 10.12 | 0.09 | 3320.1 |
| 72 | 2.5 | 70 | 60 | 85.87 | 9.5 | 122.01 | 38.54 | 19.93 | 15.62 | 18.62 | 9.99 | 0.09 | 3216.7 |
| 73 | 2.5 | 70 | 70 | 85 | 9.8 | 114.05 | 39.25 | 18.84 | 14.7 | 17.54 | 9.85 | 0.09 | 3065.4 |
| 74 | 2.5 | 70 | 80 | 84 | 10.3 | 104.9 | 40.08 | 17.53 | 13.6 | 16.23 | 9.69 | 0.09 | 2873.3 |
| 75 | 2.5 | 70 | 90 | 82.75 | 10.8 | 94.82 | 41.03 | 16 | 12.32 | 14.69 | 9.54 | 0.09 | 2638.9 |
| 76 | 2.5 | 80 | 50 | 87.12 | 9 | 126.58 | 38.41 | 20.48 | 16.08 | 19.18 | 10 | 0.1 | 3185.6 |
| 77 | 2.5 | 80 | 60 | 86 | 9.3 | 119.93 | 39.05 | 19.64 | 15.37 | 18.33 | 9.87 | 0.1 | 3084.8 |
| 78 | 2.5 | 80 | 70 | 85.12 | 9.8 | 112.07 | 39.8 | 18.58 | 14.48 | 17.27 | 9.72 | 0.1 | 2940.2 |
| 79 | 2.5 | 80 | 80 | 84.12 | 10 | 103.05 | 40.67 | 17.3 | 13.41 | 15.99 | 9.56 | 0.1 | 2754.8 |
| 80 | 2.5 | 80 | 90 | 83 | 10.5 | 93.06 | 41.67 | 15.8 | 12.15 | 14.49 | 9.41 | 0.1 | 2529 |
| 81 | 3 | 50 | 50 | 87.5 | 9.5 | 158.45 | 37.87 | 25.72 | 20.47 | 24.41 | 10 | 0.07 | 3929.9 |
| 82 | 3 | 50 | 60 | 86.62 | 9.8 | 150.28 | 38.44 | 24.62 | 19.55 | 23.31 | 9.88 | 0.07 | 3828.9 |
| 83 | 3 | 50 | 70 | 85.75 | 10 | 140.54 | 39.12 | 23.25 | 18.4 | 21.95 | 9.74 | 0.07 | 3689.8 |
| 84 | 3 | 50 | 80 | 84.75 | 10.5 | 129.4 | 39.9 | 21.61 | 17.02 | 20.3 | 9.59 | 0.07 | 3507.4 |
| 85 | 3 | 50 | 90 | 83.37 | 11 | 117.09 | 40.79 | 19.7 | 15.42 | 18.39 | 9.44 | 0.07 | 3273.6 |
| 86 | 3 | 60 | 50 | 87.37 | 9.3 | 156.45 | 37.95 | 25.44 | 20.24 | 24.14 | 9.99 | 0.08 | 3748 |
| 87 | 3 | 60 | 60 | 86.62 | 9.5 | 148.36 | 38.54 | 24.36 | 19.33 | 23.06 | 9.86 | 0.08 | 3645.5 |
| 88 | 3 | 60 | 70 | 85.75 | 10 | 138.69 | 39.24 | 23.02 | 18.21 | 21.71 | 9.72 | 0.07 | 3504 |
| 89 | 3 | 60 | 80 | 84.62 | 10.3 | 127.66 | 40.04 | 21.41 | 16.85 | 20.1 | 9.57 | 0.07 | 3321.7 |
| 90 | 3 | 60 | 90 | 83.37 | 10.8 | 115.44 | 40.96 | 19.52 | 15.27 | 18.21 | 9.41 | 0.07 | 3088 |
| 91 | 3 | 70 | 50 | 87.25 | 9.3 | 154.24 | 38.16 | 25.11 | 19.96 | 23.81 | 9.94 | 0.08 | 3569.9 |
| 92 | 3 | 70 | 60 | 86.5 | 9.5 | 146.19 | 38.77 | 24.06 | 19.08 | 22.76 | 9.81 | 0.08 | 3464.1 |
| 93 | 3 | 70 | 70 | 85.62 | 9.8 | 136.66 | 39.49 | 22.75 | 17.98 | 21.44 | 9.66 | 0.08 | 3325 |
| 94 | 3 | 70 | 80 | 84.62 | 10.3 | 125.7 | 40.32 | 21.16 | 16.65 | 19.86 | 9.51 | 0.08 | 3142.1 |
| 95 | 3 | 70 | 90 | 83.37 | 10.8 | 113.6 | 41.28 | 19.32 | 15.1 | 18.01 | 9.35 | 0.08 | 2912.4 |
| 96 | 3 | 80 | 50 | 87.75 | 9 | 151.74 | 38.65 | 24.73 | 19.64 | 23.42 | 9.82 | 0.1 | 3423.7 |
| 97 | 3 | 80 | 60 | 86.75 | 9.3 | 143.77 | 39.3 | 23.72 | 18.79 | 22.41 | 9.69 | 0.09 | 3333.8 |
| 98 | 3 | 80 | 70 | 85.87 | 9.5 | 134.34 | 40.05 | 22.43 | 17.71 | 21.13 | 9.54 | 0.09 | 3198.8 |
| 99 | 3 | 80 | 80 | 84.75 | 10 | 123.52 | 40.92 | 20.89 | 16.42 | 19.58 | 9.37 | 0.09 | 3021.4 |
| 100 | 3 | 80 | 90 | 83.62 | 10.5 | 111.55 | 41.93 | 19.08 | 14.9 | 17.77 | 9.21 | 0.09 | 2799 |

## 4.3.2. Response Interactions

***4.3.2.1.*** Interaction of Combustion Parameters

The primary objective for presenting the 3D surface plots for modelled combustion parameters is to justify the impacts observed in the various emissions and performance parameters. The included combustion parameters in this study were combustion duration (CD), peak in-cylinder pressure (PP), and crank-angle associated with the development of PP (CA-PP). The RSM-developed regression models for the response variables of CD, PP, and CA-PP are presented as equations-(71), (72), and (73), respectively. For PG-operated SI engines, a low CD might signify unstable combustion. This is because the flame speed for PG is relatively slower compared to the other conventional fuels [49]. Moreover, a longer CD necessarily signifies more combustion completeness and subsequently increased heat and work output [129]. It can be observed from Figure 4.3.4 that the CD increases significantly (maximum by 7.4%) with the full-range increase in Pressure at intake valve closure (PIVC). With PIVC increase, the relative in-cylinder temperature, pressure, and turbulence increase [102]. And consequently, the energy density in the induced fuel-air charge enhances, and results in more stable and prolonged combustion [102]. With the increase in PIVC, a significant increase in PP (maximum by 1.58 times) is also observed, which suitably justifies the previously mentioned phenomena of enhanced combustion stability. The inputs of 3 bars PIVC with minimum SSPG-blend and LIVC levels, resulted in a maximum of 158.45 bars of in-cylinder pressure. Such intense PP signified PIVC limitations towards cylinder endurability constraints and thus, the PIVC of greater than 3 bars was not considered for evaluation. Moreover, with the increase in LIVC, a gradual CD reduction is also observed (minimum by 3.79%). As LIVC increases, the trapped fuel-air charge inside the cylinder reduces. This subsequently reduces the charge available for combustion[128] and thus the CD declines. As LIVC is introduced to affect the Miller cycle strategy and enhance the thermal efficiency, it is identified as a significant parameter for

optimization for the yield of best engine performance. Moreover, increasing PIVC also imparts a simultaneous decrease (maximum 6.08%) in the observed CA-PP (Figure 4.3.4). This certainly results from the densifying of intake air-fuel charge through intake-boosting, which simultaneously increases the combustion stability and shortens the CA-durations for attainment of peak PP at greater PIVCs [102, 130].

$$\begin{aligned} CD = {} & + 81.95301 + 5.55883\times PIVC - 0.093448\times SSPG + 0.020898\times LIVC - \\ & 0.001056\times PIVC\times SSPG - 0.005515\times PIVC\times LIVC - \\ & 0.000110\times SSPG\times LIVC - 0.738286\times PIVC^2 + 0.000827\times SSPG^2 - \\ & 0.000698\times LIVC^2 \end{aligned} \tag{71}$$

$$\begin{aligned} PP = {} & -17.64591 + 71.88963\times PIVC + 0.031679\times SSPG + 0.590111\times LIVC - \\ & 0.057508\times PIVC\times SSPG - 0.337635\times PIVC\times LIVC + \\ & 0.000650\times SSPG\times LIVC + 0.107086\times PIVC^2 - 0.000840\times SSPG^2 - \\ & 0.004576\times LIVC^2 \end{aligned} \tag{72}$$

$$\begin{aligned} CA\text{-}PP = {} & + 10.73867 - 0.802300\times PIVC + 0.005360\times SSPG - 0.020800\times LIVC - \\ & 0.000880\times PIVC\times SSPG - 0.001150\times PIVC\times LIVC + \\ & 0.000030\times SSPG\times LIVC + 0.160000\times PIVC^2 - 0.000150\times SSPG^2 + \\ & 0.000432\times LIVC^2 \end{aligned} \tag{73}$$

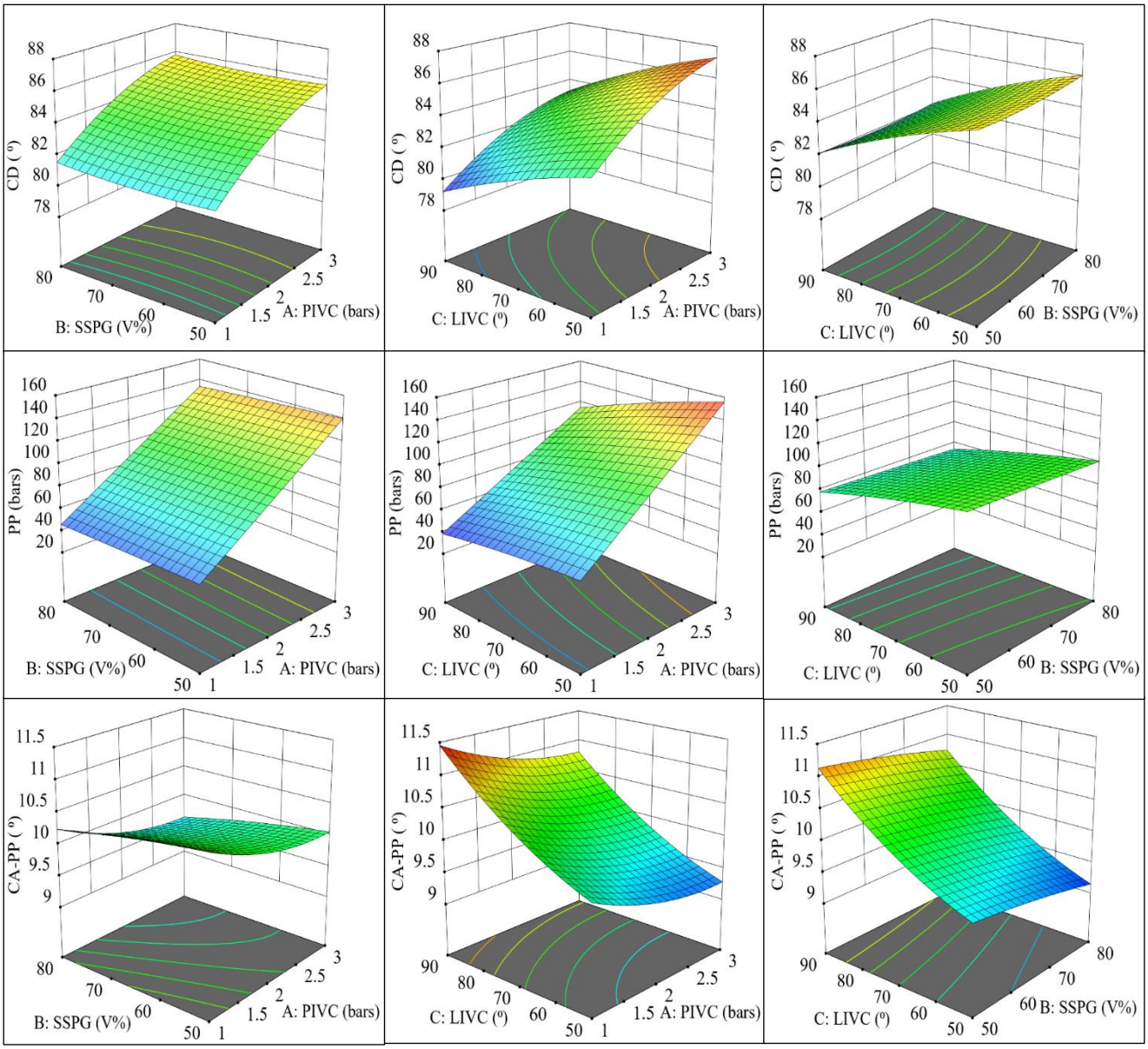


Figure 4.3.4. Simultaneous impacts on combustion parameters

***4.3.2.2.*** Interaction of performance parameters

Variations in the modelled performance parameters are presented in Figure 4.3.5. The RSM-developed regression models for the considered engine performance and emission responses are presented as equations-(74-78) and (79,80), respectively. Corresponding to simultaneous input variations, it is observed that both ITE and power representing parameters of IMEP and BP, fairly increase with PIVC rise (minimum by 2.63%, 233%, and 275% respectively). Such variation patterns are also collinear with the simultaneous observed rise in CD and PP(Figure

4.3.4). This verifies the benefits associated with longer CD, such as greater combustion completion and heat release [129]. IMEP and BP are observed to present 3D surface patterns that are similar to each other for the simultaneous input variable interactions. This verifies the simulation model predictions for similarities in engine power outputs that evolve at different engine ends. IMEP represents engine power at the piston-head[110], whereas Brake power (BP) signifies net power at the crankshaft [131]. The simulated results also present the conventional trend of ITE increase (maximum by 7.89%) with simultaneous power (IMEP and BP) decrease (maximum by 0.25 and 0.1 times), respectively, corresponding to a full ranged increase of LIVC. Increasing LIVC certainly reduces the trapped intake air-fuel charge, however, it also simultaneously enhances the effective expansion or power delivery stroke for the specific amount of fuel consumption [117, 128]. This enables a desired increase in thermal efficiency is also possible. Moreover, a minor ITE increment (maximum by 2.6%) is also observed corresponding to a full-range increase in SSPG fraction. This could be attributed to the presence of hydrogen content in the SSPG. With the increase in SSPG-fraction, the $H_2$ content also increases, which increases both net-flame speed and calorific value[191]. Through simulation, a maximum ITE of 41.93 % was attainable corresponding to peak PIVC, SSPG-blend fraction, and LIVC-settings. A simultaneous reduction in the IMEP and BP outcomes also observed corresponding with the particular SSPG fraction, which is certainly attributed to the lower CV associated with the PG fraction, as pointed out in [195, 204].

Moreover, similar trends of ITE and IMEP increase with respect to intake boosting could be verified from the investigations of Brequigny-et-al [26]. These verifications affirm suitable justifications that are stated corresponding to the observed performance parameters variations in regards to various decision parameter settings. Comparsion among the SSPG-blended fuel (60V%) simulated engine performance and the neat methane-based SI Engine performance (in Ref-[26]) reveals a significant improvement in BP (minimum 4.2 times) via consideration of 3 bar-intake boosting.

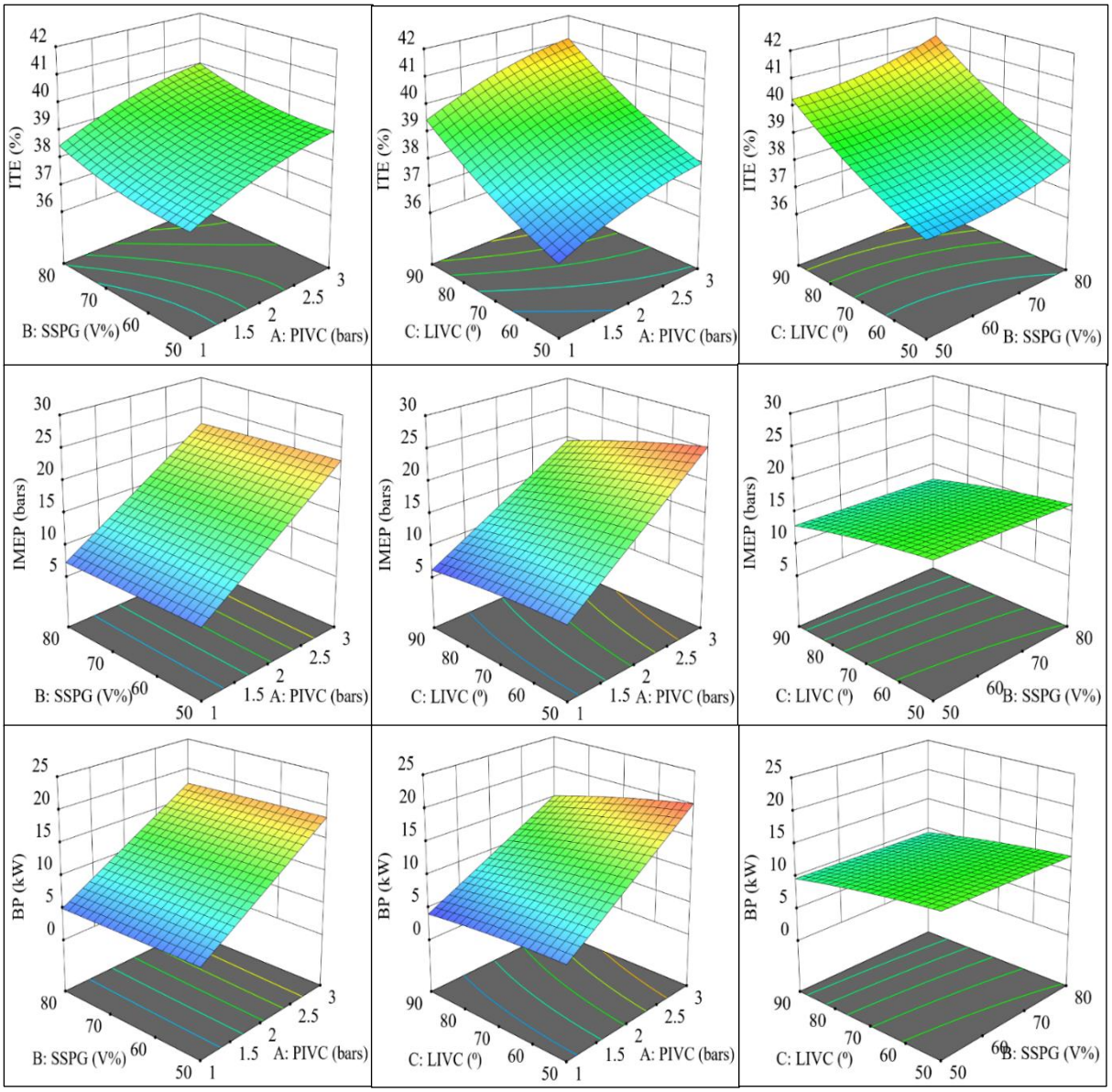


Figure 4.3.5. Simultaneous impacts on performance parameters

***4.3.2.3.*** Interaction of BSEC and emission

The effects of simultaneous input factor variations on the BSEC and emission models are presented in Figure 4.3.6. It is observed that BSEC significantly reduces corresponding to the increase in PIVC (maximum by 13.04%). As BSEC theoretically represents the inverse of BTE [135], the lower BSEC typically confirms effective combustion and enhanced energy conversion at greater PIVC levels [189]. A favourable BSEC decrease is also observed

corresponding to both, increasing SSPG and LIVC. It is possibly attributed to simultaneously increasing $H_2$ content and effective expansion-stroke elongation, respectively. CO-emissions majorly indicate combustion incompleteness [153, 219]. Thus, the CO development is observed to have a minimum tendency at greater PIVC and low SSPG inputs, where the combustion is estimated to be more stable and involves more heat release pertaining to higher CVs. On the other hand, as Zeldovich mechanism was utilized for NO-modelling, NO-modelling was a function of reduced-temperature and reduced-pressure formulations[220]. As increased PIVCs characterized better energy conversion and increased in-cylinder PP and **NTP**, the NO generation and emission significantly increased simultaneously with the increase of PIVC (maximum by 104%). Thus, an intense trade-off is also observable in Figure 4.3.6 among the CO and NO-emission. When CO-emission decreased at greater PIVCs, the NO-response peaked. Further, with the increase in SSPG-fraction, the H/C ratio of the fuel decreases, and the inert gas faction increases. Decreased H/C results in a significant CO increase (maximum by 35%)[51, 52, 221]. Whereas increased inert gases' fractions reduce SSPG CV[26], which consequently reduces the heat release and cylinder temperature. This further accounts for simultaneous NO reduction[220] (maximum by 21.4%). Similarly, with increasing LIVC, the trapped fuel-charge mass decreases. This reduces the in-cylinder heat liberation and thereby, the temperature decreases[26] which could further reduce the NO response.

$$\begin{aligned} ITE = {} & +38.25347 + 1.49481 \times PIVC - 0.133572 \times SSPG - 0.027826 \times LIVC + \\ & 0.000904 \times PIVC \times SSPG + 0.002820 \times PIVC \times LIVC + \\ & 0.000231 \times SSPG \times LIVC - 0.245143 \times PIVC^2 + 0.001117 \times SSPG^2 + \\ & 0.000587 \times LIVC^2 \end{aligned} \quad (74)$$

$$\begin{aligned} IMEP = {} & - 4.25632 + 11.51912 \times PIVC + 0.003232 \times SSPG + 0.113172 \times LIVC - \\ & 0.008820 \times PIVC \times SSPG - 0.049645 \times PIVC \times LIVC + \\ & 0.000209 \times SSPG \times LIVC + 0.053857 \times PIVC^2 - 0.000142 \times SSPG^2 - \\ & 0.000884 \times LIVC^2 \end{aligned} \quad (75)$$

$$\begin{aligned} BP = {} & - 4.69428 + 9.66627 \times PIVC + 0.003006 \times SSPG + 0.095194 \times LIVC - \\ & 0.007472 \times PIVC \times SSPG - 0.041670 \times PIVC \times LIVC + \end{aligned} \quad (76)$$

$$0.000171 \times SSPG \times LIVC + 0.045429 \times PIVC^2 - 0.000118 \times SSPG^2 - 0.000741 \times LIVC^2$$

$$BMEP = -5.61262 + 11.51759 \times PIVC + 0.004243 \times SSPG + 0.113680 \times LIVC - 0.008818 \times PIVC \times SSPG - 0.049689 \times PIVC \times LIVC + 0.000205 \times SSPG \times LIVC + 0.055114 \times PIVC^2 - 0.000148 \times SSPG^2 - 0.000885 \times LIVC^2 \quad (77)$$

$$BSEC = +13.22083 - 2.63643 \times PIVC + 0.033892 \times SSPG - 0.001054 \times LIVC - 0.000988 \times PIVC \times SSPG - 0.004475 \times PIVC \times LIVC - 0.000053 \times SSPG \times LIVC + 0.523000 \times PIVC^2 - 0.000263 \times SSPG^2 + 0.000013 \times LIVC^2 \quad (78)$$

$$CO = +0.180853 - 0.029607 \times PIVC - 0.001944 \times SSPG - 0.000118 \times LIVC - 0.000160 \times PIVC \times SSPG - 0.000035 \times PIVC \times LIVC - 1.8 \times 10^{-6} \times SSPG \times LIVC + 0.005714 \times PIVC^2 + 0.25 10^{-4} \times SSPG^2 + 1.785 10^{-6} \times LIVC^2 \quad (79)$$

$$NO = +2889.40131 + 1419.85319 \times PIVC - 37.78234 \times SSPG + 3.63970 \times LIVC - 0.473960 \times PIVC \times SSPG + 0.131050 \times PIVC \times LIVC + 0.06202 \times SSPG \times LIVC - 164.45857 \times PIVC^2 + 0.139770 \times SSPG^2 - 0.178379 \times LIVC^2 \quad (80)$$

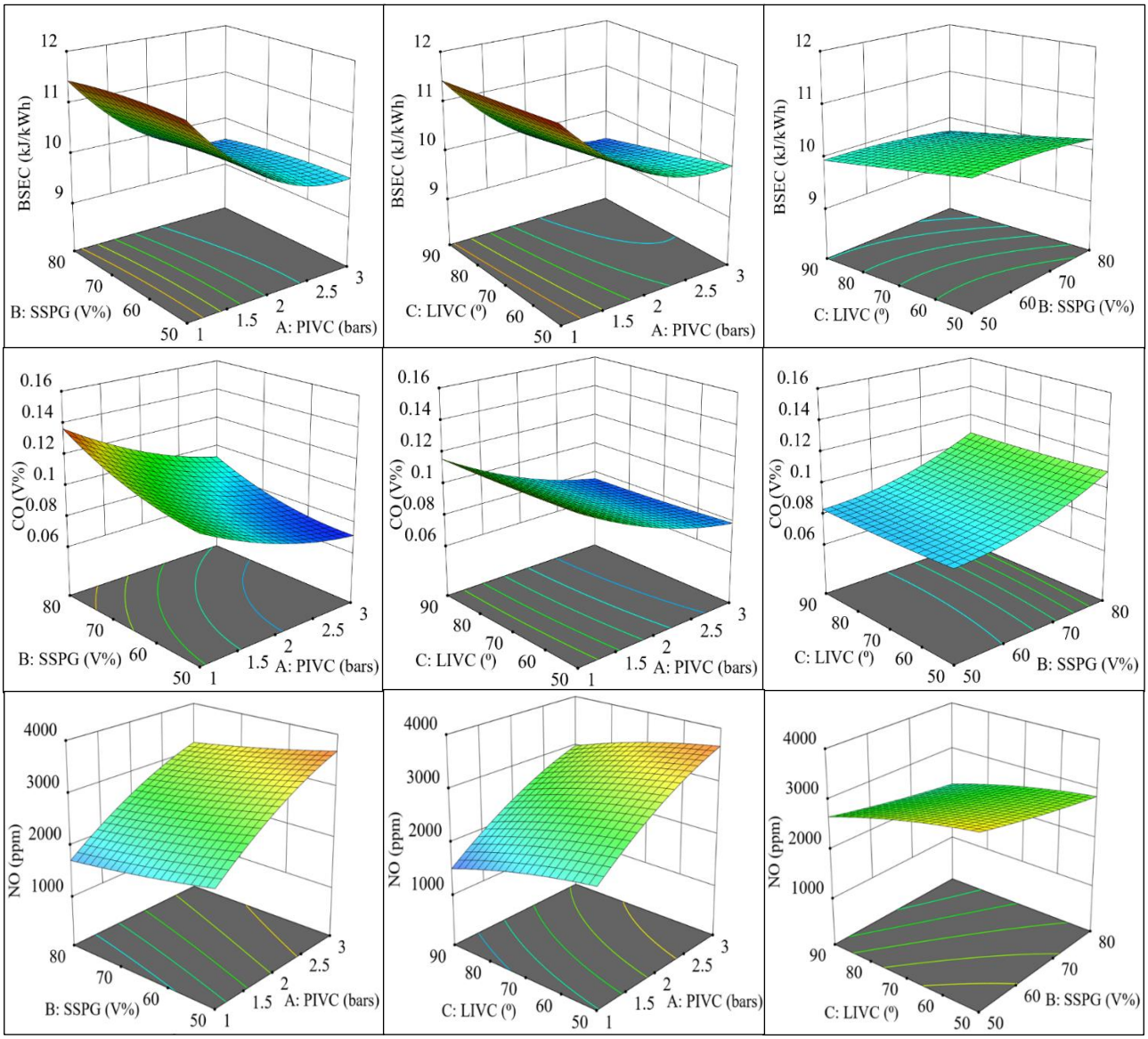


Figure 4.3.6. Simultaneous impacts on BSEC and emission parameters

## 4.3.3. Optimization and Overall-desirability

### *4.3.3.1.* Optimal Results

The desirability-function approach was considered for the optimization. Thus, the RSM-optimizer solution characterizing maximum composite desirability value is announced as the optimal solution[193]. Figure 4.3.7 presents a ramp-view of the optimal. The peak intake boosting of 3 bars PIVC was predicted as the optimal operating input parameter for the simulated dual-fuel SI Engine. The simultaneous optimal SSPG blend fraction was 76.94 (V%)

for 77.32º (CA-ABDC) LIVC. The predicted values of simultaneous performance and emission responses were 40.46% ITE, 21.35 (bars) of IMEP, 16.8 (kW) BP, 20.04 (bars) BMEP, 9.48 (kJ/kWh) BSEC, and emissions of 0.0854 (V%) CO, 3094.16 (ppm) NO, respectively.

***4.3.3.2.*** The desirability of the optimal solution

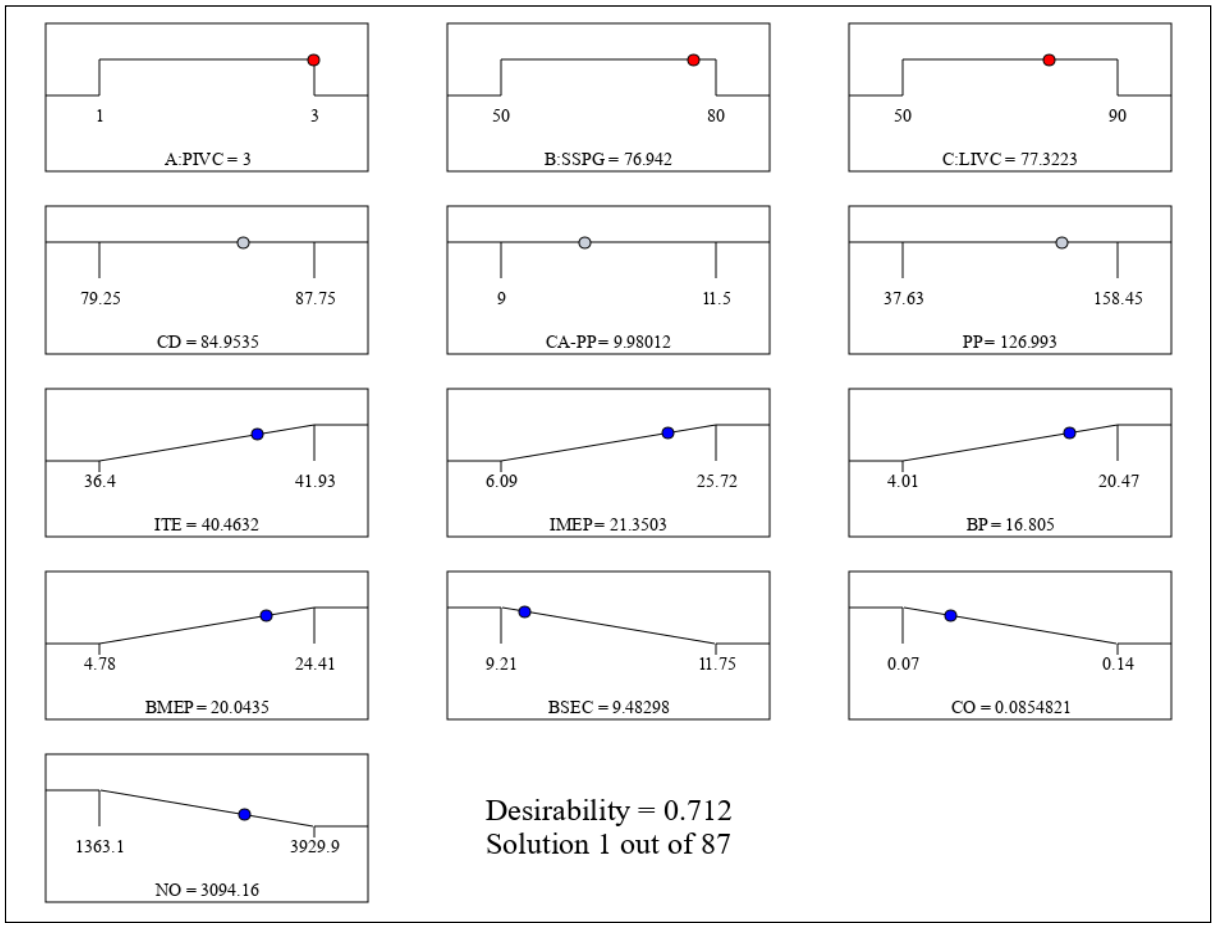


Figure 4.3.7. Optimal results ramp view

The individual desirability values for all the parameters are depicted in Figure 4.3.8-**(A).** Although the individual desirability values decline because of the high degree of trade-offs[193], the presented optimal results acquire a satisfactory degree of composite desirability. The composite desirability for the presented optimal results was 0.712. Typically, a result with composite desirability of more than 0.7, and $R^2$-values greater than 80% is considered highly acceptable[217]. As the acquired $R^2$-values were considerably high (> 97 %), the presented RSM-based optimal is also very acceptable. Figure 4.3.8-(B) presents the contour plots for

Composite Desirability. It is observed that greater PIVCs are always desirable. On the other hand, simultaneous SSPG and LIVC settings close to 74-80 (V%) and 80 (CA-ABDC), respectively should always portray composite desirability greater than 0.706. Table 4.14 presents some fitting results in decreasing-desirability order. Additionally, Table 4.15 presents the confirmation run outcomes for verifying the RSM-predicted optimum responses with the actual parametric simulation results for the optimum operating parameters, and found deviation error from the prediction to be less than 5%.

Table 4.14: Fitting solutions with decreasing Composite Desirability values (D)

| PIVC | SSPG | LIVC | ITE | IMEP | BP | BMEP | BSEC | CO | NO | (D) |
|---|---|---|---|---|---|---|---|---|---|---|
| 3 | 76.94 | 77.32 | 40.46 | 21.35 | 16.80 | 20.04 | 9.48 | 0.085 | 3094.16 | 0.712 |
| 3 | 77.56 | 78.45 | 40.60 | 21.15 | 16.64 | 19.85 | 9.46 | 0.088 | 3064.91 | 0.709 |
| 3 | 71.59 | 81.87 | 40.59 | 20.76 | 16.31 | 19.46 | 9.47 | 0.081 | 3076.50 | 0.707 |
| 3 | 79.993 | 67.977 | 39.87 | 22.63 | 17.88 | 21.33 | 9.59 | 0.093 | 3214.27 | 0.704 |
| 3 | 64.730 | 85.740 | 40.68 | 20.28 | 15.91 | 18.98 | 9.48 | 0.075 | 3095.44 | 0.701 |
| 2.982 | 68.005 | 90.000 | 41.22 | 19.33 | 15.11 | 18.02 | 9.38 | 0.078 | 2939.55 | 0.697 |
| 3 | 57.149 | 89.221 | 40.82 | 19.83 | 15.53 | 18.52 | 9.47 | 0.072 | 3140.92 | 0.692 |
| 3 | 54.276 | 84.617 | 40.34 | 20.71 | 16.27 | 19.40 | 9.55 | 0.071 | 3301.62 | 0.687 |
| 3 | 68.987 | 50.001 | 38.11 | 25.23 | 20.06 | 23.93 | 10.03 | 0.082 | 3599.06 | 0.647 |

Table 4.15: Confirmation run for Optimum responses

| **Parameters** | units | Predicted optimum: | Simulation results: | Deviation from predictions |
|---|---|---|---|---|
| **CD** | ºCA | 84.95 | 85 | 0.05% |
| **CA-PP** | ºCA-ATDC | 9.98 | 9.8 | -1.8% |
| **PP** | bars | 126.9 | 126.9 | 0% |
| **ITE** | (%) | 40.46 | 40.82 | 0.9% |
| **IMEP** | (kW) | 21.35 | 21.6 | 1.17% |
| **BP** | (kW) | 16.81 | 17.03 | 1.31% |
| **BMEP** | (kW) | 20.04 | 20.30 | 1.3% |
| **BSEC** | (MJ/kWh) | 9.48 | 9.38 | -1.05% |

| | | | | |
|---|---|---|---|---|
| **CO** | (V%) | 0.085 | 0.089 | 4.7% |
| **NO** | (ppm) | 3094.16 | 3075.9 | -0.6% |

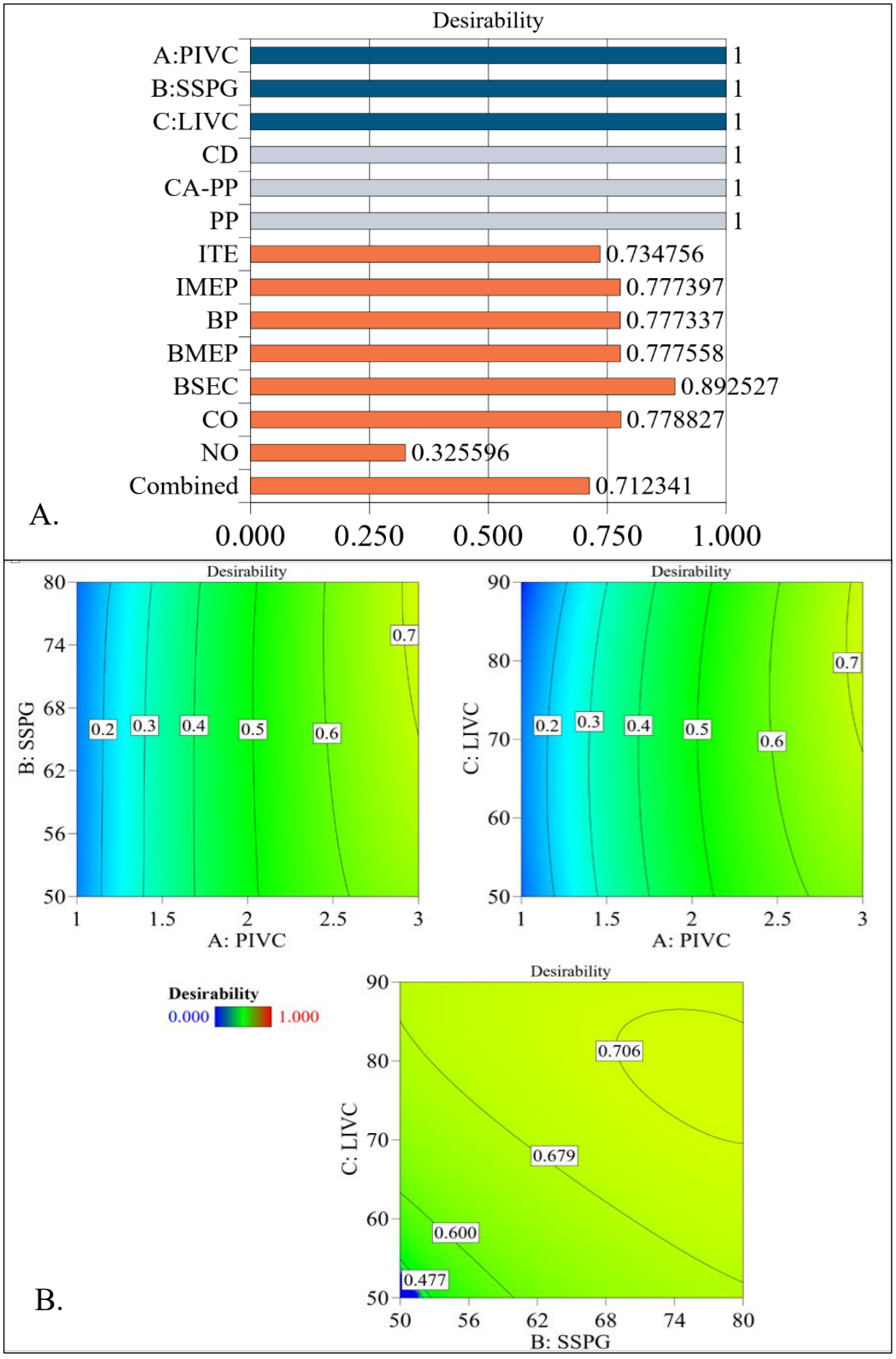


Figure 4.3.8. (A)-Individual desirability of optimal responses, (B)-Composite desirability contours

### 4.3.4. Significant analysis findings

In this study, Pressure-boosting of intake charge at IVC (PIVC), SSPG-blend fraction, and Late-inlet valve closures (LIVC) were varied. According to the results evaluation, major trade-off patterns were observed between engine output power and the efficiency respective to the LIVC variations, and CO-NO emissions respective to the SSPG variations. The simulation results are consistent with data from the literature. Accordingly, the following conclusions were reached:

- The quasi-dimensional thermodynamic model was effectively employed to simulate the engine performance and emissions for a boosted dual-fuelled-mode operation.
- A maximum indicated thermal efficiency of 41.93 % could be obtained for peak settings of PIVC, SSPG-blend fraction, and LIVC.
- Optimum operating parametric values were found as 3 bars of PIVC, 76.94 (V%) of SSPG-blend fraction, and about $77^0$ (CA-ABDC) LIVC.
- The RSM-predicted optimum responses were 40.46% ITE, 21.35 bars IMEP, 16.8 kW of BP, 20.04 bars BMEP, 9.483 kJ/kWh of BSEC, and CO, NO emissions responses of 0.085 (V%), 3094.16 ppm respectively.
- A composite desirability of 0.712 was acquired for the RSM-based optimal solution.
- Indicated efficiency was found more affected by LIVC variations than by increasing the intake boosting.

In summary, the thermodynamics-based numerical modelling and the subsequent data analysis through RSM and ANOVA analysis revealed that boosting the intake charge in DF-SI engines significantly favours the performance and emissions except that for the NO.

## 4.4. Analysis with variable equivalence ratio

Decentralized power generation through a gasifier-engine system has been an attractive alternative source for reducing dependency on the power grid and environmental impact. The major challenge of dual fuel (DF) mode engine run is to deal with setting operating parameters for optimizing efficiency-power-emission. In such cases when early prediction is required, a simulation tool of adequate precision can be utilized to predict DF mode engine performance cost-effectively. Therefore, this study aims to simulate the enhancement of thermal efficiency by employing a variable LIVC strategy with a 12.0:1 geometrical compression ratio miller cycle, and mitigation of fuel consumption and emission of DF SI engine fuelled with sewage sludge producer gas and methane blend using a quasi-dimensional thermodynamic model (QDTM). The model is validated with the experimental one, subsequently, the QDTM is applied to the parametric investigation of inputs ( blends, LIVC, equivalence ratio) on the indicated thermal efficiency, brake power, brake-specific fuel consumption (BSFC) and emissions (CO and NO). To consolidate the performance-emissions trade-off via operating parameters, optimization has been performed using a response surface methodology (RSM) statical approach.

In summary, the objectives for this study were as follows:

- Identification of parameters that lay significant influences on performance efficiency, power output and emissions according to the ANOVA results.
- Identifying the inputs, that potentially result maximum power output and engine efficiency outcomes.
- To address the significant trade-offs in the engine performance and emission responses.
- To optimize the operational inputs according to engine performance enhancement and emissions decrease.

### 4.4.1. Impacts of equivalence ratio variations

This study also employs the QDTM technique to model and study the impacts of variable ERs on the power cycle and resultant engine performance and emission parameters. Total 60 sets of parametric operating conditions were considered, comprising the range of 25%, 50% and 75% SSPG blends, 0.8, 0.9, 1.0, and 1.1 engine equivalence ratio, and 50, 60,70, 80, $90^0$ ABDC-LIVC crank angles settings. The results of these simulation inputs have been depicted in the section- *4.4.2*.

Figure 4.4.1 represents the flowchart and layout for both the modelled QDTM-based algorithm framework and the executed fundamental sections of multi-objective optimization. The power cycle starts from Inlet valve closure (IVC) and terminates at the end of the expansion phase (EVO). Thus, it comprises a partial compression phase, a complete combustion phase, and a partial expansion phase. Engine specifications considered for the modelling are presented in Table 4.16. QDTM applies fundamental thermodynamic mass and energy conservation models on the system while requiring thermochemical properties input, like the net CV of inducted fuel blends [66, 129]. Thus, the considered ASTM-standard mixture properties are referenced, calculated, and also presented for different fuel-blend proportions in Table 4.16 itself.

Table 4.16: Particular model considerations (engine specifications, fuel properties)

| **Engine Particulars** | **Specification** |
|---|---|
| Start of ignition (crank angle) | 30-45 bTDC *(variable)* |
| Stroke (mm) | 103.2 |
| Bore Diameter (mm) | 91.0 |
| Geometrical Compression ratio (r) | 12 |
| Length of connecting rod (mm) | 136.5 |
| RPM | 1500 |
| PG density | density: 1.1 ($kg/m^3$) |
| PG fraction with methane (by volume%) | 10-90% *(variable)* |

| | |
|---|---|
| Equivalence ratio | 0.8-1.1 *(variable)* |
| Inlet valve closing | 50-90$^0$CA-aBDC*(variable)* |
| Inspected fuels: | SSPG25, SSPG50, SSPG75 |

| **Fuels** | **Composition of fuel (V%)** | **Calorific Value (MJ/kg)** | **Reference** |
|---|---|---|---|
| SSPG | $CH_4$: 3% | 4.05 | [26, 49] |
| | $H_2$: 13% | | |
| | $CO_2$: 15% | | |
| | CO: 16% | | |
| | $N_2$: 53% | | |
| $CH_4$ | 100% $CH_4$ | 50.33 | [49] |
| SSPG25 | 25% SSPG+75% $CH_4$ | 35.59 | Calculated |
| SSPG50 | 50% SSPG+50% $CH_4$ | 21.28 | |
| SSPG75 | 75% SSPG+25% $CH_4$ | 11.70 | |

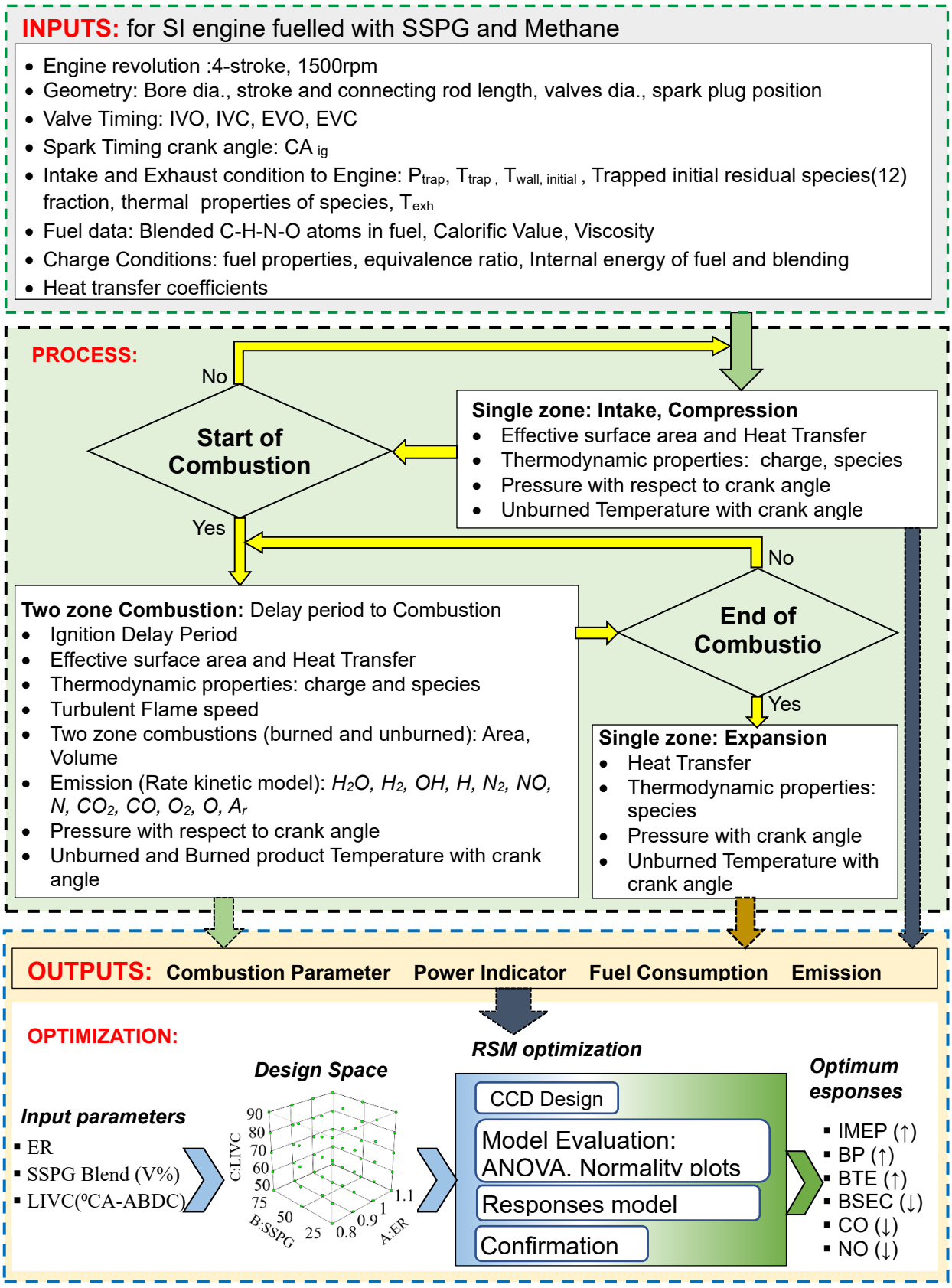


Figure 4.4.1. Schematic of the operational layout

### 4.4.2. Simulation validation and novel outcomes

Figure 4.4.2-**(A)** presents pressure vs. crank angle results traced from both the QDTM outcomes as well as the cited experimental results from-[49]. Simulation-generated in-cylinder pressure variations were observed to trace the actual experimental results very closely. The figure also shows that the deviation in peak pressure (pp) attained with crank angle and respective indicated mean effective pressure is less than 2%. The crank angle positions corresponding to the peak pressure were also observed to match the actual results very closely, although the modelled crank-angle trace deviates by a few CA-degrees during early compressions. Furthermore validation, the QDTM simulation model was constrained to a fixed 35ºBTDC SOI and 10 CR engine operation. It must be noted that the cited experimental results[49] are traces of 100 pressure-crank angle cycle variations, where irregular misfiring affects the performance outputs. Thus, for validation purposes, the highest-pressure range was considered. Figure 4.4.2-(B,C,D) further illustrates the closeness of QDTM-obtained brake power from the experimental findings corresponding to the different equivalence air-fuel ratios and varying intake fuel blend proportions (50%, 40%, and 20% SSPG blend with methane). The quasi-dimensional model is thus validated and henceforth implemented using FORTRAN to assess the engine performance (energy Consumption efficiency, power) and emissions variations corresponding to differing ER, SSPG blending, and LIVC inputs in the investigation. The simulated results have been tabulated in Table 4.17 according to the pattern of the DoE-based design matrix.

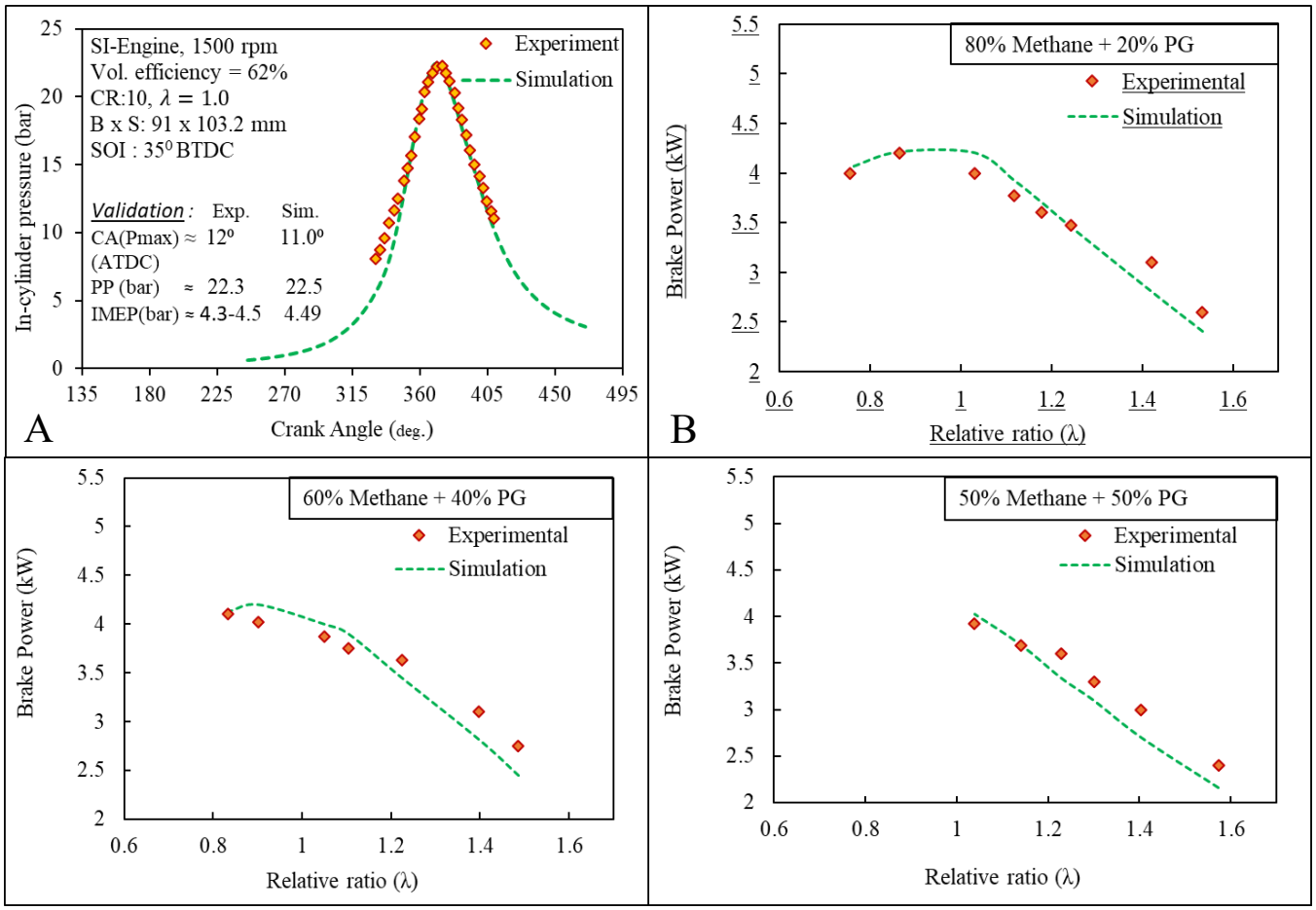


Figure 4.4.2. Simulation Validation for neat and blended SSPG

Table 4.17: Simulated results as per the Design matrix

| | Inputs | | | Outputs | | | | | |
|---|---|---|---|---|---|---|---|---|---|
| TN | ER | SSPG (V%) | LIVC (ABDC) | IMEP (bar) | BP (kW) | BTE (%) | BSEC (MJ/kWh) | CO (V%) | NO (ppm) |
| 1 | 0.8 | 25 | 50 | 6.24 | 4.13 | 26.9 | 13.382 | 0.12 | 2597.9 |
| 2 | 0.8 | 25 | 60 | 5.966 | 3.906 | 26.97 | 13.347 | 0.12 | 2452.3 |
| 3 | 0.8 | 25 | 70 | 5.626 | 3.622 | 26.9 | 13.382 | 0.11 | 2276 |
| 4 | 0.8 | 25 | 80 | 5.22 | 3.281 | 26.76 | 13.453 | 0.11 | 2020.4 |
| 5 | 0.8 | 25 | 90 | 4.749 | 2.886 | 26.41 | 13.631 | 0.11 | 1795.3 |
| 6 | 0.8 | 50 | 50 | 6.1 | 4.0192 | 28.29 | 12.727 | 0.12 | 2074.8 |
| 7 | 0.8 | 50 | 60 | 5.84 | 3.8 | 28.33 | 12.706 | 0.12 | 1949.7 |
| 8 | 0.8 | 50 | 70 | 5.514 | 3.527 | 28.33 | 12.706 | 0.12 | 1798.5 |

| | | | | | | | | | |
|---|---|---|---|---|---|---|---|---|---|
| 9 | 0.8 | 50 | 80 | 5.122 | 3.199 | 28.24 | 12.748 | 0.12 | 1630.8 |
| 10 | 0.8 | 50 | 90 | 4.666 | 2.817 | 27.87 | 12.918 | 0.12 | 1442.6 |
| 11 | 0.8 | 75 | 50 | 5.9 | 3.85 | 28.29 | 12.727 | 0.14 | 1670.7 |
| 12 | 0.8 | 75 | 60 | 5.654 | 3.645 | 28.39 | 12.68 | 0.14 | 1567.1 |
| 13 | 0.8 | 75 | 70 | 5.3479 | 3.388 | 28.43 | 12.665 | 0.14 | 1443.5 |
| 14 | 0.8 | 75 | 80 | 4.976 | 3.076 | 28.34 | 12.703 | 0.14 | 1304.8 |
| 15 | 0.8 | 75 | 90 | 4.542 | 2.712 | 28.03 | 12.844 | 0.14 | 1152.1 |
| 16 | 0.9 | 25 | 50 | 6.787 | 4.595 | 26.9 | 13.382 | 0.33 | 4373.2 |
| 17 | 0.9 | 25 | 60 | 6.478 | 4.335 | 26.9 | 13.382 | 0.33 | 4306.5 |
| 18 | 0.9 | 25 | 70 | 6.095 | 4.015 | 26.83 | 13.418 | 0.33 | 4214.7 |
| 19 | 0.9 | 25 | 80 | 5.64 | 3.633 | 26.69 | 13.489 | 0.33 | 4087.2 |
| 20 | 0.9 | 25 | 90 | 5.115 | 3.193 | 26.27 | 13.703 | 0.33 | 3909.2 |
| 21 | 0.9 | 50 | 50 | 6.644 | 4.47 | 28.43 | 12.663 | 0.34 | 3849.7 |
| 22 | 0.9 | 50 | 60 | 6.345 | 4.224 | 28.48 | 12.642 | 0.34 | 3772.1 |
| 23 | 0.9 | 50 | 70 | 5.976 | 3.915 | 28.43 | 12.663 | 0.34 | 3667.1 |
| 24 | 0.9 | 50 | 80 | 5.538 | 3.547 | 28.29 | 12.727 | 0.34 | 3525.4 |
| 25 | 0.9 | 50 | 90 | 5.03 | 3.121 | 27.82 | 12.94 | 0.34 | 3336.4 |
| 26 | 0.9 | 75 | 50 | 6.419 | 4.286 | 28.71 | 12.539 | 0.39 | 3194.5 |
| 27 | 0.9 | 75 | 60 | 6.139 | 4.052 | 28.76 | 12.516 | 0.39 | 3109.2 |
| 28 | 0.9 | 75 | 70 | 5.79 | 3.76 | 28.76 | 12.516 | 0.39 | 2997.1 |
| 29 | 0.9 | 75 | 80 | 5.37 | 3.41 | 28.63 | 12.574 | 0.39 | 2851.4 |
| 30 | 0.9 | 75 | 90 | 4.88 | 3 | 28.29 | 12.727 | 0.39 | 2666.7 |
| 31 | 1 | 25 | 50 | 7.212 | 4.951 | 26.34 | 13.667 | 0.72 | 2795.3 |
| 32 | 1 | 25 | 60 | 6.873 | 4.667 | 26.27 | 13.703 | 0.72 | 2812.9 |
| 33 | 1 | 25 | 70 | 6.456 | 4.317 | 26.2 | 13.738 | 0.72 | 2833.4 |
| 34 | 1 | 25 | 80 | 5.961 | 3.903 | 26 | 13.845 | 0.72 | 2851.1 |
| 35 | 1 | 25 | 90 | 5.394 | 3.426 | 25.61 | 14.058 | 0.72 | 2865.8 |
| 36 | 1 | 50 | 50 | 7.058 | 4.822 | 27.91 | 12.897 | 0.75 | 2631.4 |
| 37 | 1 | 50 | 60 | 6.732 | 4.55 | 27.91 | 12.897 | 0.75 | 2641.3 |
| 38 | 1 | 50 | 70 | 6.33 | 4.212 | 27.85 | 12.927 | 0.74 | 2648.7 |
| 39 | 1 | 50 | 80 | 5.852 | 3.8109 | 27.68 | 13.004 | 0.74 | 2651.3 |
| 40 | 1 | 50 | 90 | 5.305 | 3.352 | 27.28 | 13.195 | 0.74 | 2642.7 |
| 41 | 1 | 75 | 50 | 6.8 | 4.61 | 28.37 | 12.691 | 0.82 | 2444.9 |

| | | | | | | | | | |
|---|---|---|---|---|---|---|---|---|---|
| 42 | 1 | 75 | 60 | 6.499 | 4.354 | 28.42 | 12.668 | 0.82 | 2441.3 |
| 43 | 1 | 75 | 70 | 6.12 | 4.035 | 28.37 | 12.691 | 0.82 | 2432.3 |
| 44 | 1 | 75 | 80 | 5.667 | 3.656 | 28.21 | 12.762 | 0.82 | 2413.2 |
| 45 | 1 | 75 | 90 | 5.143 | 3.216 | 27.83 | 12.937 | 0.82 | 2375.5 |
| 46 | 1.1 | 25 | 50 | 7.208 | 4.948 | 24.31 | 14.806 | 2.36 | 712.8 |
| 47 | 1.1 | 25 | 60 | 6.867 | 4.662 | 24.26 | 14.841 | 2.36 | 722.5 |
| 48 | 1.1 | 25 | 70 | 6.449 | 4.312 | 24.2 | 14.877 | 2.36 | 734.5 |
| 49 | 1.1 | 25 | 80 | 5.954 | 3.896 | 23.97 | 15.019 | 2.36 | 747.2 |
| 50 | 1.1 | 25 | 90 | 5.386 | 3.421 | 23.63 | 15.233 | 2.36 | 747.8 |
| 51 | 1.1 | 50 | 50 | 7.07 | 4.834 | 25.94 | 13.876 | 2.47 | 663.2 |
| 52 | 1.1 | 50 | 60 | 6.748 | 4.562 | 25.98 | 13.855 | 2.46 | 687 |
| 53 | 1.1 | 50 | 70 | 6.348 | 4.227 | 25.94 | 13.876 | 2.45 | 717.1 |
| 54 | 1.1 | 50 | 80 | 5.871 | 3.827 | 25.79 | 13.961 | 2.44 | 753.1 |
| 55 | 1.1 | 50 | 90 | 5.322 | 3.367 | 25.44 | 14.153 | 2.42 | 793.6 |
| 56 | 1.1 | 75 | 50 | 6.86 | 4.656 | 26.78 | 13.441 | 2.65 | 853.9 |
| 57 | 1.1 | 75 | 60 | 6.551 | 4.397 | 26.83 | 13.417 | 2.64 | 869.8 |
| 58 | 1.1 | 75 | 70 | 6.169 | 4.076 | 26.78 | 13.441 | 2.64 | 887.2 |
| 59 | 1.1 | 75 | 80 | 5.711 | 3.693 | 26.64 | 13.511 | 2.63 | 962.4 |
| 60 | 1.1 | 75 | 90 | 5.174 | 3.242 | 26.24 | 13.722 | 2.65 | 895.2 |

### 4.4.3. Formulations for Desirability

Optimization operation was required to optimize multiple objectives, such as output power and efficiency improvement, along with the simultaneous decrease in both CO and NO emissions. Therefore, the strategy of multi-objective optimization is employed [191]. RSM-model (Figure 3.2.2) of the Design of Experiments (DOE) strategy was used for performing the multi-objective optimization through fewer test iterations, and lesser computational time[163, 199]. In this study, the optimal result was obtained with the desirability approach, where the diverse optimization goals of individual optimization parameters are reduced to maximization of the Composite desirability(D) alone[196, 198]. *D* is a function of Individual desirability(*d*) values and the assigned levels of importance (*i*) particular to the specific optimization parameters

[196]. *d* is further a function of parametric upper and lower limits (*U*, *L*) and their assigned optimization weights(*w*), that define the desirability function for the set goals [196]. Formulations for Individual desirability and Composite desirability have already been presented in equations-54 and 55, respectively [196-198].

### 4.4.4. Impacts analysis

The impacts of the factor parameters are initially inspected by observing the distribution of the residuals using the normal probability plots. Fine tracing is confirmed as the residuals were distributed close to normal distribution[190]. Then, the effects of simultaneously varying input variables (ER, SSPG, and LIVC) on each of the considered output parameters are discussed in the following sub-sections.

Concerning the statistical-based RSM-generated regression modelling, the discrepancy between the statistically expected and the actual outputs are represented through residuals. To determine whether the residuals deviate from random distribution (normalcy), the normal probability plots were used[194]. Figure 4.4.3 shows the normal probability plots for all the response parameters. A perfectly normally distributed residual is indicated by the red line. As all output response residuals were found to closely match the normality, the corresponding regression models could effectively trace the actual simulation results [195]. The small observed discrepancies could likely result from the ineffectiveness of the regression models in tracing higher-order terms accurately.

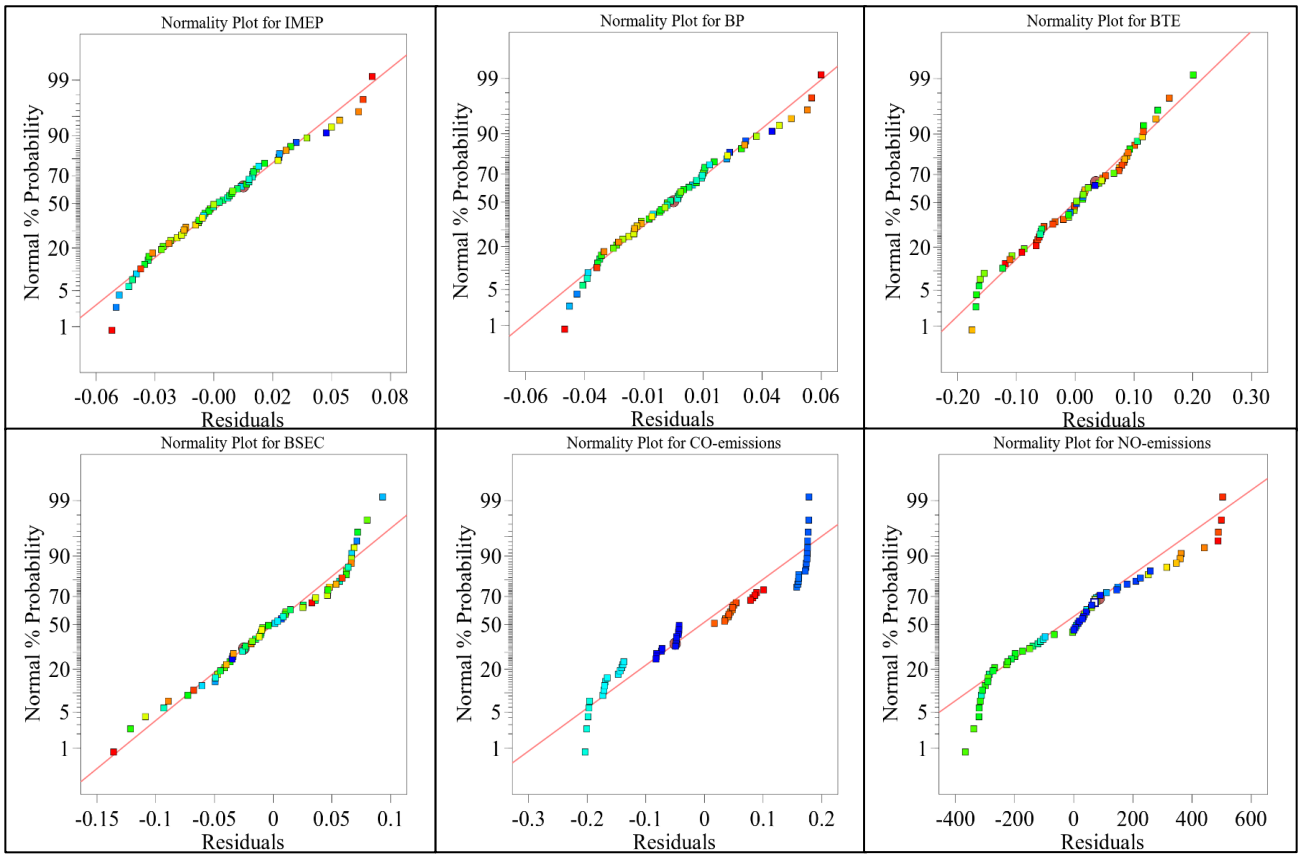


Figure 4.4.3. Normal Probability plots

***4.4.4.1.*** Indicated mean-effective pressure

The indicated mean-effective pressure (IMEP) represents engine power regardless of its size (displacement volume). Hence, it is a vital parameter for comparing the varying-sized engines [110]. It is the ratio of indicated power to displacement volume[110]. Figure 4.4.4 portrays the effects of simultaneous input variations on IMEP. It is observed that IMEP initially increases with increasing ER and then peaks at the 1.04-1.1 ER range for any simultaneous SSPG-fraction or LIVC inputs. Similar IMEP effects corresponding to ER variations are also reported in the recent work of Brequigny-et-al [26] for neat methane or PG-fuelled engine operations. Simulation results show about a 14.8% IMEP increase from ER 0.8 to 1, and then a 0.28% increase from ER 1 to 1.1. The drastic initial IMEP increase might pertain to the increasing fuel content of a leaner mixture. This lets more fuel take part in complete combustion and

results release of greater power[129]. The following gradual increase in IMEP could pertain to the simultaneously decreasing thermal efficiency[129]. An increase in the SSPG fraction is also found to decrease IMEP but relatively slightly. This decrement must pertain to the low SSPG CV and the consequently low power output [204]. Simultaneous increase of thermal efficiency with SSPG increment marginalizes the decrease in IMEP as well. With LIVC increase, the IMEP response persistently decreases (max. by 23%). This effect is certainly attributed to the decreased intake charge induced by delayed IVC [128].

#### *4.4.4.2.* Brake Power

Brake power (BP) is the power offered at the crankshaft after expenditure on internal frictional and other thermal losses [131]. The effects of simultaneous input variations on BP are also shown in Figure 4.4.4. Similar to IMEP, the power-representing response of BP also increases with increasing ER, majorly when the input charge is leaner. BP increased by as much as 18.7% with the increase of ER from 0.8 to unity. Such an effect is possibly attributed to increased fuel content, which takes part in complete combustion and liberates more heat and output work when the input-ER is increased. Besides, with an increase of SSPG at the intake, the BP is also found to decrease with relatively low sharpness (by max. 6.03%), possibly because of low CV of SSPG [195]. With delayed IVC, the BP is observed to decrease more sharply (maximum by 30.86%). This also could be attributed to the decreasing trapped fuel-air charge during suction-stroke when the LIVC is increased [128]. Collinear to the regression-developed 3D-trends, the simulation results indicate the occurrence of maximum BP, as 4.951 (kW) for greater ER(1), and simultaneous least SSPG-blend(25%) and least LIVC(50º) inputs.

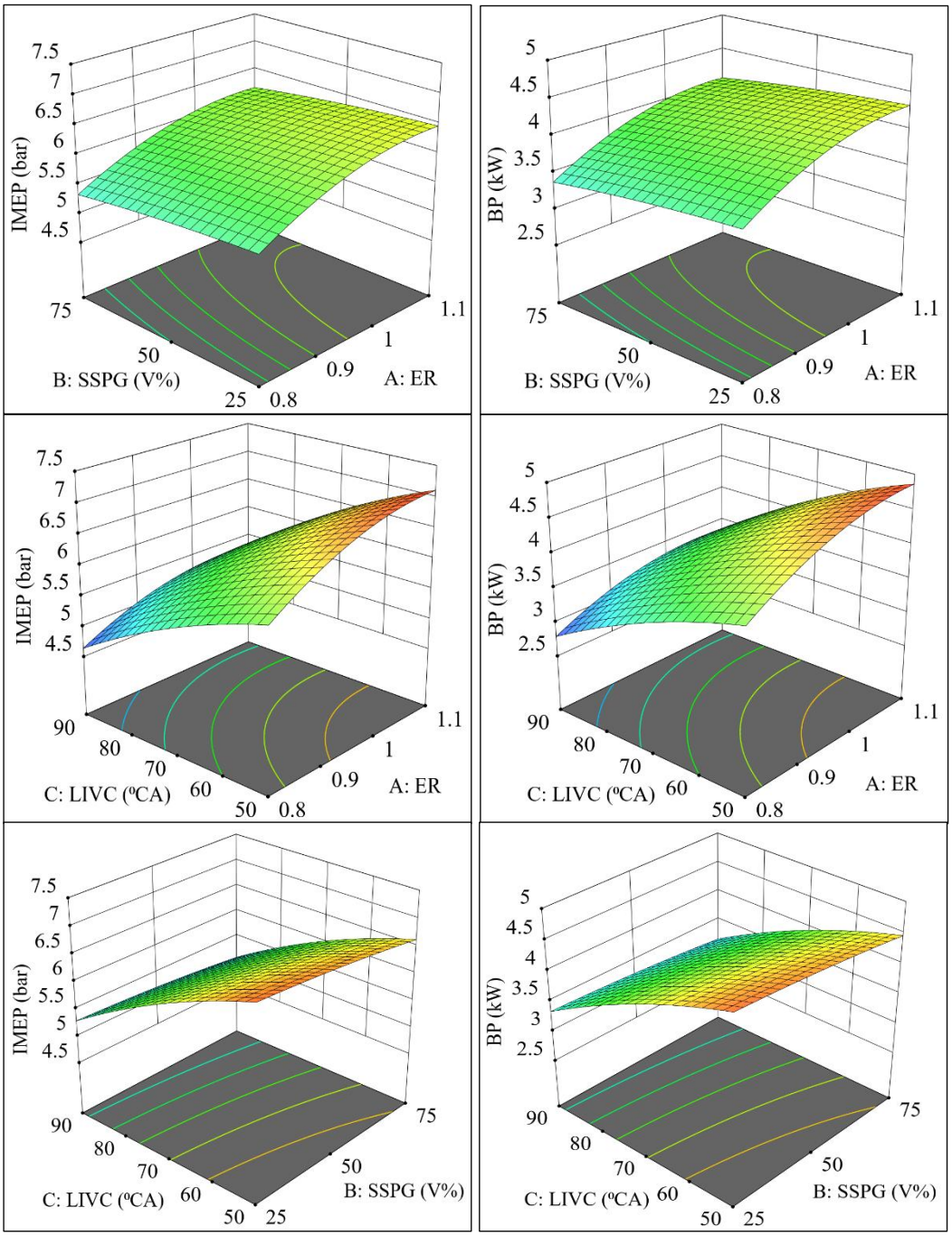


Figure 4.4.4. Simultaneous effects on power-representing parameters

***4.4.4.3.*** Brake Thermal Efficiency

Brake thermal efficiency (BTE) is a vital performance parameter to compare the fuel-to-power conversion in IC engine operations[110]. Figure 4.4.5 shows the impacts of simultaneous input variations on BTE. It was observed that relative to the increase in ER, BTE exhibits a minor initial increment pattern, followed by a sharper decline from around 0.86-0.92 ER. Maximum

BTE variations were observed for 75% SSPG fraction and 50º LIVC, where a 1.48% initial increase from 0.8 to 0.9 ER, followed by a 6.72% decrease was observed from 0.9 to 1.1 ER. This prominent decline in thermal efficiency with increasing ER could signify the enhanced incomplete combustion of fuel blends occurring inside the chamber, as claimed in [129]. Besides this, increasing the SSPG fraction is observed to increase BTE gradually (by a minimum of 5.16%). This pertains to the improved combustion resulting from increased $H_2$, CO, and other readily combustible content in SSPG intake [48]. It is also noticed that increasing the input response of LIVC results in a slight decrease of BTE (max. by 1.46%). This is due to the decreasing trapped fuel-air charge and volumetric efficiency when LIVC is increased, which lowers heat release and enhances incomplete combustion, which results in lower BTE [128]. The maximum BTE of 28.76% was observed for 0.9 ER, 75% SSPG, and both 60º and 70º LIVC inputs, which is in line with the observed effects.

***4.4.4.4.*** Brake-specific energy consumption

The parameter brake-specific energy consumption (BSEC) is considered in this study as this research utilizes two fuel compositions (methane and SSPG) with varying energy densities [134, 135]. The product of the net calorific value and the BSFC determined BSEC [189]. Figure 4.4.5 also depicts the effects of simultaneous input variations on BSEC. BSEC is typically inversely proportionate to the engine brake thermal efficiency [135]. Therefore, an inverse trend to BTE could be verified for BSEC relative to simultaneous variations in input parameters. With ER increase, the BSEC is observed to typically increase by a minimum of 11.75%. BSEC increase typically depicts combustion deterioration [189], thereby confirming ineffective combustion at greater ERs. This could arise due to the presence of significant inert gas concentrations ($N_2$ = 53% and $CO_2$ = 15%) in PG. The presence of these significants decreases LHV and reduces energy input [26]. BSEC is also observed to decrease with the increase of SSPG-fraction(by a minimum of 4.89%) certainly due to increasing conversion

efficiency attributing to improved combustion resulting from increased $H_2$ content in SSPG intake [48]. With the LIVC increase, the BSEC response is also found to increase a little (by at most 2.46%). This increase could certainly pertain to the decrease in volumetric efficiency as valve closure is delayed[128].

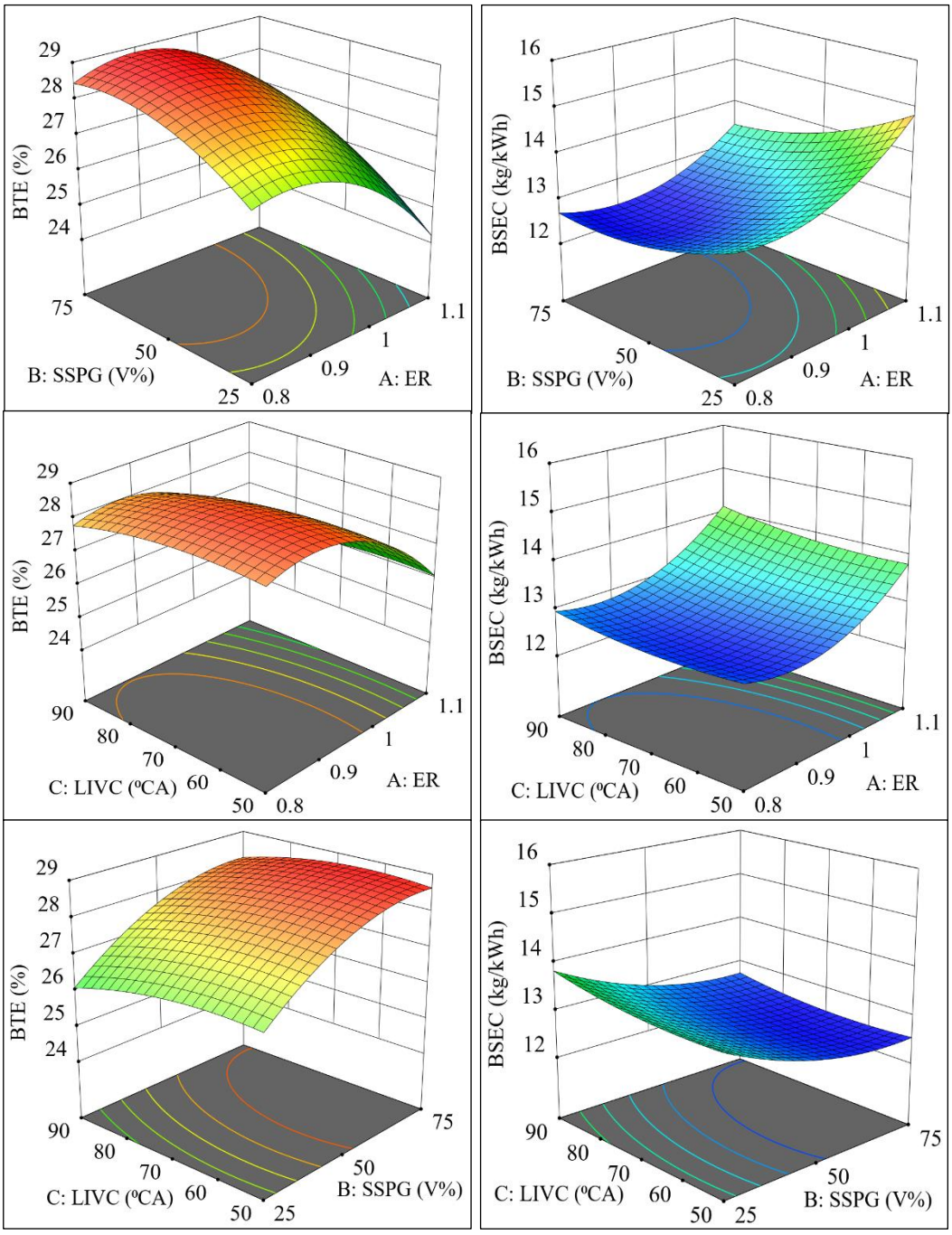


Figure 4.4.5. Simultaneous effects on efficiency-representing parameters

***4.4.4.5.*** CO emission

Carbon monoxide (CO) emission from IC engines is an important parameter to check the combustion quality as it chiefly indicates incomplete combustion [153, 207]. Figure 4.4.6 depicts the predicted effects of simultaneous input variations on CO emission. It is observed that increasing ER results in a simultaneous exponential-type rise in CO emissions. The maximum increase in CO was observed for 90º LIVC and 75% SSPG fraction, where CO outputs are 0.14, 0.9, 0.82, and 2.65(V%) respective to ER inputs of 0.8, 0.9, 1 and 1.1 (1.943% max. rise). Greater ERs result in lower BTE and increased BSEC outputs possibly due to deteriorated combustion inside the cylinder[129]. Incomplete combustion would result in increased CO-emission output[129]. It is observed that with increasing SSPG-fraction, the CO-emission gradually increased by around 12.28%. Increasing SSPG-fraction at intake could cause combustion instability due to decreasing flame speed of fuel-air charge [110, 191]. This consequently increases the CO-emission. PG has a low flame speed, calorific value, and even flammability limit as discussed in the introduction. Therefore, many works [39, 45, 222, 223] reported reduced brake power and unstable combustion by PG application in IC engines as fuel. Increasing LIVC is further observed to lay a minor decrease in CO response (by at most 8.33%). This decrement could be attributed to the low carbon content in PG-blended fuel composition[26]. As anticipated, the minimum CO-emission at the exhaust valve was computed to be 0.11 V% using the QDTM simulation for 0.8 ER, 25% SSPG, and all the 70º, 80º and 90º LIVC input settings, thus justifying the discussed CO-development reasonings.

***4.4.4.6.*** NO emission

The Zeldovich mechanism was used to project NO emission pertaining to its non-equilibrium behavior [220]. Nitrogen fraction at the intake charge is greater attributed to its greater fraction in both SSPG (53 V%) and the induced air (78 V%). Nitrogen is an inert gas at normal temperature and it only reacts at temperatures over $1100^0$C, producing nitrogen oxides [208,

209]. Effects of simultaneous input variations on NO-emission are also presented in Figure 4.4.6. It is observed that NO-emission initially increases with an increase in ER. Further, it peaks at 0.86-0.98 ER range and then decreases precipitously for any SSPG% or LIVC input values. The obtained NO-emission trend is in good agreement with the experimentally found nitrogen oxide variations from those from Szwaja [49]. Initially, the NO-emission increases with the rise in ER (by a minimum of 131.46% between ER 0.8 to 0.9). This might be attributed to an increase in the fuel content, which enables more combustion and increased chamber temperature. The following NO-emission decrease at greater ERs (by at least 664.3% from ER 0.9 to 1.1) possibly occurs for decreased improper combustion, and consequently reduced chamber temperature. Increasing SSPG also stimuluses NO decrease (by at most 26.95%) attributing to lowering in-cylinder temperature as combustion-heat release decreases. This attributes to increase of inert gases factions like $N_2$ and $CO_2$, which decreases LHV of SSPG [26]. Increasing the LIVC parameter also results in a NO-emission decrease by max 10.61%. As LIVC increases, the volumetric efficiency necessarily decreases, which tends to decrease end-gas temperature as well [154]. Therefore, the NO generation also tends to decrease along with an expected reduction in knocking.

Similar to the CO-NO tradeoff patterns, the trends in CO-$NO_X$ tradeoffs could also be verified with respect to richer Methane-SSPG fuel-blend equivalence ratios in the experimental reference work of Szwaja et al. [49]. The work also considers similar engine configuration and fuel blend compositions. Neat methane, along with all the fuel blends, present a similar trend of increase in CO emissions and decrease in the NO or $NO_X$ emissions in both performed simulation study or the referred experimental study in the richer equivalence ratio fuel domain. A 0.98 times reduction in NO emission is predicted through the simulation for the application of 60 V% SSPG-blend fuel relative to neat methane-based SI engine performance.

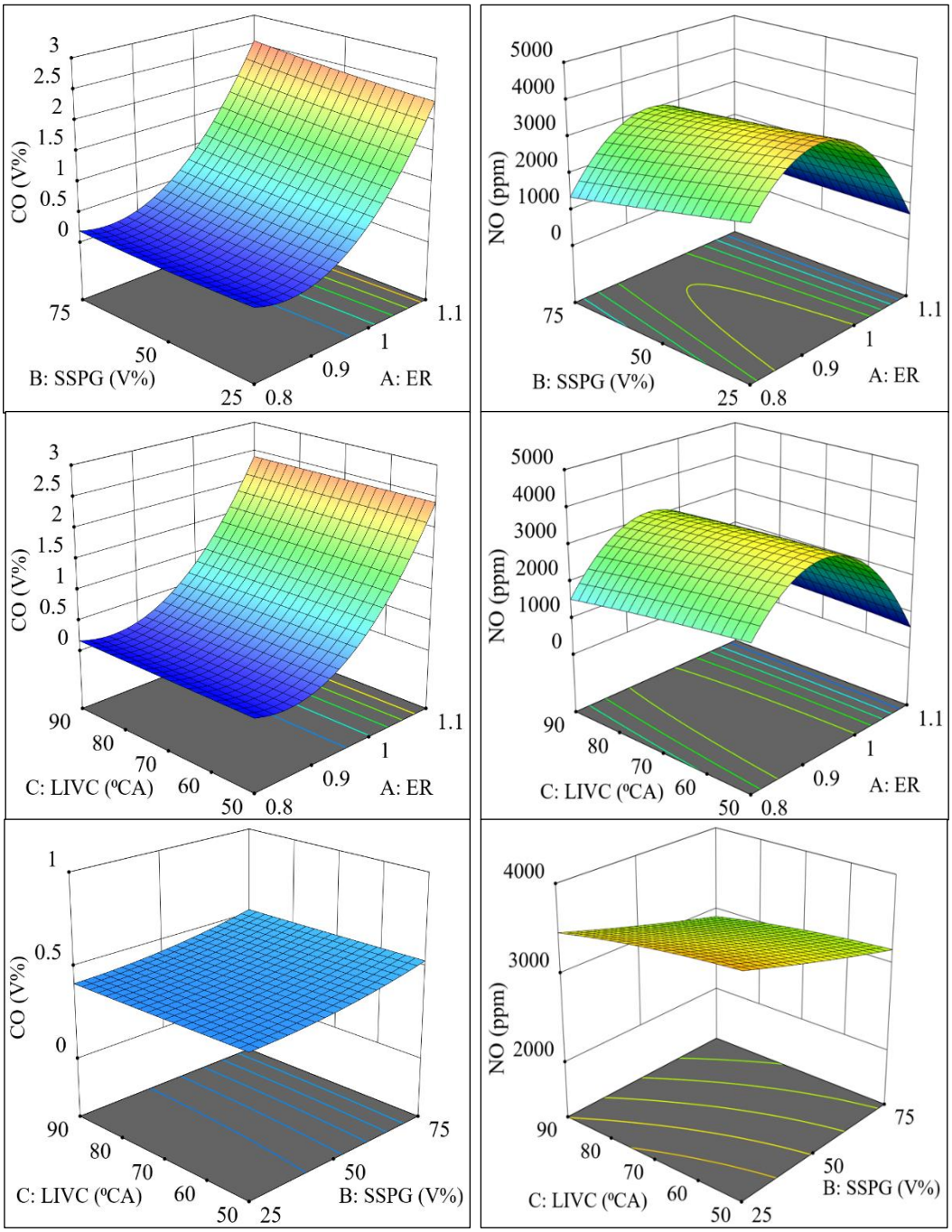


Figure 4.4.6. Simultaneous effects on considered emission parameters

Table 4.18: Relative engine performance improvements in the investigations

| | **Experimental works (100 % methane)** | **Performed Simulation (methane + SSPG)** | **% inc. or dec.** |
|---|---|---|---|
| **IMEP** | 4.5 bar (neat $CH_4$, [49]) | 6.79 ($CH_4$-blending) | 32% ↑ |
| **BMEP** | 5.49 bar(neat $CH_4$, [49]) | 6.11 ($CH_4$-blending) | 10.94% ↑ |
| **BP [49]** | 3.95 kW(neat $CH_4$, [49]) | 4.079 (LIVC Miller Cycle) | ~ |

| | | | |
|---|---|---|---|
| **BTE** | 21.8 (neat $CH_4$, [49]) | 27.95 (LIVC Miller Cycle) | 27.4% ↑ |
| **BP** | 5.4 kW (60 V% PG, [26]) | 22.6 bars (60 V% PG, 3bars PIVC) | 4.2 times ↑ |
| **NO** | 5370 ppm | 2631 ppm | 0.49 times ↓ |

### 4.4.5. Optimization and confirmation, findings

RSM-based multi-objective optimization operation considering the constrained configurations resulted in an optimum dataset that retained a cumulative desirability value of 0.843. Cumulative Desirability is a dimensionless number that depicts the overall desirability of the optimized result with regard to the optimization goals [131]. Individual desirability values for IMEP, BP, BTE, BSEC, CO, and NO were found to be 0.51, 0.51, 0.968, 0.97, 0.99, 0.627 and 0.843, respectively. Typically, a result with a composite desirability of more than 0.7, with an $R^2$-value greater than 80% is considered highly acceptable[217]. With considerably high $R^2$-values of responses and composite desirability, the RSM depiction of the model results was adequate. The optimum IMEP, BP, BTE, BSEC, and CO, NO emissions are respectively found as 5.9063 (bar), 3.8558 (kW), 28.6001%, 12.596 (MJ/kWh), 0.1349 (V%), and 2045.29 (ppm). The optimum independent inputs of ER, SSPG, and LIVC are found as 0.8143, 68.2374(V%), and 55.9339º (ABDC) respectively. The ramp view of the optimizer results and the individual desirability corresponding to all the response parameters are also presented in Figure 4.4.7 and Figure 4.4.8. Regression model accuracy is further established by running a confirmation simulation run at the optimum inputs. Table 4.19 presents the optimum results, results obtained from the confirmation-run and the calculated deviations among them.

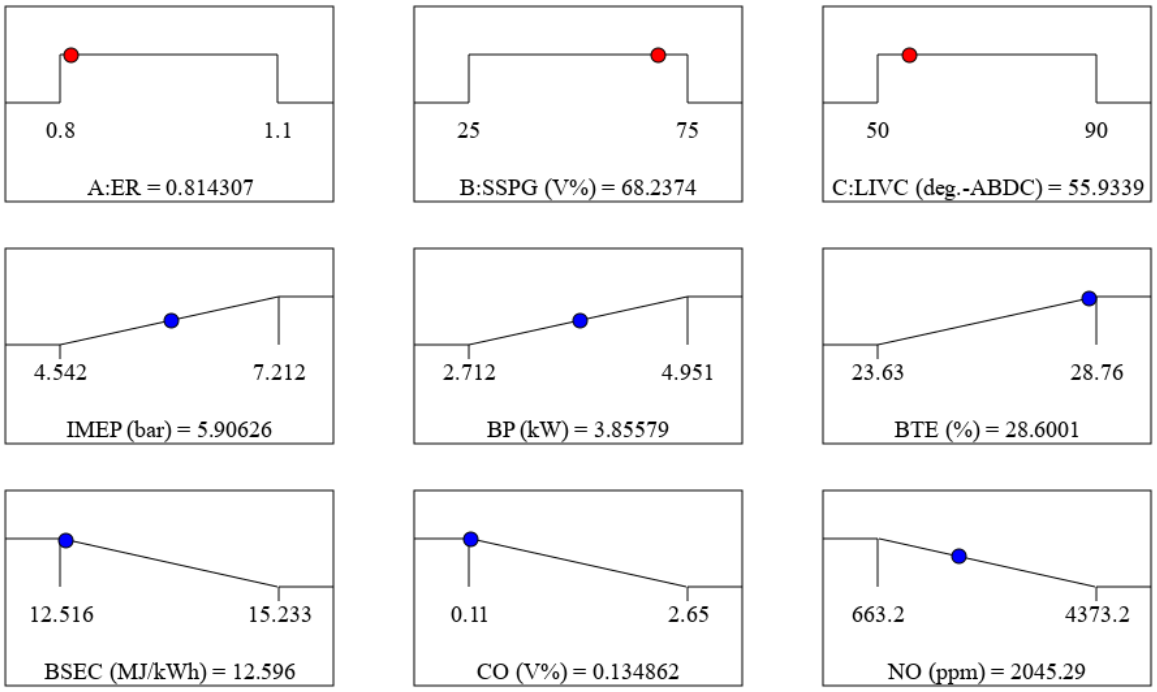


Figure 4.4.7. Ramp-view of optimized results

Table 4.19: Optimum responses and confirmation run

| **Parameters** | **IMEP (bar)** | **BP (kW)** | **BTE (%)** | **BSEC (MJ/kWh)** | **CO (V%)** | **NO (ppm)** |
|---|---|---|---|---|---|---|
| Predicted optimum responses: | 5.906 | 3.856 | 28.600 | 12.596 | 0.135 | 2045.29 |
| Simulation model results: | 5.925 | 3.872 | 28.496 | 12.633 | 0.16 | 1951.6 |
| Maximum: | 7.212 | 4.951 | 28.76 | 15.233 | 2.65 | 4373.2 |
| Minimum: | 4.542 | 2.712 | 23.63 | 12.516 | 0.11 | 663.2 |
| Deviation in predictions (%): | -0.712 | -0.714 | 2.02 | -1.36 | -0.98 | 2.52 |

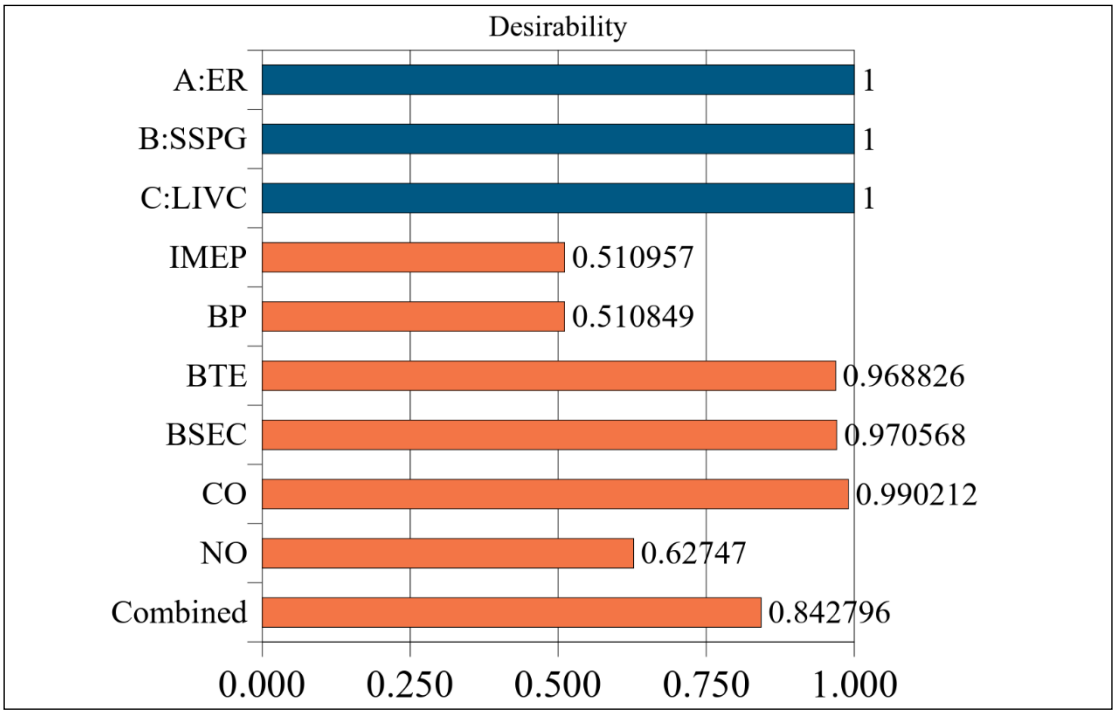


Figure 4.4.8. Parametric individual desirability values

With the close degree of accuracy projected between the statistical model results and the validated QDTM model outcomes, the following chief conclusions could be made:

- the undertaken methodology is found to have significant prediction capability for the DF-SI engine performance.
- According to ANOVA-analyzed results, the variations in SSPG and LIVC laid greater influences on performance efficiency and output power respectively.
- Engine efficiency and power output showed a significant trade-off pattern. Initially, BTE increases with ER and attains a maximum of 28.76% at 0.9 ER, thereafter the BTE decreases with further ER increment.
- With the increase in the input-factor parameter of the SSPG-blend fraction, defined for the intake fuel composition, BTE increases, BSEC decreases and BP also decreases marginally. On the other hand, with LIVC increase, the BTE response increases however the IMEP and BP decrease.

- Significant tradeoffs are also observed among the CO and NO emissions at the ER-variational range of 0.9 to 1.1. ER increase resulted in around 1.94 times increase in CO-emission and 6.64 times decrease in NO-emissions.
- The maximum brake thermal efficiency was 28.76% at 0.9ER, 75% PG, and LIVC $70^0$ABDC, while the maximum brake power was 4.95 kW at 1.0 ER, 25% SSPG, and $50^0$ABDC-LIVC.
- Optimum operating input parameters were found as 0.814 ER, 68.237% SSPG, and $55.93^0$ (ABDC-CA) LIVC.

## 4.5. Analysis of Lean-burn performance

Producer gas is a captivating alternative fuel for SI engines. However, owing to the low calorific value, the gas-powered engine suffers power and efficiency derating. Lean burn improves efficiency; however, it reduces engine power. Therefore, novel investigation strategies of intake-pressure boosting and Late inlet-valve close (LIVC)-Miller cycle are chosen to improve the lean burn SI engine power and efficiency. Quasi-dimensional thermodynamic simulation is employed to evaluate SI engine performance impacts when running on Sewage sludge-based producer gas (SSPG) and methane blend for a fixed 1500 rpm and 0.8 equivalence ratio lean mixture combustion. With an objective to determine the best operational range of SSPG-fueled engine-genset, multi-objective optimization is performed over the simulated outcomes. Design-of-experiment configured 75 simulation trial outcomes set were employed through RSM to predict the optimal inputs. Therefore, orienting towards originality, the present research study is linked to the goals as presented below:

- To extend the quasi-dimensional thermodynamic modelling code for simulating the dual-fuelled SI engine performance with Late inlet-valve closure and boosted intake pressure.
- Prediction and Performance assessment of lean burn SI engine operating with three input variables (SSPG Blending with Methane, LIVC, and SOI).
- Determination of optimum input conditions using the RSM optimizer tool to maximize brake-thermal and fuel-specific energy efficiency-cum-power, besides minimizing emissions.
- Prediction of additional power and efficiency improvement by employing the intake pressure boosting strategies.

## 4.5.1. Validation (performance and emissions)

***4.5.1.1.*** Simulation Model Validation

The experimental findings from ref.[49] are utilized to validate the programmed quasi-dimensional (QD) model. To do so, the pressure vs. crank angle outputs from both, the referred experimentation report and the simulation model, were compared. The acknowledged results are presented simultaneously in the plots within Figure 4.5.1.-(A). The crank angle deviations corresponding to the experimental and simulated pressure outcomes were found within 5%. Additionally, the crank angle position corresponding to the peak pressure match precisely. To inspect the QD model closeness with the experimental outcomes for 20%, 40%, and 50% SSPG-methane blend operations, Figure 4.5.1.-(B,C,D) present BP versus relative air-fuel ratios plots. Observed deviation from the experimental BP outcomes was also within 6.6% for various blend proportions. The minuscule encountered deviations could account for the misfiring and multi-cyclic variations in experimental results. Overall, the model traced the experimental results very closely and henceforth, the validated QD model is further implemented for obtaining the performance and emission outcomes for the various innovative input parameter combinations.

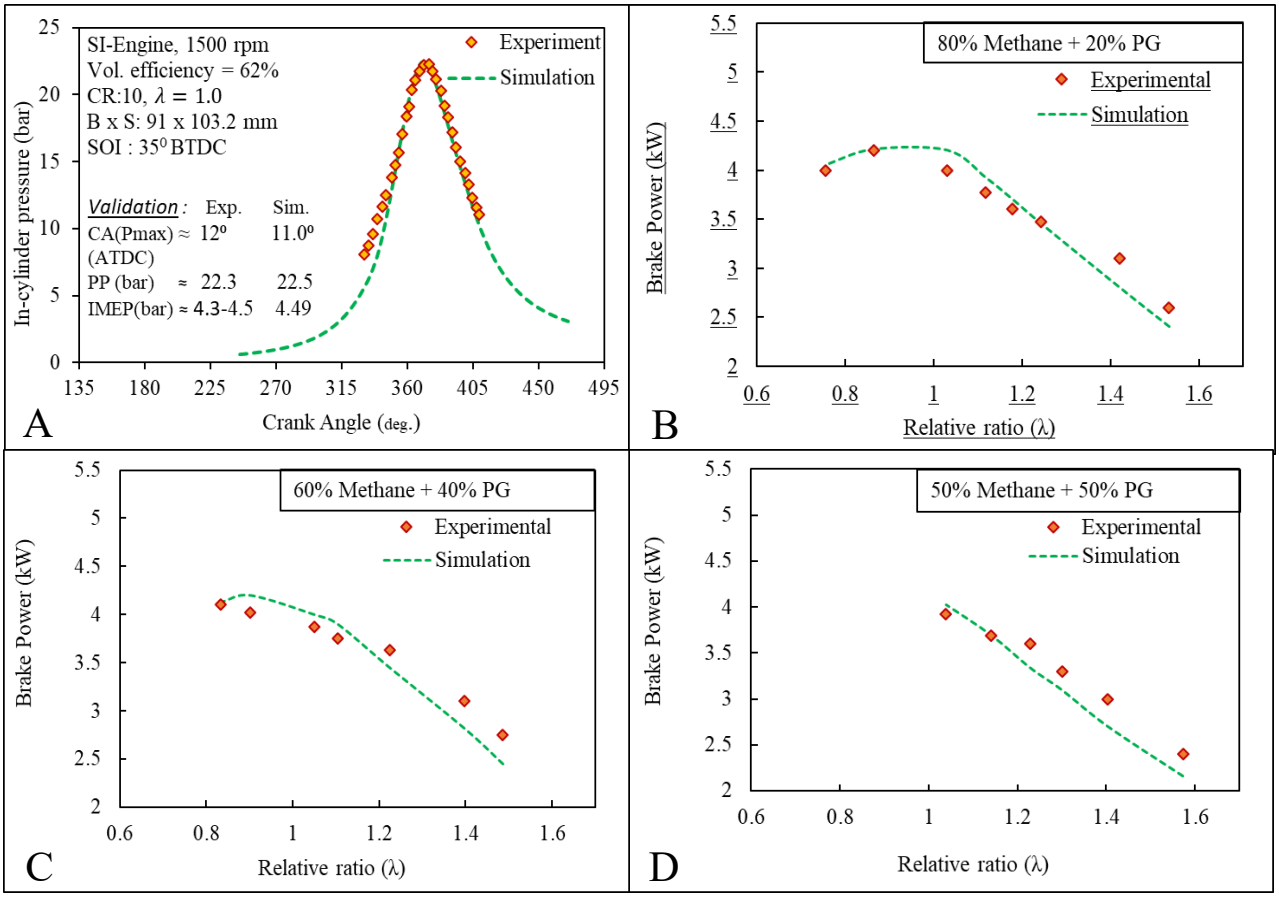


Figure 4.5.1. Simulation Validation for neat and blended SSPG

## 4.5.2. Numerical vs. Prediction of regressions

A design matrix was constructed considering an organized iteration of the simulation model as per subsequent variations of individual input parameters. This resulted in a design matrix of 75 data sets. Figure 4.5.2 consolidates the accurate tracing of QDTM model outcomes by the RSM-obtained statistical model. It collectively depicts the predicted versus actual output plots for all the output parameters. In these plots, the ordinate represents predicted response values, and the abscissa represents actual simulation outcomes. Thus, the inclined diagonal bisecting line represents a perfectly matching trace [169]. The predicted data points are observed to lie remarkably close to the QD model's actual outcomes. Thus, the regression model is found to predict the actual simulation outcomes very precisely [169, 211].

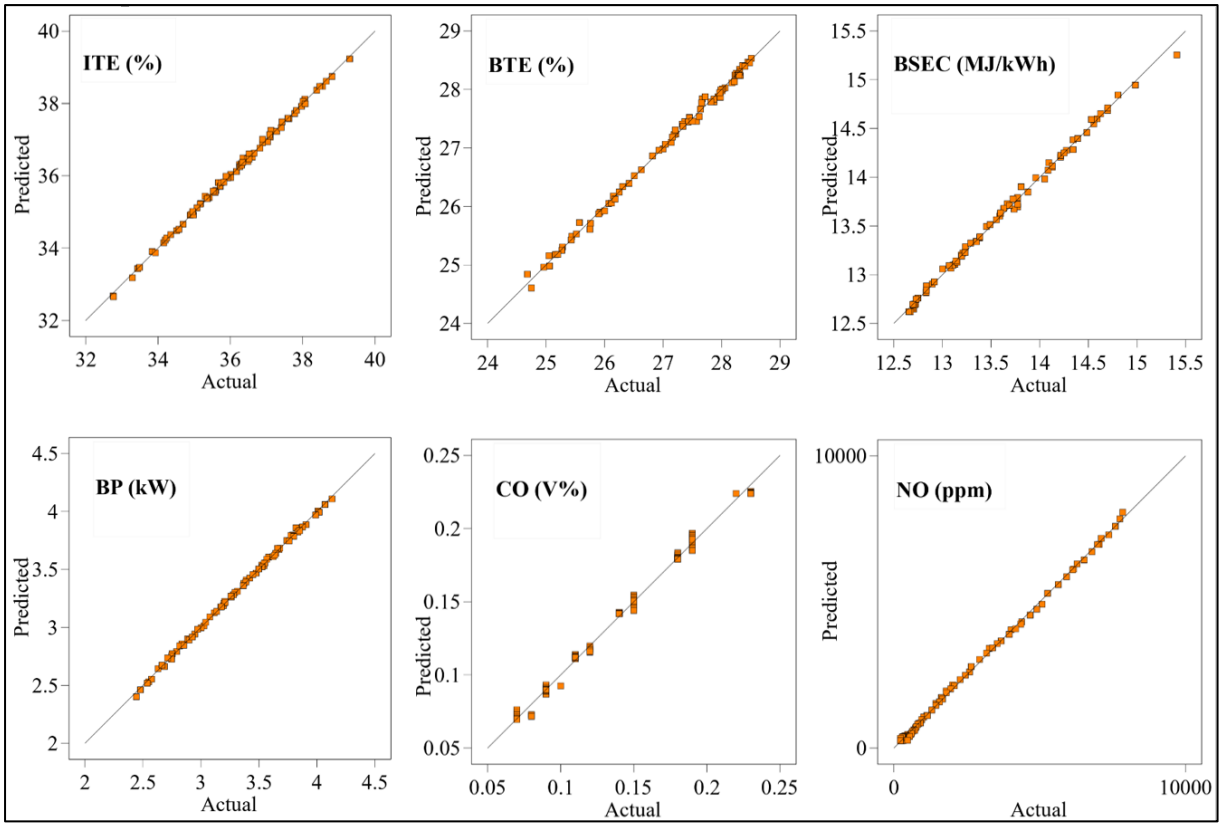


Figure 4.5.2. Numerical vs. Predicted response plots

### *4.5.2.1.* RSM regression analysis

Six diverse output parameters, including four performance (ITE, BTE, BSEC, and BP) and two emissions parameters (CO and NO emissions) are considered as responses in the RSM analysis, the correspondingly developed regression models are inclusive in application[224]. Regression models corresponding to each performance and emissions response are also presented in the supplementary file as equations 1-6.

Concerning the regression analysis, a greater coefficient of determination ($R^2$) for responses conveys a precise tracing of actual QD-model outcomes by the fitting coefficients in the regression equation [190, 195]. For this RSM model, the obtained $R^2$-values of all responses remain satisfactorily high (greater than 0.99). Further, general constraints for a consistent fit are that the predicted and adjusted $R^2$ values ($R_{pred}^2$ and $R_{adj}^2$) should vary by less than 0.2, with $R_{adj}^2$ being closer to unity for effective response estimation [191]. The $R^2$-values, along with

predicted and adjusted $R^2$-values for each response parameter are presented through fit statistics shown in Table 4.20. Additionally, Adeq. Precision is significantly more than 4. It is a signal-to-noise proportion factor that assists regression fit verification. All required constraints are well within the satisfactory constraints, thus the statistical model is expected to effectively predict the exact outcomes.

Table 4.20: Fit Statistics

| **Particular** | **ITE** | **BTE** | **BSEC** | **BP** | **CO** | **NO** |
|---|---|---|---|---|---|---|
| **$R^2$** | 0.9983 | 0.9967 | 0.9968 | 0.9989 | 0.9949 | 0.9989 |
| **Adjusted $R^2$** | 0.9981 | 0.9963 | 0.9964 | 0.9987 | 0.9942 | 0.9987 |
| **Predicted $R^2$** | 0.9976 | 0.9953 | 0.9954 | 0.9984 | 0.9930 | 0.9985 |
| **Adeq. Precision** | 275.4861 | 153.5464 | 176.0666 | 296.4273 | 121.2789 | 247.3834 |

***4.5.2.2.*** ANOVA for the quadratic regression model

RSM-obtained results are subjected to ANOVA analysis to assess their goodness of fit [190]. These analysis results are presented in Table 4.21 and Table 4.22 in supplementary file respectively, for the performance and emission responses. F-values signify the degree of influence. Greater F-values for a particular factor (or input) indicate its higher influence on the corresponding response [195]. Whereas, p-value is a significant indicator of a valid response model. Less than 0.05 p-value confirms the model's significance [202].

Table 4.21: ANOVA analysis for the performance parameters

| **Source** | **df** | **ITE** | | **BTE** | | **BSEC** | | **BP** | |
|---|---|---|---|---|---|---|---|---|---|
| | | F-value | p-value | F-value | p-value | F-value | p-value | F-value | p-value |
| **Model** | 9 | 4301.66 | < 0.0001 | 2193.19 | < 0.0001 | 2283.27 | < 0.0001 | 6547.95 | < 0.0001 |
| **A-SSPG** | 1 | 806.09 | < 0.0001 | 9.42 | 0.0031 | 4314.84 | < 0.0001 | 2417.44 | < 0.0001 |
| **B-LIVC** | 1 | 15622.27 | < 0.0001 | 406.68 | < 0.0001 | 284.60 | < 0.0001 | 50159.92 | < 0.0001 |
| **C-SOI** | 1 | 891.24 | < 0.0001 | 772.93 | < 0.0001 | 592.24 | < 0.0001 | 272.11 | < 0.0001 |
| **AB** | 1 | 80.07 | < 0.0001 | 21.66 | < 0.0001 | 21.77 | < 0.0001 | 73.31 | < 0.0001 |

| | | | | | | | | |
|---|---|---|---|---|---|---|---|---|
| **AC** | 1 | 970.26 | < 0.0001 | 840.77 | < 0.0001 | 705.43 | < 0.0001 | 230.15 | < 0.0001 |
| **BC** | 1 | 898.23 | < 0.0001 | 785.40 | < 0.0001 | 679.21 | < 0.0001 | 273.93 | < 0.0001 |
| **$A^2$** | 1 | 219.43 | < 0.0001 | 52.91 | < 0.0001 | 1111.69 | < 0.0001 | 33.35 | < 0.0001 |
| **$B^2$** | 1 | 108.28 | < 0.0001 | 215.48 | < 0.0001 | 168.08 | < 0.0001 | 591.90 | < 0.0001 |
| **$C^2$** | 1 | 19119.03 | < 0.0001 | 16633.45 | < 0.0001 | 12671.61 | < 0.0001 | 4879.43 | < 0.0001 |

Table 4.22: ANOVA analysis for the emission parameters

| **Source** | **df** | **CO** | | **NO** | |
|---|---|---|---|---|---|
| | | F-value | p-value | F-value | p-value |
| **Model** | 9 | 1422.45 | < 0.0001 | 6366.76 | < 0.0001 |
| **A-SSPG** | 1 | 791.77 | < 0.0001 | 1306.22 | < 0.0001 |
| **B-LIVC** | 1 | 10.56 | 0.0018 | 462.04 | < 0.0001 |
| **C-SOI** | 1 | 11546.36 | < 0.0001 | 49986.98 | < 0.0001 |
| **AB** | 1 | 3.96 | 0.0508 | 1.70 | 0.1966 |
| **AC** | 1 | 63.34 | < 0.0001 | 583.93 | < 0.0001 |
| **BC** | 1 | 0.1077 | 0.7438 | 123.93 | < 0.0001 |
| **$A^2$** | 1 | 145.64 | < 0.0001 | 0.1237 | 0.7262 |
| **$B^2$** | 1 | 0.1539 | 0.6961 | 7.44 | 0.0082 |
| **$C^2$** | 1 | 240.11 | < 0.0001 | 4828.46 | < 0.0001 |

It is observed in ANOVA tables that the p-value of each response model is within the required degree of significance. Thus, the overall statistical model is valid and significant. Attributing to greater F-values, the engine's BP outcome and Indicated thermal efficiency (ITE) are found highly influenced by LIVC-variation. Spark timing (SOI) variation is found to lay greater influence over BTE, whereas the blend-proportion (SSPG) variations influence the Brake specific energy consumption (BSEC) greatly. The CO and NO emission at the IVC is found very sensitive to the SOI variation pertaining to significant F-values and satisfactory p-values. This effect certainly relates to the significant influence of spark timing over the combustion performance in SI Engines [191]. Considering the square-term interactions, SOI variation laid a prominent influence over all the considered engine-performance responses.

### 4.5.3. Optimum Prediction, confirmation

According to the laid optimization configurations and constraints, the obtained optimal result of maximum composite desirability(D) is considered for declaration. Figure 4.5.3 presents these optimal outcomes in a ramp-view mode. Aiming for better performance and lesser emissions, the optimal input conditions are found as 49.717% SSPG blend, 63.305º LIVC (ABDC), and about 38.69º SOI (BTDC). The corresponding response outcomes as per the multi-objective prediction were 36.56% ITE, 28.24% BTE, 12.703 (MJ/kWh) BSEC, 3.69 (kW) BP, 0.11(V%) of CO emission and 1601.15 ppm NO emission. Moreover, Table 4.23 presents the outcomes from the simulation-based confirmation run for verification of the predicted optimum. The prediction deviation is found satisfactory and less than 5%.

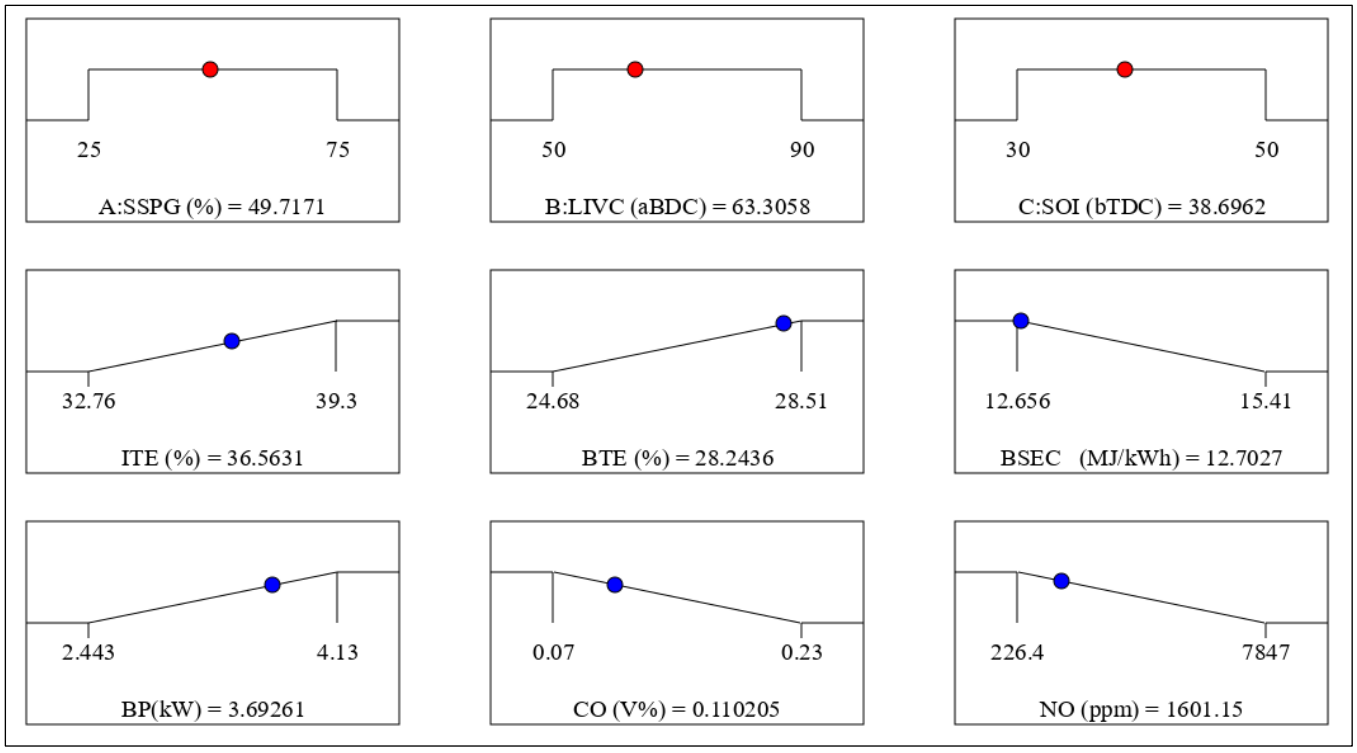


Figure 4.5.3. Ramp-view of optimized results

Table 4.23: Confirmation run for optimum responses

| **Parametric responses:** | **ITE (%)** | **BTE (%)** | **BSEC (MJ/kWh)** | **BP (kW)** | **CO (V%)** | **NO (ppm)** |
|---|---|---|---|---|---|---|
| Predicted optimum responses: | 36.56 | 28.24 | 12.702 | 3.69 | 0.11 | 1601.15 |
| Simulation-model results: | 37.0 | 28.65 | 12.560 | 3.76 | 0.11 | 1530.10 |
| Deviation in predictions (%): | -1.18% | -1.43% | 1.13% | -1.86% | 0 % | 4.64% |

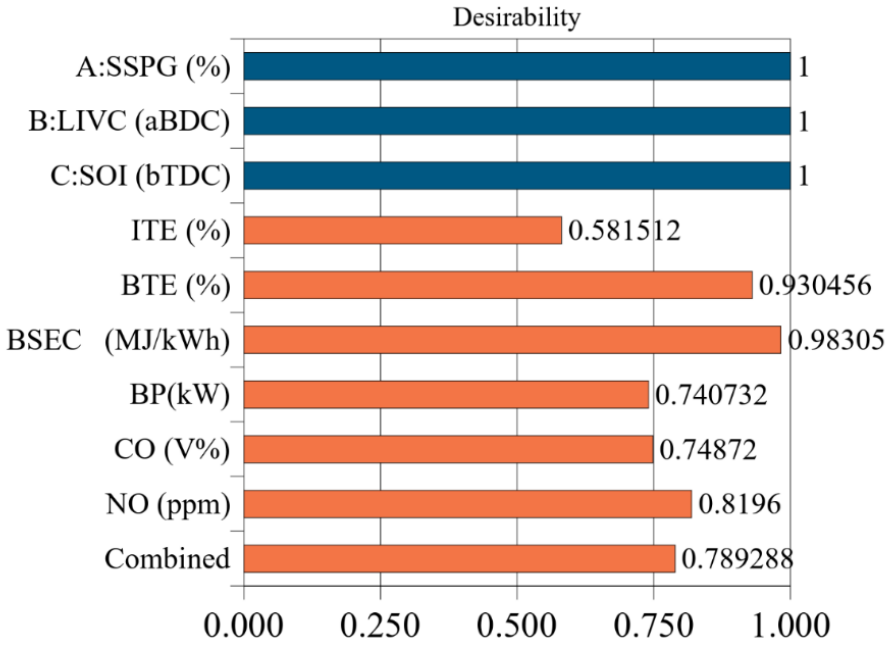


Figure 4.5.4. Parametric Individual desirability values

Individual desirability(d) values for the optimal variables are also shown in Figure 4.5.4. The desirability value is dimensionless. And, it ranges from 0 to 1, where 0 represents an unacceptable result, and 1 indicates a desirably constrained ideal result[131]. Typically, an optimization outcome with desirability(D) of exceeding 0.8, and $R^2$-values greater than 0.8 (80%) depicts a passable optimization result[217]. The D for the generated statistical model values 0.798, with the $R^2$-values of all responses being greater than 0.99. Thus, D is satisfactorily close to the critical degree of significance, and the optimization model is considered acceptable. Based on the optimal results presented in Figure 4.5.3, the optimal BTE and BSEC responses are observed attaining close to the maximum and minimum limits respectively, and therefore retain greater desirability values. However, from Figure 4.5.4, it is

noticed that both ITE and BP display relatively lower d. As already discussed, the indicated efficiency and the output power demonstrate high trade-offs relative to LIVC variation. As the conducted multi-objective optimization laid equal weightage for both power and efficiency response terms, the d for both ITE and BP dropped. To overcome this limitation, an innovative action of boosting intake pressure at IVC could benefit.

### 4.5.4. Intake boosting and findings

An increase in LIVC has been observed to increase ITE and also BTE, though up to 60º CA delay. However, power reduces, and this can be effectively improved by primarily available techniques of intake pressure boosting and increasing CR[26, 102]. In comparison to these strategies, the intake pressure boosting strategy is found more effective in improving SI engine power, especially in the case syngas-fuelled SI engine without compromising the efficiency[102]. This is certainly attributed to an increase in volumetric efficiency and increased syngas fuel input[102]. To confirm IVC-pressure boosting benefits, the QDTM-based simulation was utilized in this study, which includes the strategy to further improve the optimized input/output as shown in Figure 4.5.3 (inputs: 49.717% SSPG blend, 63.305º LIVC and about 38.69º SOI). Accordingly, the simulated impacts of boosting the intake pressure at IVC from 0.75 to 1.25 and 1.5 bars on engine performance are presented in Figure 4.5.5. It could be observed that boosting intake pressure to 1.5 bars resulted in around a 2.63% increase in ITE with a 1.9 times increment in output BP as well. A significant reduction in BSEC, by nearly 18% is also observed. However, boosting intake pressure considerably increased the NO-emission (by about 0.49 times), whereas the CO-emission declined by 0.18 times. The increment in NO is certainly attributed to increased chamber temperature and pressure pertaining to intake-pressure boosting[26]. Thermal NO contributes the major fraction in the $NO_X$ formation[186] and its emission could be reduced utilizing the additions of conventional catalytic exhaust after-treatment systems[26]. Thus, in overall, this result shows that the

strategy of 0.8 ER lean-burn mixture with boosted intake pressure could lead to an increase in both BP as well as BTE. As a result, this approach demonstrates that it might be effectively used to improve the additional power and efficiency of SI engines.

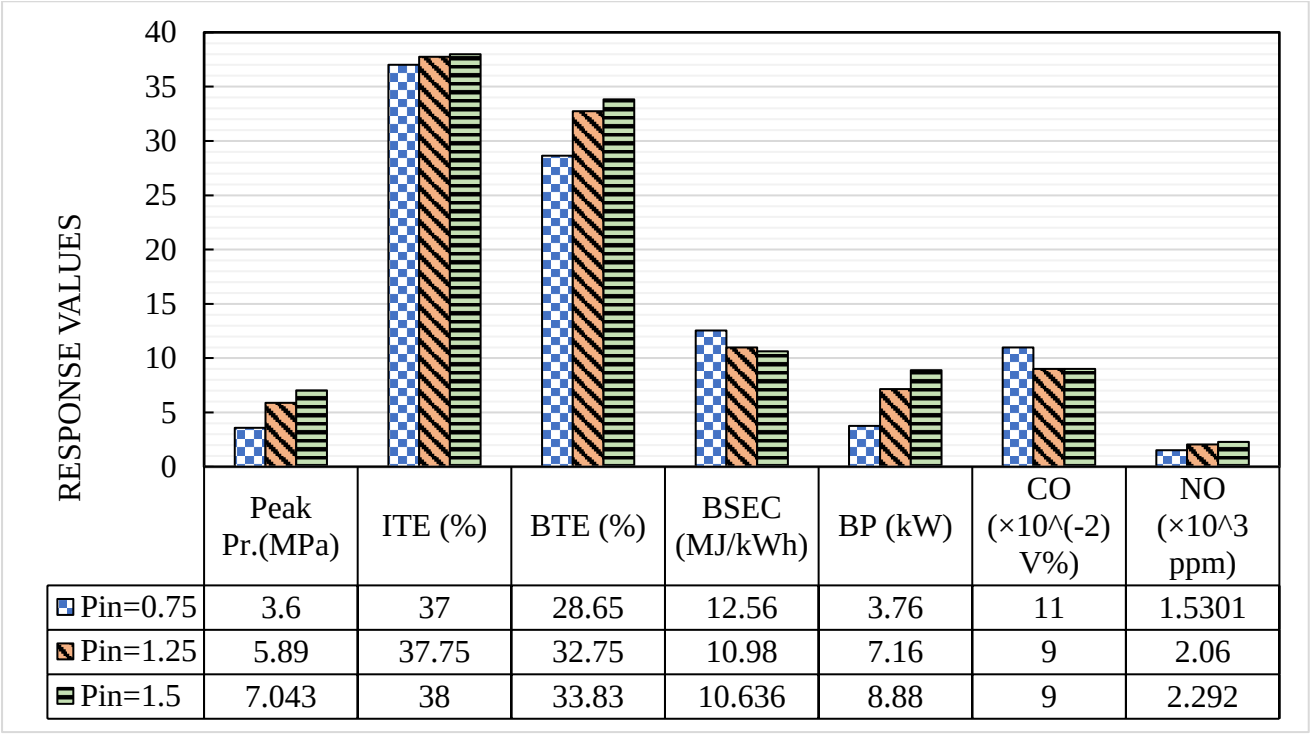


| | Peak Pr.(MPa) | ITE (%) | BTE (%) | BSEC (MJ/kWh) | BP (kW) | CO (×10^(-2) V%) | NO (×10^3 ppm) |
|---|---|---|---|---|---|---|---|
| Pin=0.75 | 3.6 | 37 | 28.65 | 12.56 | 3.76 | 11 | 1.5301 |
| Pin=1.25 | 5.89 | 37.75 | 32.75 | 10.98 | 7.16 | 9 | 2.06 |
| Pin=1.5 | 7.043 | 38 | 33.83 | 10.636 | 8.88 | 9 | 2.292 |

Figure 4.5.5. Effects of Boosting Intake Pressure

Based on simulation results, the following significant conclusions have been drawn:

- A quasi-dimensional thermodynamic model was validated and used to simulate parametric responses of dual fuel mode spark ignition engine, with successful analysis through RSM-based optimization.
- Indicated thermal efficiency increases with increment of LIVC, the maximum ITE was found to be 39.3% at LIVC 90ºABDC, 40º SOI, 75% SSPG. However, the BSEC tends to be unfavorable beyond 70º LIVC (ABDC).
- The optimum magnitudes of operating conditions were obtained as 49.71% SSPG-blend, 63.3º (ABDC) LIVC, and 38.7º (BTDC) SOI.

- The optimum response outputs are 36.56% ITE, 28.24% BTE, 12.7(MJ/kWh) BSFC, 3.6(kW) BP, 0.11(V%) CO, and about 1601 ppm NO-emission.
- With the application of a boosted intake charge from 0.75 to 1.5 bars, ITE improved by 2.7% and the BP increased by around 1.36 times. Regarding emission, CO-emission decreased by 0.18 times, however, NO emission increased by 0.49 times as a demerit.

In summary, the thermodynamic numerical method and RSM-based optimization execution revealed that the application of the miller cycle strategy by increasing LIVC resulted in a slight increase in indicated thermal efficiency and a decrease in CO, and NO emissions, with an unfavorable decrease in output power. However, applying boosted intake pressure at IVC, showed a beneficial increase in both output power (BP) as well as thermal efficiencies (ITE and BTE). Moreover, in the future, the present numerical model could be very helpful in thermodynamic and experimental studies on SI engines considering other engine parameters and when fueled with other alternate fuels.

## 4.6. Extending QDTM to PG-Propane blends

In this study, the novel approach of blending grape wood-based producer gas with propane as fuel has been investigated to increase the power and efficiency of SI engines while reducing pollutants. Similar to the simulation approaches applied in previous investigations, the SI engine performance analysis for these particular fuel blends was also carried out with QDTM and RSM-based regression, and multi-objective optimization strategies. To accomplish the quasi-dimensional thermodynamic modelling, a similar simulation model was employed with two-zone(burn and unburn zone) combustion to mimic SI engine performance at 1500 rpm. However, the thermo-physical and chemical properties of the specific compone ts of the intake fuel were altered. Table 4.24 presents these particular thermophysical properties.

Table 4.24: Values for Propane-Grape PG blend constants

| **Value** | **PG** | **Propane** |
|---|---|---|
| *A* | 2.0 | 2.18-0.8(Ø-1.0) |
| *B* | -0.4 | -0.16 +0.22(Ø-1.0) |
| $S_{ref}$ | 0.56-0.827(Ø-1.186)$^2$ | 0.342-1.387(Ø-1.08)$^2$ |
| *Polynomial Coefficient for Internal energy(J/kmolK)* | $U_1$= -490.4x10$^5$ | $U_1$= -0.7722x10$^8$ |
| | $U_2$= 20050.34 | $U_2$= -14.532x10$^3$ |
| | $U_3$= 1.3988 | $U_3$= 155.48 |
| | $U_4$= 5.1931x10$^{-3}$ | $U_4$= 0.05447 |
| | $U_5$= 1.70609x10$^{-6}$ | $U_5$= 8.4227x10$^{-6}$ |
| | $U_6$= -1.4003x10$^7$ | $U_6$= 50.99x10$^6$ |

Satisfactory model validation was observed by utilizing an experimental report and thereafter the simulation was run as per the Design of Experiment's RSM strategy to envisage parametric impacts and confirm multi-objective optimization. To enhance the SI engine performance, equivalence ratio (ER), compression ratio (CR), ignition timing (IT), and propane blending fraction (BF) with PG were considered as parametric operating settings. Also, to determine the

best operating condition, an optimization was conducted with the best response of performance regarding Brake-thermal efficiency (BTE), Brake-mean effective pressure (BMEP), Brake specific fuel consumption (BSFC), and emissions reduction of Carbon monoxide (CO), Nitrous monoxide (NO). Response regressions were modelled using ANOVA, and optimal output responses were predicted accurately using an RSM-based response optimizer. Moreover, to determine the minimum utilization of propane for best response of engine performance an additional case of multi-objective optimization was carried out. Overall, it was found that blending and optimization strategies provided improvement in SI engine performance.

Thus, considering the above research gap, this study aimed to promote grape-based PG fuel generation through gasification by an assurance of simulated assessment of engine performance and CO-NO emissions. Accordingly, the present study includes the following main objectives:

- To study the compatibility of dual fuel mode engine operation using QDTM-simulation approach to assist better engine operating prediction.
- To interpret the variation of engine performance and emission responses with regard to the variations in the four decision/input parameters.
- To demonstrate the specific response sensitivities towards various factor parameters through ANOVA.
- Determining the optimum operating setting for envisaging the best engine response (i.e., enhanced performance and diminished emissions).

The energy transition necessitates the adoption of new energy sources and sustainable technologies. In this respect, optimizing operating variables can significantly improve the performance of the engine for decentralized electricity generation. Further, this article will

guide engine researchers on modelling and optimization techniques for improving the performance of dual-fuel SI engines using PG fuels with blends.

## 4.6.1. QDTM yields with Propane-blending

***4.6.1.1.*** Simulation methods overview

Intending to assess the performance proofing before experimentation and saving substantial resources, cost, and time investment, an engine modelling and simulation tool could offer a more anticipated platform[54-57]. It enables parametric engine performance predictions particularly in the early phases of engine design [58]. Literature works present the available engine simulation methodologies as zero/one-dimensional (0D/1D) [55, 59], multi-zone-capable three-dimensional (like, CFD) and quasi-dimensional modelling techniques [55, 60], and Computational Fluid Dynamics (CFD) modelling [61, 62]. The QD model circumvents the limitations of 0D and 1D models and thus is a more accurate simulation technique [54]. Besides this, the 3D-CFD simulation depends on the sizes of the computational mesh and requires higher computational resources. Therefore, the QD combustion modelling is substantially practiced to predict and investigate the SI turbulent combustion without penalizing the prediction accuracy [63]. It has been reviewed in the literature [68, 70, 72, 73] that despite the rising attention on biomass and gasification-based alternate fuel sources for SI engines, very few publications report on the quasi-dimensional numerical modelling and on further integration of optimization to declare the optimal settings which best enhance the engine performance and reduce emissions. Thus, utilizing grape-producer gas blended with propane as fuel composition for predicting engine performance responses through the FORTRAN-coded QDTM model and Response surface methodology (RSM) is a novelty in this literature.

### 4.6.2. Validation (performance, emissions)

Both the experimentally inferred [39] and the simulated in-cylinder pressure versus crank angle tracings are plotted simultaneously in Figure 4.6.1-(A and B). Figure 4.6.1-(A) represents validation plots for neat propane-based engine operations, whereas Figure 4.6.1-(B) displays the trace maps for the engine simulation outcome when constrained with the input blended fuel composition of 45 % Propane with 55% PG. For validation purposes, the SI engine specifications were set collinear with the experimental specifications (272 $cm^3$ displacement volume and 10 CR). Information regarding the model validation is detailed within the figures. Simulation traced experimental outcomes very closely during both the compression and expansion periods. With respect to Figure 4.6.1-(A and B), the experimental to simulated peak pressure difference was observed to be 0.3% error with 5º CA for pure propane and 5% error with 4º CA for 55% PG-blend with propane. However, small deviations of less than +1.33% and -0.4% were observed for the 55% PG-blend and the 100% propane operations, respectively corresponding to the crank-angle positions at attained peak pressures. These minute deviations might possibly be attributed to cycle-to-cycle variations and misfiring that are prone in experimental results [39]. For further consolidation of the model validation, the model's validation has been presented with respect to Pressure-CA, output brake power with respect to PG-blends, and CO, NO emissions.

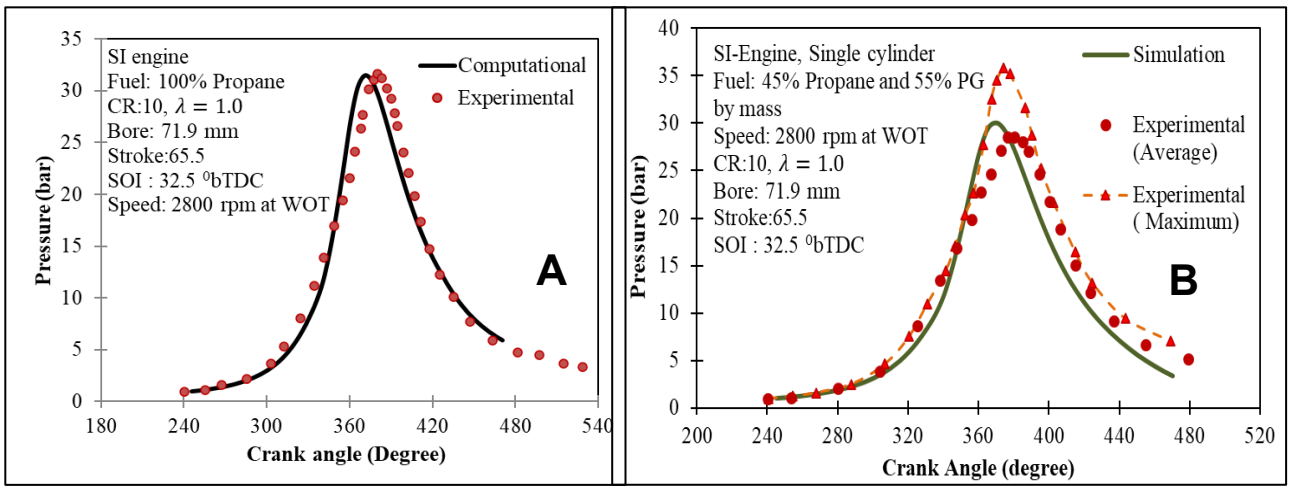


Figure 4.6.1. Simulated and Experimental outcomes for validation

For further consolidation of the developed QDTM-based simulated prediction model, the modelled in-cylinder pressure-crank angle (P-θ), output BP and the CO and NO-emissions are validated at the following, using an available experimentation reference (Swaja et. al. [49]). Accordingly, the engine specifications, PG-calorific value, and the PG composition (as 16% CO, 13% $H_2$, 3% $CH_4$, 53% $N_2$, and 15% $CO_2$ (volume-fraction percentages) were set.

The simultaneous trace of simulated and experimental P-θ curves are plotted in Figure 4.6.2. Figure 4.6.3 additionally confirmed the close trace by QDTM for the BP for the methane-PG blend. With a satisfactory degree of closeness in the traced experimental outcomes (less than 5%), the QDTM simulation model is considered valid for predicting the dual-fuel engine performance with PG. Figure 4.6.4 presents the simulated and experimental CO-outcomes plotted together. Pertaining to the close tracing capability of the experimental CO-outcomes, the QDTM-based simulation is considered valid for CO-emissions. As the reference experimentation[49] lacked NO outcomes, it was validated for three different PG-compositions (as variety-A, B, and C) using the experimental results from reference-[225]. By incorporating the specific engine specifications of the reference work, the simulated NO-outcome deviated only by 0.04 to 0.08 (*g/kWh*, absolute deviation) (Table 4.25).

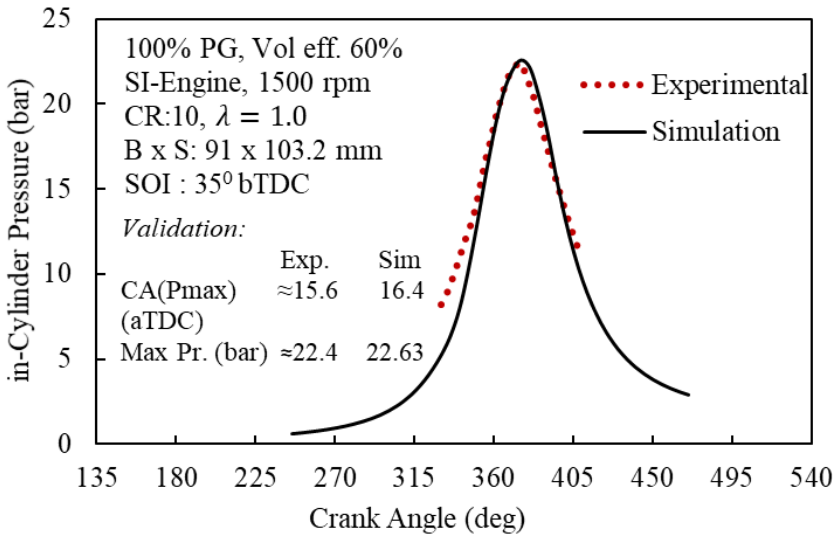

Figure 4.6.2. P-crank angle validation

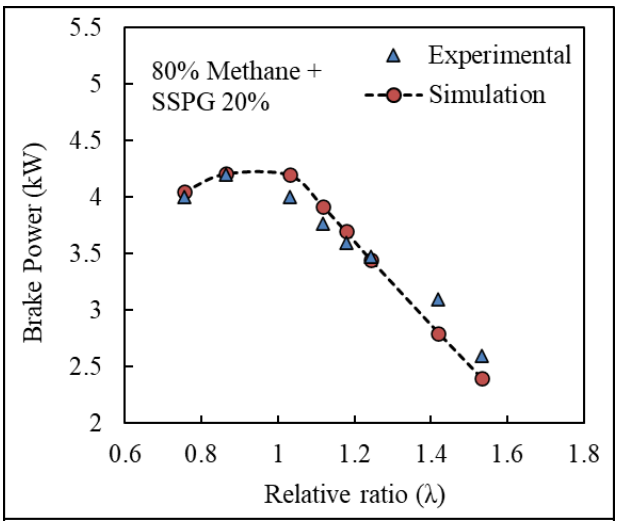


Figure 4.6.3. BP- Relative ratio validation

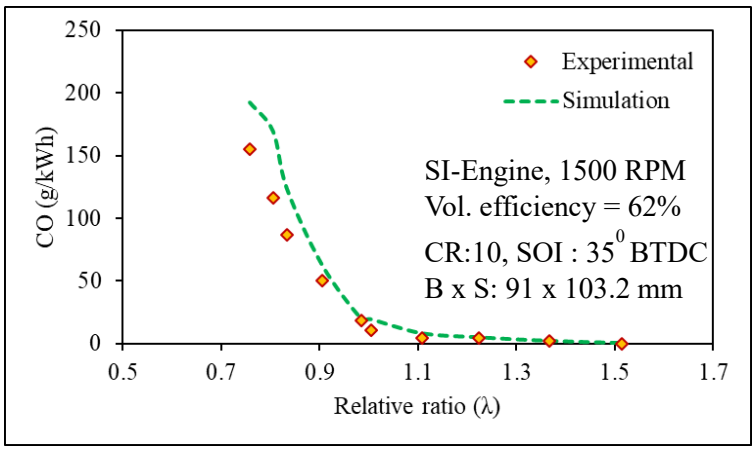


Figure 4.6.4. CO- Relative ratio emission validation

Table 4.25: Validation for NO

| PG-types | PG-composition | | | | | Experimental NO (g/kWh) | Simulated NO (g/kWh) | Deviation (g/kWh) |
|---|---|---|---|---|---|---|---|---|
| | $H_2$ | CO | $CH_4$ | $CO_2$ | $N_2$ | | | |
| A | 16 | 18 | 1 | 12 | 53 | 1.15 | 1.12 | 0.03 |
| B | 16 | 18 | 2.5 | 12 | 51.5 | 0.81 | 0.85 | -0.04 |
| C | 16 | 18 | 4 | 12 | 50 | 0.87 | 0.79 | 0.08 |

### 4.6.3. Effective propane-blending extent

The effectiveness of the adopted QDTM simulation model is initially validated and then simulated iteratively as per the organized design matrix. The obtained results are respectively presented in Table 4.26.

Table 4.26: Parameter settings plan along with the responses and simulation results

**For 20 (V%) Propane blend fraction in PG-Propane mix:**

| Trial no. | **BF** (V%) | **ER** | **CR** | **IT** (ºCA) | **CD** (ºCA) | **CA** (ºCA) | **PP** (bars) | **BMEP** (bars) | **BSFC** (kg/kWh) | **CO** (V%) | **NO** (ppm) |
|---|---|---|---|---|---|---|---|---|---|---|---|
| 1 | 20 | 0.9 | 10 | 37.5 | 147.65 | 9.2 | 34.852 | 5.7 | 0.825 | 0.36 | 2100.1 |
| 2 | 20 | 0.9 | 10 | 42.5 | 155.15 | 7.7 | 42.29 | 6.058 | 0.776 | 0.44 | 3504.6 |
| 3 | 20 | 0.9 | 10 | 45 | 157.65 | 7.2 | 45.07 | 6.0828 | 0.773 | 0.47 | 4008.2 |
| 4 | 20 | 0.9 | 12 | 37.5 | 147.65 | 7.2 | 41.24 | 5.709 | 0.804 | 0.36 | 2118.8 |
| 5 | 20 | 0.9 | 12 | 42.5 | 152.65 | 6.4 | 47.038 | 6.002 | 0.765 | 0.42 | 3028.9 |
| 6 | 20 | 0.9 | 12 | 45 | 155.15 | 5.9 | 50.054 | 6.077 | 0.756 | 0.45 | 3488.1 |
| 7 | 20 | 0.9 | 14 | 37.5 | 147.65 | 5.9 | 47.4 | 5.667 | 0.795 | 0.36 | 2106.9 |
| 8 | 20 | 0.9 | 14 | 42.5 | 155.15 | 4.9 | 57.95 | 6.06 | 0.745 | 0.46 | 3480.6 |
| 9 | 20 | 0.9 | 14 | 45 | 157.65 | 4.4 | 61.94 | 6.088 | 0.742 | 0.49 | 3958.9 |
| 10 | 20 | 1 | 10 | 37.5 | 147.65 | 9.4 | 37.55 | 6.373 | 0.811 | 0.82 | 1620.2 |
| 11 | 20 | 1 | 10 | 42.5 | 152.65 | 8.4 | 42.84 | 6.58 | 0.785 | 0.88 | 2054.1 |
| 12 | 20 | 1 | 10 | 45 | 155.15 | 7.9 | 45.77 | 6.614 | 0.781 | 0.91 | 2283.2 |
| 13 | 20 | 1 | 12 | 37.5 | 147.65 | 7.4 | 44.112 | 6.399 | 0.788 | 0.82 | 1529.8 |
| 14 | 20 | 1 | 12 | 42.5 | 152.65 | 6.7 | 50.502 | 6.622 | 0.762 | 0.89 | 1955.5 |
| 15 | 20 | 1 | 12 | 45 | 155.15 | 6.2 | 54.05 | 6.657 | 0.758 | 0.92 | 2180.7 |
| 16 | 20 | 1 | 14 | 37.5 | 147.65 | 6.2 | 50.793 | 6.392 | 0.776 | 0.82 | 1467.6 |
| 17 | 20 | 1 | 14 | 42.5 | 152.65 | 5.4 | 58.3 | 6.624 | 0.749 | 0.89 | 1884.1 |
| 18 | 20 | 1 | 14 | 45 | 155.15 | 5.2 | 62.217 | 6.659 | 0.745 | 0.92 | 2093.2 |
| 19 | 20 | 1.2 | 10 | 37.5 | 119.15 | 9.7 | 38.106 | 6.45 | 0.927 | 5.31 | 188.4 |
| 20 | 20 | 1.2 | 10 | 42.5 | 108.77 | 8.4 | 43.55 | 6.64 | 0.9008 | 5.27 | 248.3 |
| 21 | 20 | 1.2 | 10 | 45 | 99.77 | 7.9 | 46.707 | 6.701 | 0.8936 | 5.28 | 294.2 |
| 22 | 20 | 1.2 | 12 | 37.5 | 117.77 | 7.7 | 44.901 | 6.491 | 0.901 | 5.25 | 175.6 |

| | | | | | | | | | | | |
|---|---|---|---|---|---|---|---|---|---|---|---|
| 23 | 20 | 1.2 | 12 | 42.5 | 104.65 | 6.7 | 51.63 | 6.714 | 0.871 | 5.22 | 242 |
| 24 | 20 | 1.2 | 12 | 45 | 104.4 | 6.4 | 54.836 | 6.734 | 0.868 | 5.2 | 264.2 |
| 25 | 20 | 1.2 | 14 | 37.5 | 120.15 | 6.2 | 51.42 | 6.472 | 0.889 | 5.23 | 162.2 |
| 26 | 20 | 1.2 | 14 | 42.5 | 105.65 | 5.7 | 59.302 | 6.713 | 0.857 | 5.19 | 223.5 |
| 27 | 20 | 1.2 | 14 | 45 | 103.9 | 5.2 | 63.39 | 6.74 | 0.853 | 5.16 | 247.3 |

**For 40 (V%) Propane blend fraction in PG-Propane mix:**

| Trial no. | **BF** | **ER** | **CR** | IT | **CD** | **CA** | **PP** | **BMEP** | **BSFC** | **CO** | **NO** |
|---|---|---|---|---|---|---|---|---|---|---|---|
| 28 | 40 | 0.9 | 10 | 37.5 | 147.65 | 9.4 | 36.102 | 6.06 | 0.5211 | 0.33 | 2269.3 |
| 29 | 40 | 0.9 | 10 | 42.5 | 152.65 | 8.4 | 41.308 | 6.32 | 0.5004 | 0.39 | 3253.5 |
| 30 | 40 | 0.9 | 10 | 45 | 155.15 | 7.9 | 43.923 | 6.366 | 0.496 | 0.41 | 3738.6 |
| 31 | 40 | 0.9 | 12 | 37.5 | 147.65 | 7.4 | 42.57 | 6.09 | 0.506 | 0.34 | 2265.9 |
| 32 | 40 | 0.9 | 12 | 42.5 | 152.65 | 6.7 | 48.855 | 6.36 | 0.485 | 0.39 | 3248.1 |
| 33 | 40 | 0.9 | 12 | 45 | 155.15 | 6.2 | 52.025 | 6.41 | 0.482 | 0.42 | 3722.8 |
| 34 | 40 | 0.9 | 14 | 37.5 | 147.65 | 6.2 | 49.174 | 6.088 | 0.4989 | 0.34 | 2284.2 |
| 35 | 40 | 0.9 | 14 | 42.5 | 152.65 | 5.4 | 56.31 | 6.358 | 0.4778 | 0.4 | 3221.7 |
| 36 | 40 | 0.9 | 14 | 45 | 155.15 | 5.2 | 60.034 | 6.413 | 0.473 | 0.43 | 3683.6 |
| 37 | 40 | 1 | 10 | 37.5 | 147.65 | 9.9 | 39.193 | 6.78 | 0.515 | 0.79 | 1713.4 |
| 38 | 40 | 1 | 10 | 42.5 | 152.65 | 8.7 | 44.78 | 6.944 | 0.503 | 0.85 | 2151.7 |
| 39 | 40 | 1 | 10 | 45 | 153.65 | 8.4 | 46.015 | 6.952 | 0.502 | 0.87 | 2242 |
| 40 | 40 | 1 | 12 | 37.5 | 147.65 | 7.9 | 46.063 | 6.84 | 0.498 | 0.79 | 1618.5 |
| 41 | 40 | 1 | 12 | 42.5 | 152.65 | 6.9 | 52.838 | 7.013 | 0.486 | 0.85 | 2048.7 |
| 42 | 40 | 1 | 12 | 45 | 154.65 | 6.7 | 55.836 | 7.019 | 0.486 | 0.88 | 2229.6 |
| 43 | 40 | 1 | 14 | 37.5 | 147.65 | 6.4 | 53.073 | 6.864 | 0.489 | 0.79 | 1552.4 |
| 44 | 40 | 1 | 14 | 42.5 | 152.65 | 5.4 | 61.04 | 7.038 | 0.477 | 0.86 | 1976.2 |
| 45 | 40 | 1 | 14 | 45 | 155.15 | 5.4 | 65.187 | 7.04 | 0.477 | 0.89 | 2184.5 |
| 46 | 40 | 1.2 | 10 | 37.5 | 110.52 | 10.2 | 39.64 | 6.86 | 0.597 | 5.22 | 172.7 |
| 47 | 40 | 1.2 | 10 | 42.5 | 100.77 | 8.9 | 45.53 | 7.04 | 0.581 | 5.19 | 238.6 |
| 48 | 40 | 1.2 | 10 | 45 | 97.77 | 8.2 | 48.78 | 7.06 | 0.5805 | 5.19 | 269.4 |
| 49 | 40 | 1.2 | 12 | 37.5 | 111.15 | 8.2 | 46.589 | 6.931 | 0.577 | 5.16 | 161.2 |
| 50 | 40 | 1.2 | 12 | 42.5 | 100.9 | 7.2 | 53.719 | 7.124 | 0.562 | 5.13 | 220.2 |

| | | | | | | | | | | | |
|---|---|---|---|---|---|---|---|---|---|---|---|
| 51 | 40 | 1.2 | 12 | 45 | 97.77 | 6.7 | 57.68 | 7.138 | 0.5609 | 5.12 | 247.8 |
| 52 | 40 | 1.2 | 14 | 37.5 | 112.15 | 6.7 | 53.65 | 6.95 | 0.566 | 5.11 | 151.8 |
| 53 | 40 | 1.2 | 14 | 42.5 | 100.77 | 5.9 | 62.012 | 7.15 | 0.5507 | 5.09 | 204.7 |
| 54 | 40 | 1.2 | 14 | 45 | 96.77 | 5.4 | 66.414 | 7.159 | 0.55 | 5.1 | 227.8 |

**For 60 (V%) Propane blend fraction in PG-Propane mix:**

| Trial no. | **BF** | **ER** | **CR** | IT | **CD** | **CA** | **PP** | **BMEP** | **BSFC** | **CO** | **NO** |
|---|---|---|---|---|---|---|---|---|---|---|---|
| 55 | 60 | 0.9 | 10 | 37.5 | 147.65 | 9.7 | 37.17 | 6.31 | 0.399 | 0.33 | 2448.7 |
| 56 | 60 | 0.9 | 10 | 42.5 | 152.65 | 8.7 | 42.395 | 6.52 | 0.386 | 0.38 | 3437.3 |
| 57 | 60 | 0.9 | 10 | 45 | 155.15 | 8.2 | 45.282 | 6.55 | 0.384 | 0.41 | 3966.1 |
| 58 | 60 | 0.9 | 12 | 37.5 | 147.65 | 7.7 | 43.883 | 6.39 | 0.3865 | 0.33 | 2449.4 |
| 59 | 60 | 0.9 | 12 | 42.5 | 152.65 | 6.9 | 50.199 | 6.58 | 0.3739 | 0.39 | 3435 |
| 60 | 60 | 0.9 | 12 | 45 | 155.15 | 6.4 | 53.703 | 6.61 | 0.372 | 0.42 | 3952.5 |
| 61 | 60 | 0.9 | 14 | 37.5 | 147.65 | 6.4 | 50.742 | 6.38 | 0.379 | 0.34 | 2469.3 |
| 62 | 60 | 0.9 | 14 | 42.5 | 152.65 | 5.7 | 58.167 | 6.607 | 0.366 | 0.39 | 3439.7 |
| 63 | 60 | 0.9 | 14 | 45 | 155.15 | 5.4 | 62.032 | 6.634 | 0.365 | 0.4 | 3913 |
| 64 | 60 | 1 | 10 | 37.5 | 145.15 | 10.9 | 37.817 | 6.919 | 0.403 | 0.76 | 1598.8 |
| 65 | 60 | 1 | 10 | 42.5 | 147.65 | 10.2 | 40.624 | 7.05 | 0.3962 | 0.79 | 1824.2 |
| 66 | 60 | 1 | 10 | 45 | 151.65 | 9.2 | 45.213 | 7.155 | 0.3905 | 0.83 | 2175.8 |
| 67 | 60 | 1 | 12 | 37.5 | 145.15 | 8.7 | 44.411 | 7 | 0.389 | 0.75 | 1504 |
| 68 | 60 | 1 | 12 | 42.5 | 147.65 | 8.2 | 47.79 | 7.14 | 0.382 | 0.78 | 1725.7 |
| 69 | 60 | 1 | 12 | 45 | 152.15 | 7.4 | 54.116 | 7.25 | 0.376 | 0.84 | 2117.7 |
| 70 | 60 | 1 | 14 | 37.5 | 145.15 | 7.2 | 51.151 | 7.04 | 0.3814 | 0.75 | 1439.7 |
| 71 | 60 | 1 | 14 | 42.5 | 147.65 | 6.7 | 55.124 | 7.184 | 0.373 | 0.78 | 1656.5 |
| 72 | 60 | 1 | 14 | 45 | 152.15 | 5.9 | 62.567 | 7.294 | 0.368 | 0.84 | 2042.1 |
| 73 | 60 | 1.2 | 10 | 37.5 | 110.65 | 11.2 | 38.05 | 6.984 | 0.4714 | 5.19 | 142.9 |
| 74 | 60 | 1.2 | 10 | 42.5 | 104.4 | 10.4 | 40.98 | 7.132 | 0.4616 | 5.18 | 176 |
| 75 | 60 | 1.2 | 10 | 45 | 97.4 | 9.2 | 47.092 | 7.272 | 0.452 | 5.16 | 237.2 |
| 76 | 60 | 1.2 | 12 | 37.5 | 111.025 | 8.9 | 44.66 | 7.068 | 0.455 | 5.13 | 132.4 |
| 77 | 60 | 1.2 | 12 | 42.5 | 104.77 | 8.4 | 48.201 | 7.223 | 0.445 | 5.12 | 163 |
| 78 | 60 | 1.2 | 12 | 45 | 95.52 | 7.4 | 55.634 | 7.36 | 0.4369 | 5.12 | 217 |

| | | | | | | | | | | | |
|---|---|---|---|---|---|---|---|---|---|---|---|
| 79 | 60 | 1.2 | 14 | 37.5 | 111.025 | 7.4 | 51.416 | 7.103 | 0.445 | 5.11 | 124.7 |
| 80 | 60 | 1.2 | 14 | 42.5 | 103.9 | 6.9 | 55.56 | 7.25 | 0.435 | 5.11 | 152 |
| 81 | 60 | 1.2 | 14 | 45 | 94.025 | 6.2 | 64.305 | 7.39 | 0.428 | 5.12 | 199.4 |

**For 80 (V%) Propane blend fraction in PG-Propane mix:**

| Trial no. | **BF** | **ER** | **CR** | IT | **CD** | **CA** | **PP** | **BMEP** | **BSFC** | **CO** | **NO** |
|---|---|---|---|---|---|---|---|---|---|---|---|
| 82 | 80 | 0.9 | 10 | 37.5 | 147.65 | 10.2 | 8.313 | 6.532 | 0.332 | 0.33 | 2655.3 |
| 83 | 80 | 0.9 | 10 | 42.5 | 152.65 | 8.9 | 43.734 | 6.689 | 0.324 | 0.38 | 3679.9 |
| 84 | 80 | 0.9 | 10 | 45 | 118.4 | 8.4 | 46.718 | 6.696 | 0.324 | 0.4 | 4211.6 |
| 85 | 80 | 0.9 | 12 | 37.5 | 147.65 | 8.2 | 45.31 | 6.613 | 0.3204 | 0.33 | 2663.6 |
| 86 | 80 | 0.9 | 12 | 42.5 | 152.65 | 7.2 | 51.88 | 6.77 | 0.3129 | 0.39 | 3684.5 |
| 87 | 80 | 0.9 | 12 | 45 | 122.65 | 6.7 | 55.27 | 6.77 | 0.3127 | 0.41 | 4172.9 |
| 88 | 80 | 0.9 | 14 | 37.5 | 145.15 | 7.2 | 48.77 | 6.486 | 0.3215 | 0.31 | 2193.5 |
| 89 | 80 | 0.9 | 14 | 42.5 | 147.65 | 6.7 | 52.47 | 6.653 | 0.3133 | 0.34 | 2887.8 |
| 90 | 80 | 0.9 | 14 | 45 | 152.65 | 5.9 | 60.203 | 6.813 | 0.3059 | 0.39 | 3692.5 |
| 91 | 80 | 1 | 10 | 37.5 | 142.95 | 11.9 | 36.93 | 7.04 | 0.342 | 0.73 | 1540.2 |
| 92 | 80 | 1 | 10 | 42.5 | 147.65 | 10.7 | 42.189 | 7.27 | 0.3311 | 0.78 | 1958.5 |
| 93 | 80 | 1 | 10 | 45 | 148.65 | 10.2 | 43.406 | 7.3 | 0.33 | 0.8 | 2050.8 |
| 94 | 80 | 1 | 12 | 37.5 | 145.15 | 9.2 | 46.183 | 7.28 | 0.323 | 0.75 | 1631.1 |
| 95 | 80 | 1 | 12 | 42.5 | 147.65 | 8.4 | 49.74 | 7.389 | 0.318 | 0.78 | 1858.6 |
| 96 | 80 | 1 | 12 | 45 | 148.65 | 8.4 | 51.216 | 7.417 | 0.317 | 0.79 | 1950.2 |
| 97 | 80 | 1 | 14 | 37.5 | 145.15 | 7.4 | 53.273 | 7.348 | 0.3148 | 0.75 | 1563.5 |
| 98 | 80 | 1 | 14 | 42.5 | 147.65 | 7.2 | 57.455 | 7.458 | 0.3102 | 0.78 | 1787.1 |
| 99 | 80 | 1 | 14 | 45 | 149.15 | 6.7 | 60.076 | 7.494 | 0.3087 | 0.8 | 1923.9 |
| 100 | 80 | 1.2 | 10 | 37.5 | 103.4 | 11.4 | 39.3 | 7.22 | 0.394 | 5.16 | 150.8 |
| 101 | 80 | 1.2 | 10 | 42.5 | 99.15 | 10.7 | 42.351 | 7.345 | 0.387 | 5.15 | 183.5 |
| 102 | 80 | 1.2 | 10 | 45 | 92.15 | 9.4 | 48.71 | 7.438 | 0.382 | 5.15 | 242.2 |
| 103 | 80 | 1.2 | 12 | 37.5 | 102.77 | 9.2 | 46.22 | 7.326 | 0.379 | 5.12 | 139.4 |
| 104 | 80 | 1.2 | 12 | 42.5 | 97.4 | 8.7 | 49.913 | 7.45 | 0.373 | 5.12 | 168.5 |
| 105 | 80 | 1.2 | 12 | 45 | 89.65 | 7.7 | 57.647 | 7.54 | 0.368 | 5.14 | 219.3 |
| 106 | 80 | 1.2 | 14 | 37.5 | 101.77 | 7.7 | 53.277 | 7.37 | 0.37 | 5.12 | 129.9 |

| | | | | | | | | | | | |
|---|---|---|---|---|---|---|---|---|---|---|---|
| 107 | 80 | 1.2 | 14 | 42.5 | 96.025 | 7.2 | 57.617 | 7.5 | 0.364 | 5.12 | 155.8 |
| 108 | 80 | 1.2 | 14 | 45 | 88.02 | 6.4 | 66.748 | 7.578 | 0.3607 | 5.15 | 200.5 |

### 4.6.4. Response Interactions

The influence of varying the Propane-blend proportions with grape-based PG fuel (BF) on the SI engine performance and emission is intercepted using the RSM-developed 3D surface plots simultaneous to ER, CR, and IT input variations as well. Discussion of their influences over BTE, BMEP, and BSFC engine performance responses and CO, NO emission responses are presented in two sections, along with the corresponding statistically developed quadratic regression models and 3D plots[199].

***4.6.4.1.*** Impacts on Performance parameters

The concurrent impacts on engine performance parameters of BTE, BMEP, and BSFC are discussed in this section. The difference between the IMEP and the empirically obtained Total-motored friction mean effective pressure (TFMEP) gives the Brake mean-effective pressure (BMEP) [132]. The differential of swept volume with the obtained BMEP results in BP whereas its quotient with the net CV of intake fuel results in BTE. Expressions that are used to integrate the engine performance parameters' models with the QDTM have been presented in equations: 8S-18S. BMEP represents a size-independent depiction of the engine brake power[116], thus it is a significant power-indicating parameter. The maximum BMEP was observed as 7.58 bars for the input operating parameters of 14 CR, 1.2 ER, and 42.5ºCA spark advance for the 20% PG-blend inputs. On the other hand, BSFC is the rate of fuel consumption to produce unit BP[221]. Lower BSFC implies greater efficiency in the conversion of specific fuel quantity into output brake power. Figure 4.6.5 demonstrates the impacts on engine performance parameters corresponding to varying input decision parameters. The corresponding regression models for BTE, BMEP, and BSFC are also presented in equations: 19S, 20S, and 21S. It is

observed from the 3D plots that greater BF inputs, along with simultaneously greater CR and IT settings would be advantageous for engine performance by increasing BTE, and BMEP. These inputs also reduce the BSFC when operating with optimum modest ER. It is also observed that, with the increase in ER, the BTE reduces significantly (max. by 16.36%). This could result from the low volumetric efficiency associated with the use of PG-fuel in an unmodified engine [48]. This effect is attributed to the reduction in the swept air volume pertaining to PG replacement at the intake fuel composition at greater ERs[48]. Reduced swept air certainly reduces the oxidizer content and without sufficient oxidization the net heat release, work output (as IMEP), and efficiency (as ITE) would degrade as observed in the figure. Additionally, an increase in BF results in significant BMEP increases (max. by 14.95%) and simultaneously decreases BSFC (max. by 59.43%). Such variation patterns essentially demonstrate the enhancements in chemical energy (in fuel) to work conversion with an increasing fraction of propane at the intake. As the neat propane-air mixture has a greater heating value (46.3 MJ/kg) compared to the Grape-based PG (4.52 MJ/kg, Table 2.4), the combustion heat release and corresponding work outputs should be more with increasing propane-fraction. It is also observed that for any BF, the BMEP peaks for richer mixtures (ER≥1.08) whereas, the BSFC tends to minimize at leaner fuel-mixes. This pattern depicts a conventional trade-off nature [82, 113], wherein the richer charge combustion confirms more heat release and power output, whereas the lean burn confirms more complete combustion, better combustion efficiency, and lower BSFC [110]. The pertaining trade-off nature signifies the multi-objective optimization objective towards finding the best operating parameter predictions to balance the power with efficiency. Additionally, peak BMEP is verified close to the modest ER optimization range in the figure, thus emphasizing the significance of multi-objective optimization for the operation. It is observed from the two-way interaction perspective that the response parameters of BTE and BSFC are more sensitive to simultaneous

changes in BF versus ER than in BF versus CR in terms of the variations range. This sensitivity could also be confirmed quantitatively through the ANOVA [193], as depicted and discussed in the ANOVA section.

A similar trend of derating power and efficiency was also observed when producer gas blends with other gaseous fuels and applications in the SI engine. This observation was attributed to the effect of lower energy density content of PG [113, 226]. Huang et al. [227] observed similar trends and obtained a maximum BTE of 26% at ER 1.0-1 for gaseous blends SI engines. Moreover, Porpatham et al. [107] observed similar trends in power and BTE results as the range of ER covered the lean misfire limit on one side to the knock limit on the rich side for the SI engine.

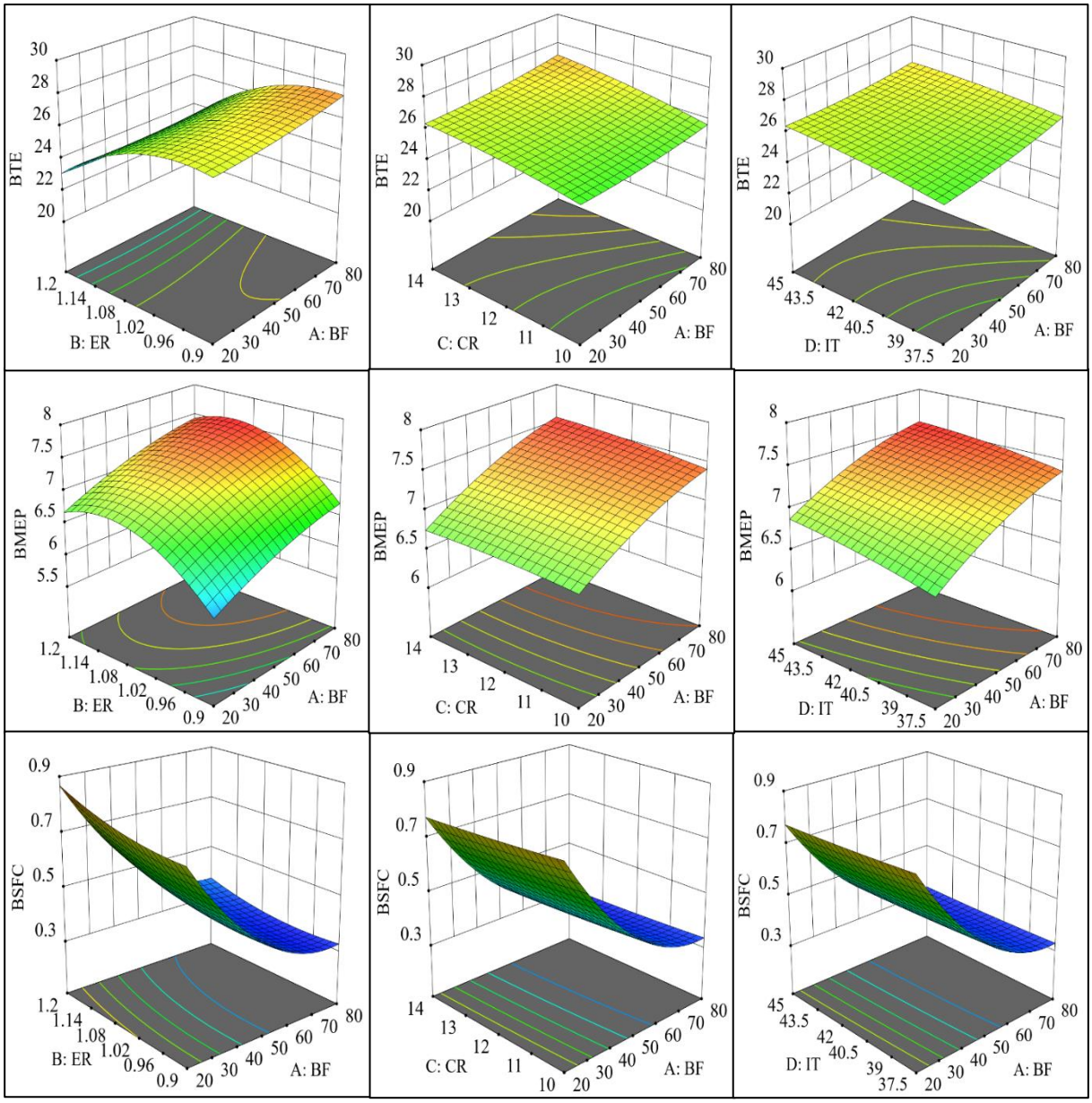


Figure 4.6.5. Impacts of BF, simultaneous CR, ER, IT variations on brake-performances

***4.6.4.2.*** Impacts on Emission parameters

The CO and NO emission parameters are exceptions to the general equilibrium algorithm, besides attributing greater reactivity and toxicity. The noxious gas of Carbon monoxide (CO) is produced during engine combustion, majorly imputing to unstable incomplete combustion, low H/C ratio in fuel compositions, or low mixture homogeneity [49, 221, 228]. On the other hand, carcinogenic Nitric oxide (NO) forms at both, the flame front and the post-flame gases. Primary factors contributing to its origin are greater gas temperature, higher oxygen

concentration, and sufficient combustion reaction time[191, 221]. A relatively greater $H_2$ and CO-contents in the utilized grape-based PG could be attributed to the increase in operational adiabatic flame temperature inside the chamber[48] and the consequent release of greater NO. However, a lower concentration of NO emission identifies improved exhaust emission characteristics[229]. Figure 4.6.6 shows the impacts of simultaneous variations in ER, CR, and IT on the CO and NO emissions corresponding to all BFs. A clear and significant trade-off is observable for CO and NO corresponding to the simultaneous BF versus ER variations. With the increase in ER, the CO-emission increases whereas the NO-emittants decrease, nearly exponentially (max. by 11.23 times increase and 13.62 times decrease, respectively). Such tradeoffs hinder the improvement in individual desirabilities of the respective emission responses and also the composite desirability of the optimal solution [193]. These trade-offs remain inline with the origin theories for the particular emittants in regard to the combustion and thermodynamic states existing inside the combustion chamber. With increasing ERs, the intake-fuel content increases and correspondingly the net content of PG also increases. Consequently, the proportion of CO and other inert gas contents(like $CO_2$ and $N_2$) also increases at the intake charge[26]. The presence of these inert contents further decreases the LHV and the chamber-temperature, attributed to the slackened exothermic oxidation [26]. This could possibly result in ineffective and improper combustion, thus increasing the CO emission and tending to decrease the NO emissions. However, with the increase in propane blend (BF), the combustion completeness and stability increase [39] and BSFC(or fuel intake) decreases (by at most 59.56% decrease). Thus, the relative amount of fuel oxidized and heat liberated for a 1500 RPM engine run could be reduced, which might result in a slight decrease in NO-emission. This is also observed clearly from simultaneous 3D plots of BF versus IT variations. Further, according to the same plot, an increase in NO emission is noticed corresponding to an increase in IT (max. by 46.78%). This pattern indicates a conventional development of an

increase in in-cylinder temperature with the advancement of ignition start (IT). IT advancement gives more combustion duration and consequent greater heat release particularly for slow flame-speed fuel like PG (at low BF). Thus, the in-cylinder temperature increases and gives rise to more NO-emission from the combustions [191]. Expression-22S and 23S present the RSM-based regression models for the emission responses of CO and NO, respectively. Though ER is observed to be the most influencing factor parameter for both CO and NO, IT also is influential regarding NO emission. Considering the two-way interaction, ER and IT would have a significant influence over the selected emissions. Towards confirming these sensitivities, the ANOVA analysis benefits and is discussed in the next section[80]. A similar trend of NO emission with the increase in PG fractions is also observed for methane-PG blends SI engine as reported by Solferini et al. [226]. Moreover, Park et al.[230] observed similar trends in NO emission with blend fractions.

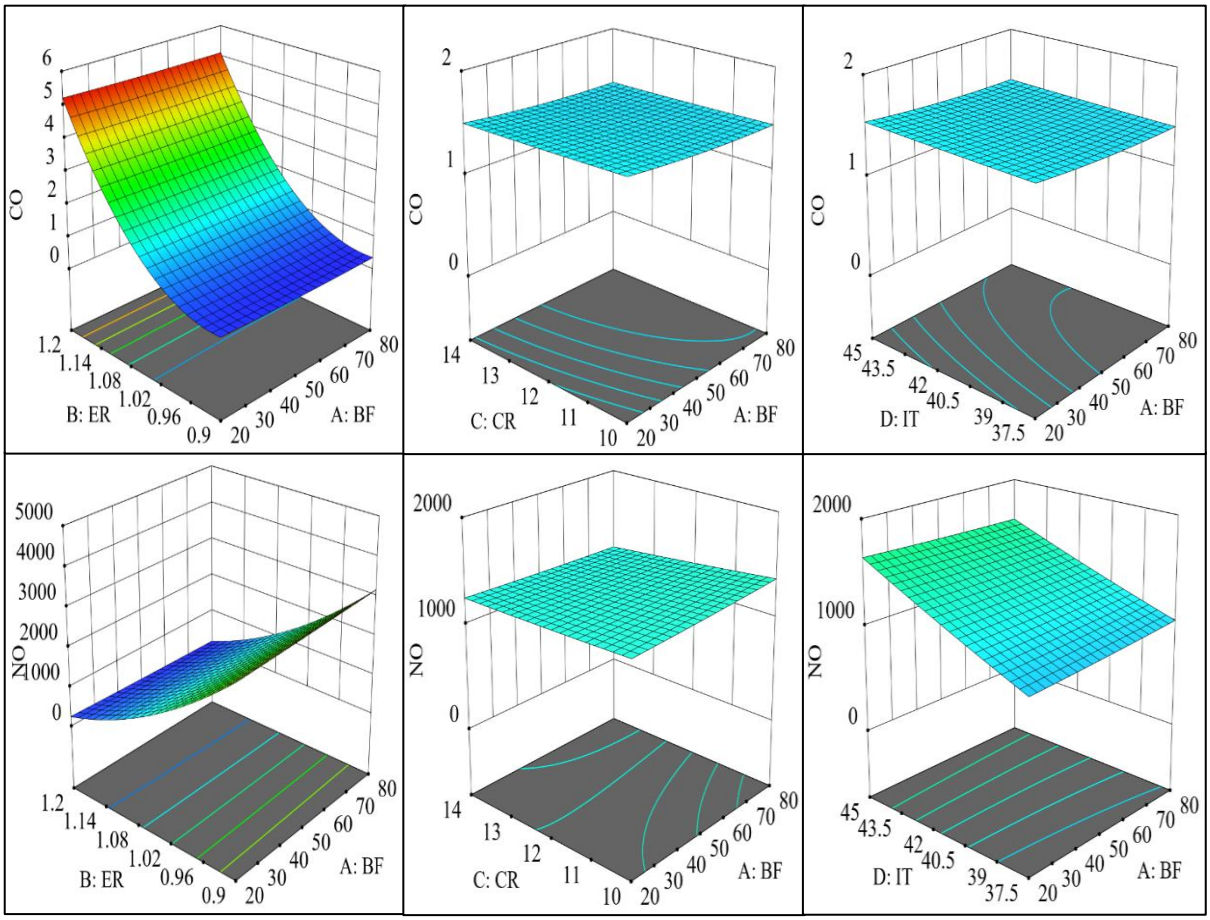


Figure 4.6.6. Impacts of BF, simultaneous CR, ER, IT variations on CO, NO emissions

## 4.6.5. Response optimizer and blending extent

Optimal results for Case-A and Case-B of multi-objective optimization are presented in Figure 4.6.7 and Figure 4.6.8, respectively. The confirmation run results are also presented in Table 4.27. For the case-A optimal results, the BTE, BMEP, and BSFC were assessed as 27.47%, 7.51 bars, and 0.3153 kg/kWh, with optimal predicted CO and NO emissions of 1.1656 (V%) and 1407.5(ppm), respectively. With respect to the input operating variables (BF, ER, CR, and IT), and apparent trafe-offs in simulated engine performance results, the innovative optimal operating optimal operating conditions were found as 79.996 (V%) BF (or, 20.004 V% of PG-blend), 1.032 ER, close-to-peak CR as 13.99 and slightly delayed ignition spark timing (41.428º CA-BTDC). Although most of the response parameters offer desirable outputs relative

to the DF PG-fuelled SI engines, the optimal BF represents nearly minimum blending of PG to be beneficial. However, for the Case-B of optimization, which is intended for more propane replacement, the optimal BF is found 46.15 V% (≈53.85 V% of PG), which represents about 1.67 times increment in the PG-blending. Further, the optimal BTE and BMEP performance decreased by just 1.89% and 3.79%, respectively, as compared to case-A. This might be attributed to the retention of the same high CR value (13.99) in the case-B of optimization as well. However, a significant increment in optimal BSFC was also noticed in case-B (28.61%). This is certainly attributed to the greater optimal PG-fraction (BF) in intake fuel (46.147 BF, or 53.853 V% of PG-blend) and the low CV of PG. This demands more PG-quantity to substitute the high-CV fuel, thus increasing the optimal BSFC for the constant RPM QDTM-modelled engine. Additionally, the CO and NO responses increase slightly (by 0.1V% and 5.7%, respectively) as compared to case-A of the optimization as compared to case A. Thus the presentation of these two optimization models also supports and provides the benefits associated with enhancing the waste wood-based PG blending at to conventional fuel. Further, the assessed individual and composite desirability levels for both the optimal results are also presented alongwith the generated optimal results in Figure 4.6.7 and Figure 4.6.8. It is observed that among all the responses, the CO and NO emission parameters feature relatively lower desirability values. This should be attributed to their higher degree of trade-off nature and establishment of optimum neither towards the minimum of CO nor towards the minimum of NO-response outcome. The decreased individual desirability values in case B lead to a decrease in the composite desirability as well. In case A, the RSM-assessed composite desirability for the best optimal solution was 0.859, whereas for case B the overall desirability further reduced to 0.728. Comparing cases A and case B, it is inferred that individual desirability values (*d*) get reduced attributing to the tradeoffs. This result is significant for the general case of optimization (case-A). Besides the results of case A&B, simulation results also

show that 60 *V%* PG (40*V%* BF) presents a max. BTE is 27.5% with BMEP as 7.159. Therefore, further PG blending might certainly result in more power derating which might also affect efficiency deterioration. Thus, 60 *V%* PG-fraction might certainly be considered an appropriate limitation for fueling the specified SI engine model.

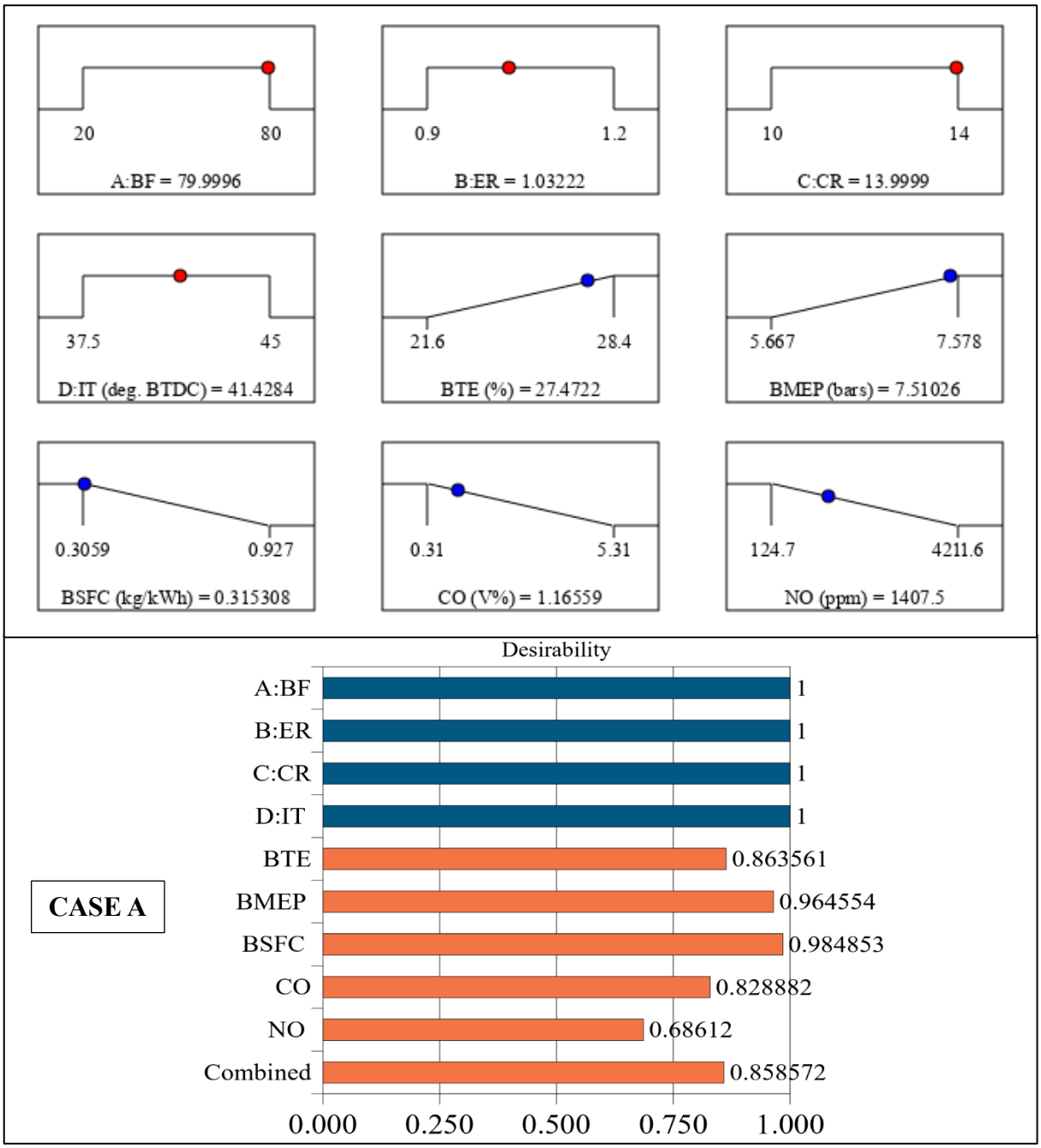


Figure 4.6.7. Optimization results for CASE-A

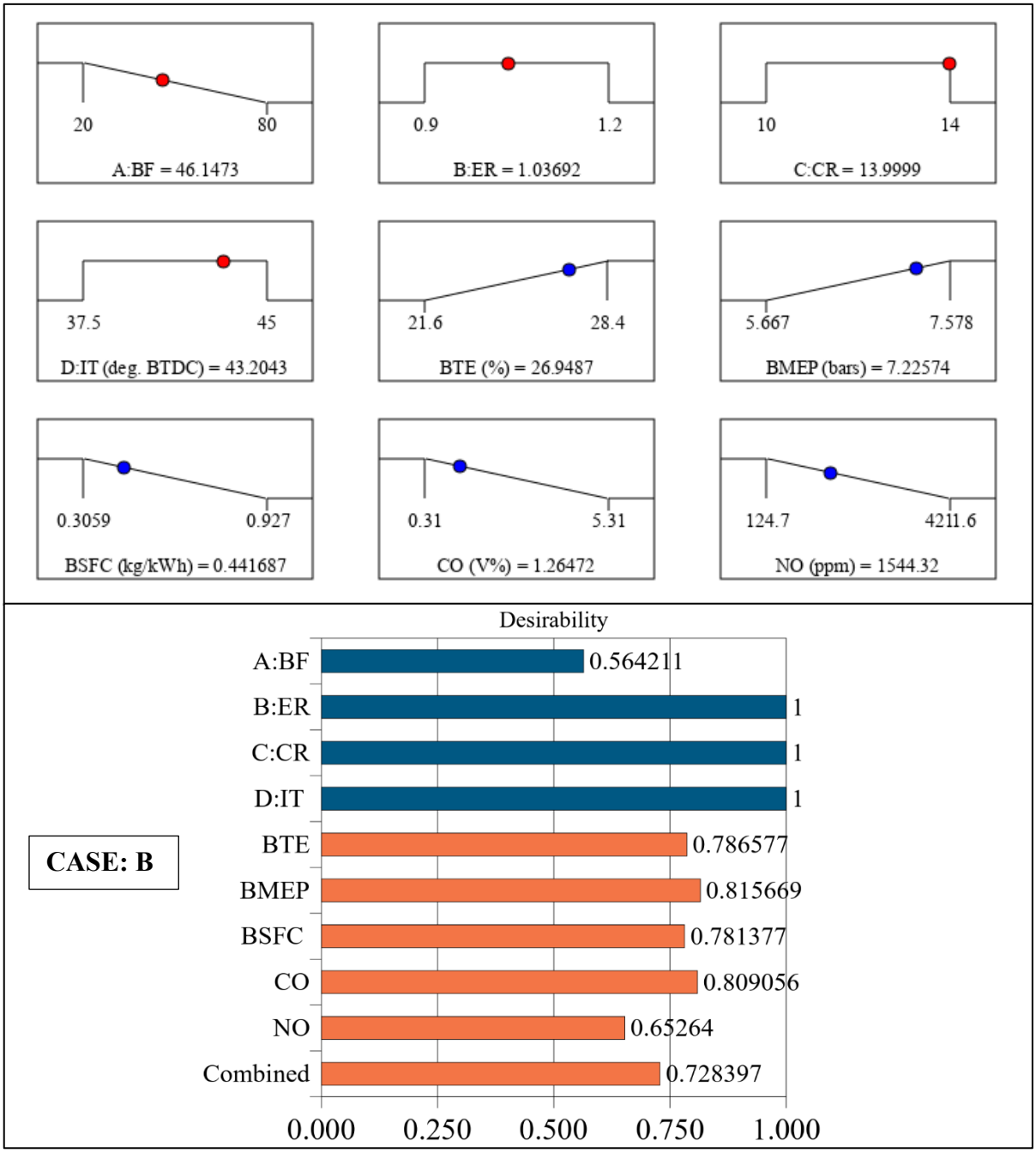


Figure 4.6.8. Optimization results for CASE-B

Table 4.27: Optimum responses confirmation run

| Parameters | BTE (%) | BMEP (kW) | BSFC (kg/kWh) | CO (V%) | CO (g/kWh) | NO (ppm) | NO (g/kWh) |
|---|---|---|---|---|---|---|---|
| **case-A** | | | | | | | |
| Predicted optimum: | 27.47 | 7.51 | 0.315 | 1.166 | 43.91 | 1407.5 | 9.33 |
| Simulation confirmation: | 27.65 | 7.55 | 0.314 | 1.17 | 44.06 | 1195.3 | 7.93 |
| Prediction deviation (%): | +1.7% | -0.4% | -3.4% | +1.6% | | 0.5% | |
| **case-B** | | | | | | | |
| Predicted optimum: | 26.95 | 7.23 | 0.442 | 1.264 | 47.61 | 1544.32 | 10.23 |
| Simulation confirmation: | 26.95 | 7.21 | 0.441 | 1.31 | 49.34 | 1265.5 | 8.39 |
| Prediction deviation (%): | | | | | | | |

### 4.6.6. Significant findings

The approach of using four independent parameters - Blending-fraction (BF), Equivalence ratio (ER), Compression ratio (CR), and Ignition timing (IT) as decision parameters was executed in simulation and through RSM-optimization to estimate the optimal performance (BMEP and BSFC) and emission parameters (CO and NO). The optimality of responses was compared respective to a case of letting the independent parameters be unconstrained, and another case of letting only the BF-operative parameter be constrained towards minimization (or PG-blend maximization), wherein the engine model delivers very comparable outputs.

The following major conclusions were drawn from the investigated study

- Increasing the propane-blending enhances the performance responses, and a simultaneous equivalence ratio increase significantly reduces the NO emission.
- An equivalence ratio of more than 1.08 could effectively counter the drawback of engine power-derating.
- Regression models were found highly accurate for predicting the output responses with ANOVA justifying the response sensitivities towards operating parameters' variations.

- Inline with the results depicted from surface plots, ANOVA results approved that the BTE and BSFC responses are most influenced by the BF*ER two-way interaction.
- Through ANOVA, ER and IT were also found most influencing factors for the CO and NO emission responses
- Optimal independent operating variables for a general case of optimization were found as 79.998(V%) BF, 1.032 ER, 13.99 CR, and slightly advanced IT of 41.42º (CA-BTDC).
- Desiring for more Grape-PG substitution resulted in shifting of optimal responses to 53.853 V% of PG-blend (or, 46.147 BF), greater ER (1.036), and slightly more advanced IT (43.20º CA-BTDC).
- Optimum dependent response parameters were found as 27.47% BTE, 7.51(bars) BMEP, 0.3153(kg/kWh) BSFC performances, and 1.166(V%) of CO and 1407.5(ppm) NO emissions.
- Individual desirabilities for the responses showing significant trade-offs like CO-NO and BTE-BMEP, show reduced individual desirability values.
- Composite desirability through the optimization was 0.859, whereas, with the setting of propane blend-fraction for minimization, the composite desirability was reduced to 0.728. With the feasible operating inputs and significant response outputs, it is recommended from the present study that Propane and grape-based PG could feasibly become a viable biomass-based energy source.